

DESIGN SOFTWARE DEVELOPMENT FOR INDUCTION MOTORS

A THESIS SUBMITTED TO
THE GRADUATE SCHOOL OF NATURAL AND APPLIED SCIENCES
OF
MIDDLE EAST TECHNICAL UNIVERSITY

BY

MUSTAFA İZGÜDEN

IN PARTIAL FULLFILLMENT OF THE REQUIREMENTS
FOR
THE DEGREE OF MASTER OF SCIENCE
IN
ELECTRICAL AND ELECTRONICS ENGINEERING

MAY 2011

Approval of the thesis:

DESIGN SOFTWARE DEVELOPMENT FOR INDUCTION MOTORS

submitted by **MUSTAFA İZGÜDEN** in partial fulfillment of the requirements
for the degree of **Master of Science in Electrical and Electronics
Engineering Department, Middle East Technical University** by,

Prof. Dr. Canan Özgen _____
Dean, **Graduate School of Natural and Applied Sciences**

Prof. Dr. İsmet Erkmen _____
Head of Department, **Electrical and Electronics Engineering**

Prof. Dr. H. Bülent Ertan _____
Supervisor, **Electrical and Electronics Engineering Dept., METU**

Examining Committee Members:

Prof. Dr. Aydın Ersak _____
Electrical and Electronics Engineering Dept., METU

Prof. Dr. H. Bülent Ertan _____
Electrical and Electronics Engineering Dept., METU

Prof. Dr. Muammer Ermiş _____
Electrical and Electronics Engineering Dept., METU

Prof. Dr. Kemal Leblebicioğlu _____
Electrical and Electronics Engineering, METU

Dr. Taylan Daş _____
ROKETSAN Inc.

Date: _____ 13/05/2011

I hereby declare that all information in this document has been obtained and presented in accordance with academic rules and ethical conduct. I also declare that, as required by these rules and conduct, I have fully cited and referenced all material and results that are not original to this work.

Name, Last name : Mustafa İZGÜDEN

Signature :

ABSTRACT

DESIGN SOFTWARE DEVELOPMENT FOR INDUCTION MOTORS

İzgüden, Mustafa

M. Sc., Department of Electrical and Electronics Engineering

Supervisor: Prof. Dr. H. Bülent Ertan

May 2011, 190 pages

The purpose of this thesis has been to convert two softwares called TPCAD (Three Phase Induction Machine Computer Aided Desing) and SPCAD (Single Phase Induction Machine Computer Aided Design) developed earlier for the design and analysis of three and single phase induction machines to meet the needs of motor manufacturing industry so that they can be run in windows environment. Furthermore, it was aimed to include features such as double cage motor analysis and design, to provide a facility designed motor lamination can be drawn for the user to see and facilitate sharing the designed lamination with other professional programs such as finite element analysis or thermal analysis etc.

As a result of this study, a user friendly design tool facilitating the design process of induction motors has been upgraded by using C++ Microsoft Visual Studio .Net programming language. TPCAD and SPCAD are tested with different commercial motors. The results show that the full load performance calculations are within the range of 5% error for both

programs. However, starting performance calculation errors are within 10% for TPCAD, and 8% for SPCAD.

Keywords: Three phase induction machine, single phase induction machine, performance analysis, optimum design, computer aided design

ÖZ

İNDÜKSİYON MOTORLARI İÇİN TASARIM PROGRAMI GELİŞTİRİLMESİ

İzgüden, Mustafa

Yüksek Lisans, Elektrik Elektronik Mühendisliği Bölümü

Tez Yöneticisi: Prof. Dr. H. Bülent Ertan

Mayıs 2011, 190 sayfa

Bu tezde motor üretim endüstrisinin ihtiyaçlarını karşılamak adına üç ve tek fazlı endüksiyon makinelerinin dizayn ve analizi için daha önce geliştirilmiş olan TPCAD (Üç Fazlı İndüksiyon Motoru Bilgisayar Destekli Tasarım) ve SPCAD (Tek Fazlı İndüksiyon Motoru Bilgisayar Destekli Tasarım) olarak isimlendirilen iki yazılımın windows ortamında çalıştırılabilmesi için gerekli değişikliklerin yapılması amaçlanmıştır. Ayrıca çift kafesli motor analiz ve dizaynı, kullanıcı için motor dizayn çiziminin çıkarılması ve dizayn edilen çizimin sonlu elemanlar analizi ya da termal analiz gibi diğer profesyonel programlarla paylaşımının sağlanması gibi ilave özelliklerin de kapsanması amaçlar dahilindedir.

Bu çalışma sonucunda, C++ Microsoft Visual Studio .Net programlama dili kullanılarak endüksiyon motorlarının dizayn sürecinde kullanılmak üzere kullanıcı dostu bir araç iyileştirilmiştir. TPCAD and SPCAD yazılımları çeşitli ticari motorlarla test edilmiştir. Her iki program için de sonuçlar, tam kapasite performans hesaplarının %5 hata aralığı içinde olduğunu

göstermektedir. Fakat, baslangıç performansı hesap hataları TPCAD için %10 ve SPCAD için %8 aralığındadır.

Anahtar Kelimeler: Üç faz indüksiyon motoru, bir faz indüksiyon motoru, performans analizi, en iyi tasarım, bilgisayar destekli tasarım

To Enuma

ACKNOWLEDGEMENTS

I would like to thank to my supervisor Prof. Dr. H. Bülent Ertan for his guidance, advice, criticism, encouragement and insight throughout the completion of the thesis.

I express my deepest gratitude to my mother Hatice Nuray İzgüden, my father Yılmaz İzgüden and my sister Esra İzgüden for their endless love, moral, and encouragement throughout my whole life.

I would like to thank Esra Cengiz for her existence, trust, endurance and everlasting love.

I sincerely thank my director Anıl Ünal for giving me valuable advices to complete my degree.

I would like to thank Elsan A.Ş. for providing test results of motors and motor data required for testing the program.

Finally, I am indebted to my close friend Tahir Onur Bakır for his encouragement to solve problems. Also, I would like to thank my friend Şenol Çelik and my cousin Yunus Gündüz for their help on the last turn.

TABLE OF CONTENTS

ABSTRACT	IV
ÖZ.....	VI
ACKNOWLEDGEMENTS	IX
TABLE OF CONTENTS	X
LIST OF TABLES.....	XV
LIST OF FIGURES	XIX
LIST OF ABBREVIATIONS.....	XXII
CHAPTERS	
1 INTRODUCTION	1
2 THREE PHASE INDUCTION MOTOR PARAMETER AND PERFORMANCE CALCULATIONS.....	3
2.1 INTRODUCTION.....	3
2.2 CALCULATION OF MACHINE PARAMETERS	3
2.3 CALCULATION OF STATOR RESISTANCE	4
2.4 CALCULATION OF ROTOR RESISTANCE	5
2.4.1 Deep-Bar Correction.....	8
2.5 CALCULATION OF MAGNETIZING REACTANCE.....	9
2.5.1 Saturation Factor	11
2.5.2 Carter's Coefficient	12

2.6 CALCULATION OF LEAKAGE REACTANCE	13
2.6.1 Slot Leakage Reactance.....	13
2.6.2 Zig – Zag Leakage Reactance.....	23
2.6.3 End Leakage Reactance.....	24
2.6.4 Skew Leakage Reactance	24
2.7 CALCULATION OF LOSSES.....	25
2.7.1 Calculation of Iron Losses.....	25
2.7.2 Friction and Windage Losses.....	27
2.8 PERFORMANCE CALCULATIONS	27
2.8.1 Calculation of Current	27
2.8.2 Calculation of Torque.....	28
2.8.3 Calculation of Output Power	29
2.8.4 Calculation of Efficiency.....	29
2.8.5 Calculation of Power Factor	30
2.8.6 Pull-Out Torque	30
2.9 DOUBLE CAGE MOTOR CALCULATIONS	31
2.9.1 Derivation of Equivalent Circuit.....	33
2.9.2 Calculation of Resistances.....	35
2.9.3 Calculation of Leakage Reactances.....	36
2.9.4 Calculation of Mutual Reactance	37
2.9.5 Modifications in Program Structure	37
3 OTHER FEATURES OF TPCAD.....	39
3.1 INTRODUCTION.....	39
3.2 PARAMETER CALCULATION FROM TESTS	39
3.2.1 Locked Rotor Test	40
3.2.2 No Load Test	42
3.3 ANALYZE A MOTOR USING PARAMETERS.....	44
3.4 ELECTRICAL POWER MEASUREMENT WITH LOSS SEGREGATION.....	46
4 SINGLE PHASE INDUCTION MOTOR PARAMETER AND PERFORMANCE CALCULATIONS.....	49

4.1 INTRODUCTION.....	49
4.2 CALCULATION OF MACHINE PARAMETERS	49
4.3 CALCULATION OF MAIN AND AUXILIARY WINDING RESISTANCES.....	51
4.4 CALCULATION OF ROTOR RESISTANCE	51
4.5 CALCULATION OF MAGNETIZING REACTANCE.....	51
4.6 CALCULATION OF LEAKAGE REACTANCE	52
4.6.1 Slot Leakage Reactance.....	52
4.6.2 Zig – Zag Leakage Reactance.....	53
4.6.3 End Leakage Reactance.....	53
4.6.4 Skew Leakage Reactance	53
4.7 CALCULATION OF LOSSES.....	54
4.7.1 Calculation of Iron Losses.....	54
4.7.2 Friction and Windage Losses.....	55
4.8 PERFORMANCE CALCULATIONS	55
4.8.1 Calculation of Full Load Performance	56
4.8.2 Combined Winding Performance	60
5 USER INTERFACE AND SOFTWARE	65
5.1 INTRODUCTION.....	65
5.2 TECHNICAL FEATURES OF TPCAD	66
5.3 STRUCTURE OF TPCAD	67
5.4 FILE MENU	69
5.4.1 New.....	69
5.4.2 Open	70
5.4.3 Print	71
5.5 CURVE MENU	72
5.5.1 B-H Curve Menu	72
5.5.2 Coreloss Curve Menu	74
5.6 ANALYSIS MENU	75
5.6.1 Graphical Performance Analysis.....	76
5.6.2 At a Power Analysis	77
5.6.3 At a Speed Analysis.....	78

5.6.4 Summary of the Analysis	79
5.6.5 Evaluation Form of the Analysis	80
5.6.6 Parameter Calculation	81
5.7 TEST MENU	82
5.7.1 Calculate Parameters Using Tests	82
5.7.2 Analyze A Motor Using Parameters	83
5.7.3 Motor Performance From Load Test	84
5.8 LAMINATION MENU	85
5.8.1 Creation of Repeating Stator Portion	87
5.8.2 Creation of Repeating Rotor Portions	95
6 TEST RESULTS AND VERIFICATION	97
6.1 INTRODUCTION.....	97
6.2 VERIFICATION OF TPCAD RESULTS	97
6.2.1 Test Motors.....	98
6.2.2 Verification of Parameter Calculation Algorithm.....	100
6.2.3 Sensitivity of Performance Calculations to Equivalent Circuit Parameters	108
6.2.4 Performance Calculation from Test Parameters and Evaluation of Model Accuracy	118
6.2.5 Performance Calculation from Motor Geometry Using TPCAD and Accuracy of TPCAD Calculation	121
6.3 VERIFICATION OF SPCAD RESULTS	127
6.3.1 Test Motors.....	127
6.3.2 Verification of Parameter Calculation Algorithm.....	129
6.3.3 Sensitivity of Performance Calculations to Equivalent Circuit Parameters	132
6.3.4 Performance Calculation from Test Parameters and Evaluation of Model Accuracy	138
6.3.5 Performance Calculation from Motor Geometry Using SPCAD and Accuracy of SPCAD Calculation	140
7 CONCLUSION.....	145

REFERENCES	150
 APPENDICES	
A TPCAD DATA ENTRY FORM	151
B SPCAD DATA ENTRY FORM	157
C ANALYSIS DATA OF TEST MOTORS - TPCAD	162
D ANALYSIS DATA OF TEST MOTORS - SPCAD	170
E TPCAD FLOWCHARTS.....	174
F SPCAD FLOWCHARTS.....	180
G B-H CURVE DATA	188

LIST OF TABLES

TABLES

Table 2-1 Look-Up Table for Deep-Bar Correction	9
Table 2-2 Distribution Factor for Three Phase Motors	15
Table 2-3 Look-Up Table of Slot Constants for Flat Bottom Trapezoidal Slots.....	18
Table 2-4 Look-Up Table of Slot Constants for Round Bottom Slots	19
Table 2-5 Look-Up Table of Bridge Permeance versus Bar Current.....	22
Table 2-6 Sample Core Loss Curve.....	26
Table 3-1 Empirical Distribution of Leakage Reactances.....	42
Table 3-2 Assumed Values for Stray-Load Loss.....	47
Table 4-1 Sample Core Loss Curve.....	55
Table 6-1 Three Phase Test Motors	98
Table 6-2 Performance Calculation Temperature for Three Phase Motors.....	99
Table 6-3 Double Cage Motors Parameter Calculations.....	101
Table 6-4 Single Cage Motors Parameter Calculations - 1	101
Table 6-5 Single Cage Motors Parameter Calculations - 2	102
Table 6-6 Coreloss Resistance Correction Factors.....	103
Table 6-7 New Air Gap Length Values of Double Cage Motors	105
Table 6-8 Comparison of Magnetizing Reactance for Double Cage Motors	105
Table 6-9 New Air Gap Length Values of Single Cage Motors	107
Table 6-10 Comparison of Magnetizing Reactance for Single Cage Motors	108

Table 6-11 Performance Variation of Double Cage Motor for Rotor Resistance	109
Table 6-12 Performance Variation of Double Cage Motor for Leakage Reactance	110
Table 6-13 Performance Variation of Double Cage Motor for Magnetizing Reactance	111
Table 6-14 Summary of Performance Variation for Double Cage Motor ...	112
Table 6-15 Performance Variation of Single Cage Motor for Rotor Resistance	113
Table 6-16 Performance Variation of Single Cage Motor for Leakage Reactance	114
Table 6-17 Performance Variation of Single Cage Motor for Magnetizing Reactance	115
Table 6-18 Summary of Performance Variation for Single Cage Motor	116
Table 6-19 Effect of Impedance on Current	117
Table 6-20 Double Cage Motors Performance Analysis (measured parameters)	119
Table 6-21 Single Cage Motors Performance Analysis - 1 (measured parameters)	119
Table 6-22 Single Cage Motors Performance Analysis - 2 (measured parameters)	120
Table 6-23 Double Cage Motors Performance Analysis (calculated performance)	122
Table 6-24 Single Cage Motors Performance Analysis - 1 (calculated performance)	122
Table 6-25 Single Cage Motors Performance Analysis - 2 (calculated performance)	123
Table 6-26 Single Cage Motors Performance Analysis - 3 (calculated performance)	124
Table 6-27 Single Cage Motors Performance Analysis - 4 (calculated performance)	124
Table 6-28 Machining Tolerances of the Motors	126

Table 6-29 No Load Current Verification.....	126
Table 6-30 Single Phase Test Motors.....	128
Table 6-31 Performance Calculation Temperature for Single Phase Motors	128
Table 6-32 Single Phase Motor Parameter Calculations - 1	129
Table 6-33 Single Phase Motor Parameter Calculations - 2	130
Table 6-34 New Air Gap Length Values of Single Phase Motors.....	131
Table 6-35 Comparison of Magnetizing Reactance for Single Phase Motors	132
Table 6-36 Performance Variation of Single Phase Motor for Rotor Resistance	133
Table 6-37 Performance Variation of Single Phase Motor for Main Winding Leakage Reactance.....	134
Table 6-38 Performance Variation of Single Phase Motor for Auxiliary Winding Leakage Reactance	135
Table 6-39 Performance Variation of Single Phase Motor for Magnetizing Reactance	136
Table 6-40 Summary of Performance Variation for Single Phase Motor...	137
Table 6-41 Single Phase Motors Performance Analysis - 1 (measured parameters)	139
Table 6-42 Single Phase Motors Performance Analysis - 2 (measured parameters)	140
Table 6-43 Single Phase Motors Performance Analysis - 1 (calculated performance)	141
Table 6-44 Single Phase Motors Performance Analysis - 2 (calculated performance)	142
Table 6-45 Single Phase Motors Performance Analysis - 3 (calculated performance)	143
Table A-1 TPCAD Motor Data Entry Form (Single Cage)	151
Table A-2 TPCAD Motor Data Entry Form (Double Cage).....	154
Table B-1 SPCAD Data Entry Form.....	157
Table C-1 Analysis Data of Single Cage Motors - 1	162

Table C-2 Analysis Data of Single Cage Motors - 2..... 165

Table C-3 Analysis Data of Double Cage Motors..... 167

Table D-1 Analysis Data of Single Phase Motors 170

Table G-1 TPCAD B-H Curve Data..... 188

Table G-2 SPCAD B-H Curve Data 189

LIST OF FIGURES

FIGURES

Figure 2-1 Equivalent Circuit of Three Phase Induction Motor.....	4
Figure 2-2 Coil Extension of Stator Windings	5
Figure 2-3 Skewed Rotor	6
Figure 2-4 Dimensions and Shapes of Stator Slots	14
Figure 2-5 Dimensions and Shapes of Rotor Slots	14
Figure 2-6 Flat Bottom Trapezoidal Slots.....	17
Figure 2-7 Round Bottom Slots.....	18
Figure 2-8 Slot Constants for Round Bottom Slots	19
Figure 2-9 Round Slots	20
Figure 2-10 Closed Slot of Rotor.....	21
Figure 2-11 Stator and Rotor Zig-Zag Leakage Flux.....	23
Figure 2-12 Flowchart of Pull-Out Torque Calculation	31
Figure 2-13 Double Cage Rotor Slot.....	32
Figure 2-14 Equivalent Circuit of Double Cage Motor.....	33
Figure 2-15 Exact Equivalent Circuit of Rotor Bars.....	33
Figure 2-16 Approximate Equivalent Circuit of Rotor Bars.....	34
Figure 3-1 Equivalent Circuit for Locked Rotor Test	40
Figure 3-2 Equivalent Circuit for No Load Test	43
Figure 4-1 Schematic Representation of Capacitor Start Motor.....	50
Figure 4-2 Equivalent Circuit of Single Phase Motor with Main Winding.....	56
Figure 4-3 Simplified Equivalent Circuit Model of Main Winding.....	56
Figure 4-4 Main and Auxiliary Winding Equivalent Circuit.....	60
Figure 5-1 Main Form of TPCAD	68

Figure 5-2 Menu Structure of TPCAD	68
Figure 5-3 New Motor Form	70
Figure 5-4 Loaded Motor Data Form.....	71
Figure 5-5 Print Form	72
Figure 5-6 B-H Curve Menu	73
Figure 5-7 Coreloss Curve Menu	75
Figure 5-8 Graphical Performance Analysis Menu.....	77
Figure 5-9 At a Power Analysis Menu	78
Figure 5-10 At a Speed Analysis Menu.....	79
Figure 5-11 Summary of Analysis Menu	80
Figure 5-12 Evaluation Form of the Analysis Menu	81
Figure 5-13 Calculated Machine Parameters Menu.....	81
Figure 5-14 Calculate Parameters Using Tests Menu	83
Figure 5-15 Analyze a Motor Using Parameters Menu	84
Figure 5-16 Motor Performance From Load Test Menu	85
Figure 5-17 Lamination Menu	86
Figure 5-18 Sample Motor Lamination.....	87
Figure 5-19 Sample Stator Slot Drawing.....	88
Figure 5-20 “C - D” Drawing.....	90
Figure 5-21 “G - H” Drawing	92
Figure 5-22 Algorithm of Drawing Stator Slot Portion	94
Figure 5-23 Algorithm of Drawing Rotor Slot Portion	95
Figure 5-24 Types of Rotor Slots	96
Figure E-1 Main Body of TPCAD	174
Figure E-2 Flowchart of the Performance Calculation.....	175
Figure E-3 Flowchart of Calc Procedure	176
Figure E-4 Flowchart of find_reactance Procedure.....	177
Figure E-5 Flowchart of comp Procedure	178
Figure E-6 Flowchart of reactance Procedure.....	179
Figure F-1 Main Body of SPCAD	180
Figure F-2 Flowchart of the Performance Calculation.....	181
Figure F-3 Flowchart of Calc Procedure	182

Figure F-4 Flowchart of CombinedCalculation Procedure	183
Figure F-5 Flowchart of find_reactance Procedure	184
Figure F-6 Flowchart of comp Procedure.....	185
Figure F-7 Flowchart of combined_performance Procedure	186
Figure F-8 Flowchart of reactance Procedure.....	187

LIST OF ABBREVIATIONS

r_1	Resistance of the Stator Winding
LMC_m	Mean Length of a Conductor of Stator Winding
C	Number of Conductor in Stator Winding
ρ_m	Resistivity of Stator Winding
$A1_m$	Cross Sectional Area of Conductor
L_1	Stator Stack Length
Γ	Coil Extension
q_m	Number of Parallel Paths in Main Winding
SK	Rotor Skew
α	Skew Angle
D_2	Rotor Outside Diameter
L_2	Rotor Stack Length
ρ_b	Resistivity of Rotor Bar
A_b	Cross Sectional Area of a Single Bar
I_b	Peak Value of the Current in a Single Bar
S_2	Number of Rotor Bars
p	Number of Poles
ρ_r	Resistivity of End Ring
D_r	Mean Diameter of End Ring
A_r	Cross Sectional Area of End Ring
CDB_r	Deep Bar Correction Factor for Rotor Resistance
t_{main}	Operating Temperature
K_\emptyset	Voltage Drop Correction Factor
K_{wm}	Distribution Factor for Main Winding
t_m	Throw of Coils
S_{1p}	Number of Stator Slots per Pole
X_m	Magnetizing Reactance
K_x	Reactance Constant
C_{sk}	Skew Constant
A_g	Air Gap Area per Pole

L_g	Effective Air Gap Length
K_1	Carter Coefficient (stator)
K_2	Carter Coefficient (rotor)
B_{sc}	Stator Core Flux Density
B_{st}	Stator Tooth Flux Density
B_{rc}	Rotor Core Flux Density
B_{rt}	Rotor Tooth Flux Density
B_g	Air Gap Flux Density
A_{sc}	Cross Sectional Area of Stator Core
A_{st}	Cross Sectional Area of Stator Tooth
A_{rc}	Cross Sectional Area of Rotor Core
A_{rt}	Cross Sectional Area of Rotor Tooth
A_g	Cross Sectional Area of Air Gap
SF	Saturation Factor
AT_{sc}	MMF Drop on Stator Core
AT_{st}	MMF Drop on Stator Tooth
AT_{rc}	MMF Drop on Rotor Core
AT_{rt}	MMF Drop on Rotor Tooth
AT_g	MMF Drop on Air Gap
ks_1	Slot Constant for Stator
ks_2	Slot Constant for Rotor
K_s	Slot Constant Referred to Primary
C_x	Distribution Factor
S_1	Number of Stator Slots
S_2	Number of Rotor Slots
X_{slot}	Slot Leakage Reactance
$X_{zig-zag}$	Zig-Zag Leakage Reactance
g	Air Gap Length
λ_1	Stator Tooth Pitches
λ_2	Rotor Tooth Pitches
D_1	Stator Bore Diameter
D_2	Rotor Outside Diameter
X_{end}	End Leakage Reactance
ACT	Weighted Average Coil Throw of Stator Windings
X_{skew}	Skew Leakage Reactance
K_{p1}	Primary Flux Factor
X	Total Leakage Reactance
CDB_x	Deep Bar Correction Factor for Rotor Reactance

X_1	Stator Leakage Reactance
X_o	Open Circuit Reactance
X_2	Rotor Leakage Reactance
K_{hi}	High Frequency Loss Constant
I_1	Stator Current
V	Phase Voltage
Z_{th}	Total Impedance of Equivalent Circuit
T	Full Load Torque
m	Phase Number
i_2'	Referred Rotor Current
r_2'	Referred Rotor Resistance
n_s	Synchronous Speed
s	Slip
P_{out}	Output Power
$P_{friction}$	Friction Loss
$P_{windage}$	Windage Loss
P_{cu_stator}	Stator Copper Loss
P_{cu_rotor}	Rotor Copper Loss
P_{in}	Input Power
r_3	Upper Cage Resistance
r_4	Lower Cage Resistance
X_4	Lower Cage Reactance
X_{mutual}	Mutual Reactance
B_{rt_upper}	Upper Cage Rotor Tooth Flux Density
B_{rt_lower}	Lower Cage Rotor Tooth Flux Density
A_{rt_upper}	Upper Cage Area
A_{rt_lower}	Lower Cage Area
AT_{rt_upper}	Upper Cage MMF Drop
AT_{rt_lower}	Lower Cage MMF Drop
Z_{locked}	Locked Rotor Impedance
V_{locked}	Locked Rotor Test Voltage
I_{locked}	Locked Rotor Test Current
r_{locked}	Locked Rotor Resistance
P_{locked}	Locked Rotor Test Power
X_{locked}	Locked Rotor Reactance
V_{noload}	No Load Test Voltage
I_{noload}	No Load Test Current
P_{noload}	No Load Test Power
P_{gap}	Power Transferred Across the Air Gap

$P_{\text{gap_net}}$	Net Output Power on the Shaft
T_{mech}	Electromechanical Torque
r_{1a}	Auxiliary Winding Resistance
R_f	Forward Field Apparent Resistance
R_b	Backward Field Apparent Resistance
X_f	Forward Field Apparent Reactance
X_b	Backward Field Apparent Reactance
Z_T	Total Apparent Resistance of Main Winding
R_T	Total Apparent Reactance of Main Winding
X_T	Total Apparent Impedance of Main Winding
E_{fm}	Main Winding Forward Field Induced Voltage
E_{bm}	Main Winding Backward Field Induced Voltage
E_{fa}	Auxiliary Winding Forward Field Induced Voltage
E_{ba}	Auxiliary Winding Backward Field Induced Voltage
K_{wa}	Auxiliary Winding Distribution Factor
I_m	Main Winding Current
I_a	Auxiliary Winding Current
Z_{Ta}	Total Apparent Resistance of Auxiliary Winding
R_{Ta}	Total Apparent Reactance of Auxiliary Winding
X_{Ta}	Total Apparent Impedance of Auxiliary Winding
R_c	Capacitor Resistance
X_c	Capacitor Reactance
D_1	Stator Bore Diameter
D	Stator Outside Diameter
d_1	Stator Tooth Depth
d_{10}	Stator Mouth Depth
d_{11}	Stator Tip Depth
w_{10}	Stator Slot Opening
w_{11}	Stator Slot Bottom Width
w_{13}	Stator Slot Top Width
d_2	Rotor Tooth Depth
d_{20}	Rotor Mouth Depth
d_{21}	Rotor Tip Depth
w_{20}	Rotor Slot Opening
w_{21}	Rotor Slot Top Width
w_{23}	Rotor Slot Bottom Width

CHAPTER 1

INTRODUCTION

Motor design and performance calculations are done for many years. When a design process is started first of all, constraints and desired performances should be determined. Then to meet these needs, an initial design is made and performance of this attempt is calculated and compared with desired requirements. If the results are satisfactory the design process is finalized, else design inputs are changed and performance output is recalculated. This process goes on until a satisfactory performance is attained and a motor is designed with desired requirements.

In early years, design process of the motors was done manually. With the growth of the computer and software area, old fashioned methods leave the calculations to the software programs. Nowadays various software programs are widely used in motor design industry. With these programs, procedures and calculations used to take a long time can be done within few seconds. These products also accelerate the design phase and make it easier to improve the motor performance of an existing calculation or design.

In this context, design software called TPCAD (Three Phase Induction Machine Computer Aided Design) and SPCAD (Single Phase Induction

Machine Computer Aided Design) are developed by Hamarat and Aftahi respectively are good examples for the purpose of design and optimization of three-phase and single-phase induction motors. ([1], [2]) Since TPCAD and SPCAD run on DOS environment, these programs become obsolete. So, in this work these two design programs are rewritten in Microsoft Visual Studio .NET environment using C++ programming language.

In this work, induction motor design softwares called TPCAD and SPCAD are improved and many new capabilities are added to the programs. Furthermore, the improvements of the performance calculations were done and compared with the test results.

The rest of this paper is organized as follows: in Chapter 2 calculation methods and models used for three phase induction machine are explained. In Chapter 3, new features added to TPCAD are explained. In Chapter 4 calculation methods and models used for single phase induction machine are explained. In Chapter 5 user interfaces are given. In Chapter 6 experiments and results are demonstrated. In Chapter 7 conclusion and ideas about future works are given.

CHAPTER 2

THREE PHASE INDUCTION MOTOR PARAMETER AND PERFORMANCE CALCULATIONS

2.1 Introduction

In this chapter, the applied methods and improvements for the design and optimization software of TPCAD are summarized. Calculation methods and equations defined in TPCAD are given in the following sections. In this section, the approach used is based on the Veinott's work. ([3])

2.2 Calculation of Machine Parameters

To calculate the performance of a motor, one needs the equivalent circuit of the motor. For design purposes, the equivalent circuit parameters need to be calculated from the dimensions of the motor and material properties. To obtain a correct model it is important to calculate the parameters accurately and use them to calculate machine performance at any value of the slip. To meet these needs, TPCAD has a feature to calculate motor parameters from the entered motor data and the motor performance. TPCAD uses the per phase equivalent circuit of a polyphase induction motor shown in Figure

2-1, to calculate the performance of the motor. User defined parameters entered to TPCAD for calculations are given in APPENDIX A. Units of these parameters are also given in APPENDIX A.

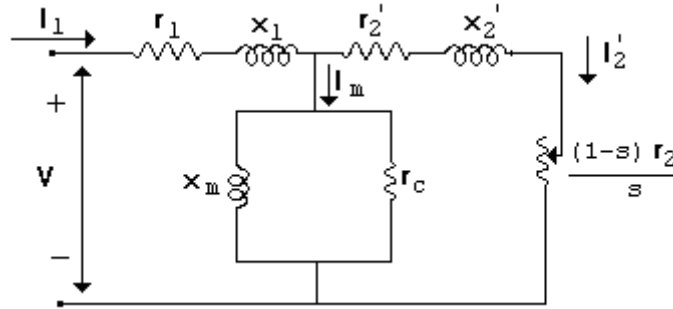


Figure 2-1 Equivalent Circuit of Three Phase Induction Motor

In the following sections, methods used in the developed software for the calculation of parameters and performance of a given induction motor will be described.

2.3 Calculation of Stator Resistance

The stator resistance of the equivalent circuit can be found from the amount of copper used in the stator windings. The resistance of the stator winding coils, r_1 , is found from,

$$r_1 = \frac{LMC_m \cdot C \cdot \rho_m}{q_m \cdot A_{1m}} \quad (2-1)$$

where LMC_m is the mean length of a conductor of stator windings and calculated from (2-2);

$$LMC_m = L_1 + \Gamma \quad (2-2)$$

In (2-2), L_1 is the stator stack length and entered to the TPCAD by the user. Γ is the coil extension of conductors of the machine (Figure 2-2) and is also entered to the program by the user.

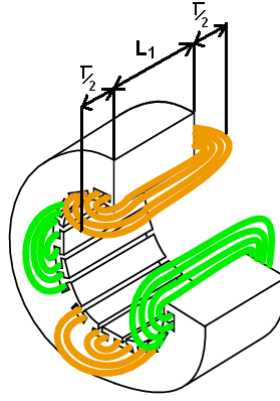


Figure 2-2 Coil Extension of Stator Windings

In (2-1), C is the total number of conductors connected in series within main windings. ρ_m is the resistivity of the stator winding material, $A1_m$ is the cross sectional area of the conductor which is used in the stator windings and q_m is the number of parallel paths in main windings. All these parameters are user defined parameters and entered by the user.

2.4 Calculation of Rotor Resistance

The rotor resistance of the equivalent circuit can be found from the bar cross section, core length, end ring dimensions and the cage materials. While calculating the resistance of the rotor cage referred to primary, the skew of the rotor bars should be accounted for Figure 2-3.

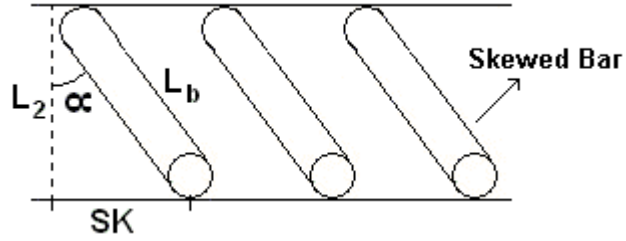


Figure 2-3 Skewed Rotor

The skew is found in terms of skew angle, α , and the rotor outside diameter, D_2 ,

$$SK = \frac{\pi \cdot \alpha \cdot D_2}{360} \quad (2-3)$$

The length of the rotor bar, L_b , is found from rotor stack length, L_2 , and rotor skew, SK,

$$L_b = \sqrt{L_2^2 + SK^2} \quad (2-4)$$

The resistance of a single bar of the rotor cage is $\frac{L_2 \cdot \rho_b}{A_b}$, where, ρ_b is the resistivity of rotor bar and A_b is the cross sectional area of a single bar. All these parameters are entered to TPCAD by the user. (APPENDIX A)

Resistance of a single bar is used to determine the I^2R loss of all the rotor bars.

$$\left(\frac{I_b}{\sqrt{2}}\right)^2 \cdot \left(\frac{L_2 \cdot \rho_b}{A_b}\right) \cdot S_2 = I_b^2 \frac{S_2 \cdot L_2 \cdot \rho_b}{2 \cdot A_b} \quad (2-5)$$

In (2-5) I_b is used as the peak value of the current in a single bar and calculated from (2-6), and S_2 is the number of rotor bars. S_2 is a user defined parameter.

$$I_b = \frac{m \cdot \sqrt{2} \cdot C \cdot K_{wm}}{S_2} \cdot I_2 \quad (2-6)$$

The total I^2R loss per phase of the two end rings is calculated from (2-7),

$$\text{End Ring } I^2R \text{ Loss} = \left(\frac{I_b S_2}{\sqrt{2} \cdot \pi \cdot p} \right)^2 \cdot \left(\frac{2 \cdot \rho_r \cdot \pi \cdot D_r}{A_r} \right) \quad (2-7)$$

Where, p is the number of poles, ρ_r is the resistivity of the end ring, D_r is the mean diameter of the end ring and A_r is the cross sectional area of end ring. While evaluating the end ring losses these parameters are used from the entered inputs by the user.

Total rotor I^2R loss is found from the addition of (2-5) and (2-7) and shown in (2-8),

$$\text{Rotor } I^2R \text{ Losses} = \frac{I_b^2}{m} \left(\frac{S_2 \cdot L_2 \cdot \rho_b}{2A_b} + \frac{S_2^2 \cdot D_r \cdot \rho_r}{\pi \cdot p^2 \cdot A_r} \right) \quad (2-8)$$

Substituting the value of I_b in (2-8), gives the total I^2R loss per phase;

$$(C \cdot K_{wm})^2 \cdot \left(\frac{L_2 \cdot \rho_b}{S_2 \cdot A_b} + \frac{2 \cdot D_r \cdot \rho_r}{\pi \cdot p^2 \cdot A_r} \right) \cdot m \cdot I_2^2 = r_2^2 \cdot I_2^2 \quad (2-9)$$

The value of the rotor resistance referred to the primary can be found from simplifying the (2-9),

$$r_2 = (C \cdot K_{wm})^2 \cdot \left(\frac{L_b \cdot \rho_b}{S_2 \cdot A_b} + \frac{2 \cdot D_r \cdot \rho_r}{\pi \cdot p^2 \cdot A_r} \right) \cdot m \quad (2-10)$$

Rotor resistance is corrected by a factor to reflect the deep bar effect. In (2-11), CDB_r is a correction factor due to the deep bar effect and detailed information is given in section 2.4.1.

$$r_2 = r_2 \cdot CDB_r \quad (2-11)$$

Calculations of equivalent circuit resistances are given in the previous sections. TPCAD can calculate performance of the motor for any given operating temperature value using these values. However, to calculate the performance of the motor for a given operating temperature, the calculated resistances have to be corrected. For that reason, to find the values at any operating temperature value, t_{main} , (2-12) is used. Operating temperature is entered to the program as final temperature by the user.

$$r_{hot} = \frac{(234.5 + t)}{(234.5 + t_{main})} \cdot r_{cold} \quad (2-12)$$

2.4.1 Deep-Bar Correction

Rotor conductors placed near the top of the slots link less flux than the conductors near the bottom, so the reactance of the top conductors is less than the bottom ones. When voltage is induced in a bar, more current flow through the top of the conductors when compared to the bottom ones. For that reason I^2r losses will be increased by this non-uniform distribution. This condition increases the effective resistance of the bar. High current density on the top of the slot increases the reluctance; however non-uniform distribution of the current decreases the effective reactance. ([3])

To calculate the deep bar effects in parallel sided rotor slots, correction factor is used from the pre-defined correction factor curves. ([3]) These curves are used in TPCAD as a look-up table. The table entered to the

program is given in Table 2-1. For the values exceeding the defined points, extrapolation is used to predict these points.

Table 2-1 Look-Up Table for Deep-Bar Correction

Bar Depth (meter)	Correction Factor for Resistance	Correction Factor for Reactance
0.0000	1.00	1.00
0.0074	1.00	1.00
0.0127	1.20	0.98
0.0330	3.00	0.60
0.0381	3.50	0.50
0.0592	4.50	0.40
0.0635	6.00	0.30

2.5 Calculation of Magnetizing Reactance

Magnetizing reactance is the ratio of the voltage induced by the fundamental component of flux to magnetizing current required to set up the flux. Total flux per pole is calculated from (2-13);

$$\phi = \frac{0.45 \cdot K_{\phi} \cdot V}{f \cdot C \cdot K_{wm}} \quad (2-13)$$

In (2-13), K_{ϕ} is the voltage drop correction factor. In the developed software it is defined as a constant and is entered by the user to find the voltage drop on the series leakage reactance. (i.e. voltage on the magnetizing branch is $K_{\phi} \cdot V$) This is an initial calculation to calculate machine parameters. When the parameters are calculated, the voltage drop on the magnetizing branch is recalculated according to the machine parameters. Calculations used in TPCAD are given in Figure E-3.

K_{wm} is the distribution factor for the main winding, and calculated from (2-14);

$$K_{wm} = \frac{\sin(S_{1p} \cdot \frac{\alpha}{2}) \cdot \sin(\frac{\pi \cdot t_m}{2 \cdot S_{1p}})}{\frac{S_{1p}}{m \cdot \sin(\frac{\alpha}{2})}} \quad (2-14)$$

where t_m is the throw of coils (number of slot pitches), α is the skew angle (degrees) and S_{1p} is the number of stator slots per pole. These parameters are entered to TPCAD by the user. (APPENDIX A)

The value of the magnetizing reactance, X_m , is found from (2-15);

$$X_m = K_x \cdot C_{sk} \cdot \frac{12.5 \cdot A_g \cdot m}{L_g \cdot SF \cdot p \cdot \sqrt{2}} \quad (2-15)$$

where K_x is the reactance constant found from (2-16), C_{sk} is the skew constant found from (2-17), A_g is the air gap area per pole found from (2-18) and L_g is the effective air gap length found from (2-19);

$$K_x = 2 \cdot \pi \cdot f \cdot 10^{-8} \cdot (C \cdot K_{wm})^2 \quad (2-16)$$

$$C_{sk} = \frac{\sin\left(\frac{\alpha}{2}\right)}{\frac{\pi \cdot \alpha}{360}} \quad (2-17)$$

$$A_g = L_1 \cdot \pi \cdot \frac{(D_2 + g)}{p} \quad (2-18)$$

$$L_g = K_1 \cdot K_2 \cdot g \quad (2-19)$$

In (2-19), K_1 and K_2 are the Carter Coefficients for stator and rotor respectively. Determinations of these coefficients are explained in section 2.5.2.

2.5.1 Saturation Factor

SF is the saturation factor defined as the ratio of total ampere turns in the stator, rotor and air gap to air gap ampere turns. To find the ampere turns of the various parts of the motor, one needs to determine the total flux per pole. Total peak flux per pole can be calculated from (2-13).

Flux densities at stator core and teeth, rotor core and teeth and the flux density in the gap are found from the equations given below;

$$B_{sc} = \frac{\phi}{A_{sc}} \quad (2-20)$$

$$B_{st} = \frac{\phi}{0.637 \cdot A_{st}} \quad (2-21)$$

$$B_{rc} = \frac{\phi \cdot K_{p1}}{A_{rc}} \quad (2-22)$$

$$B_{rt} = \frac{\phi \cdot K_{p1}}{0.637 \cdot A_{rt}} \quad (2-23)$$

$$B_g = \frac{\phi \cdot K_{p1}}{0.637 \cdot A_g} \quad (2-24)$$

Where A_{sc} , A_{st} , A_{rc} , A_{rt} , A_g are the cross sectional areas of stator core, stator teeth, rotor core, rotor teeth and the air gap respectively. The field intensity is found from the magnetization curve of the material used. Multiplying the values of the field intensity found from the curves with the

actual length of the magnetic path, ampere turn values for each part of the magnetic circuit can be found in (2-25). ([3])

$$SF = \frac{(AT_{sc} + AT_{st} + AT_{rc} + AT_{rt} + AT_g)}{AT_g} \quad (2-25)$$

Where AT_{sc} , AT_{st} , AT_{rc} , AT_{rt} , AT_g are the mmf drops on the stator core, stator teeth, rotor core, rotor teeth and the air gap respectively.

2.5.2 Carter's Coefficient

The slot openings of both stator and rotor increase the reluctance of the air gap which needs to be accounted for the calculation of the mmf drop in the air gap. The effect of the slot openings should be taken into account by assuming that the slot openings are equivalent to an increase length of air gap. That's why the gap length is increased by Carter's coefficients K_1 and K_2 corresponding to stator and rotor slot openings respectively. Calculations of these coefficients are obtained from (2-26) and (2-27) [3];

$$K_1 = \frac{\lambda_1 \cdot (5g + w_{10})}{\lambda_1 \cdot (5g + w_{10}) - w_{10} \cdot (0.5g + w_{10})} \quad (2-26)$$

$$K_2 = \frac{\lambda_2 \cdot (5g + w_{20})}{\lambda_2 \cdot (5g + w_{20}) - w_{20} \cdot (g + w_{20})} \quad (2-27)$$

In the case of closed rotor slots where w_{20} is equal to zero, the value of K_2 is assumed to be 1.0. λ_1 and λ_2 are the stator and rotor tooth pitches respectively and calculated from (2-42).

2.6 Calculation of Leakage Reactance

Leakage reactance is the reactance due to the leakage flux. This value depends on the operating conditions of the motor. Main cause of this variation is the magnetic saturation of the leakage flux paths. Saturation increases with increasing current and decreases the leakage reactance. Here, leakage reactances are taken as independent of saturation except when the rotor side has closed slots. To calculate the correct value of the reactances, they must be computed at any slip. The components of the leakage reactance are; Slot leakage (stator and rotor) reactance, Zig-zag leakage reactance, End leakage reactance and Skew leakage reactance. Calculations used in TPCAD are given in Figure E-6.

In the following sub sections, detailed information about methods used in TPCAD to calculate these reactances are described.

2.6.1 Slot Leakage Reactance

Before starting to determine the slot leakage reactance, the value of the slot constant for that slot should be found first. The slot constant is the equivalent permeance of a slot which varies due to the geometry of the slot and the arrangement of the conductors. Stator and rotor slot shapes handled in TPCAD are given in Figure 2-4 and Figure 2-5.

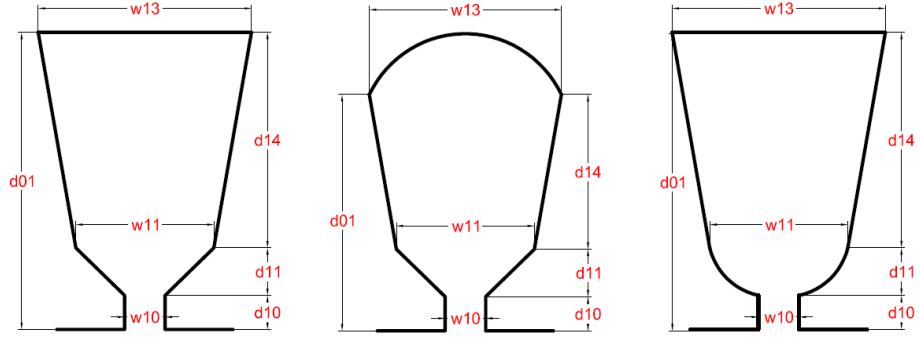


Figure 2-4 Dimensions and Shapes of Stator Slots

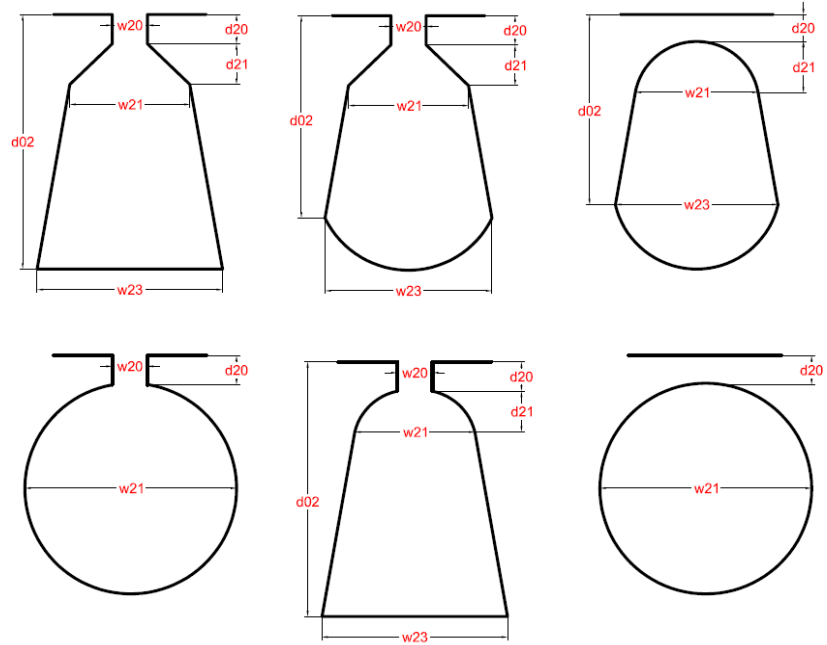


Figure 2-5 Dimensions and Shapes of Rotor Slots

Using the equations to find the slot constants mentioned in the following sections, it is possible to find the slot constant for stator, k_{s1} , and rotor, k_{s2} , respectively. The total slot constant referred to the primary side, K_s , is found from (2-28);

$$K_s = k_{s1} \cdot C_x + \frac{S_1}{S_2} \cdot k_{s2} \quad (2-28)$$

where, S_1 and S_2 are number of slots of stator and rotor respectively. All these parameters are entered to the program by the user. C_x is the distribution factor for slot leakage and is found from the equations given in Table 2-2 [3];

Table 2-2 Distribution Factor for Three Phase Motors

pup = per unit pitch	C_x
0.33 – 0.67	0.25 (6 pup - 1)
0.67 – 1.00	0.25 (3 pup + 1)
1.00 – 1.33	0.25 (7 – 3 pup)

The slot leakage reactance, X_{slot} , is determined from (2-29);

$$X_{slot} = K_x \cdot 125,5 \cdot L_1 \cdot \frac{K_s}{S_1} \cdot m \quad (2-29)$$

In (2-29), K_x is the reactance constant and calculated from (2-16).

Total leakage reactance, X , including stator and rotor reactances, is calculated from (2-30);

$$X = K_x (X_{slot} + X_{skew} + X_{end} + Z_{zig-zag}) \left(\frac{1 + CDB_x}{2} \right) \quad (2-30)$$

In (2-30), CDB_x is the deep bar correction factor for reactance. Determination of this value is detailed explained in section 2.4.1. K_x is the reactance constant found from (2-38). Calculations of skew, end and zig-zag leakage reactances are explained in the following sections.

The stator leakage reactance, X_1 , is found from (2-31);

$$X_1 = \frac{X}{\sqrt{1 + \frac{(X_0 - X)}{X}}} \quad (2-31)$$

where, X_0 is the open circuit reactance of the motor and determined from (2-32);

$$X_0 = K_x (P_m + \frac{(X_{slot} + X_{skew} + X_{end} + X_{zig-zag})}{2}) \quad (2-32)$$

where,

$$P_m = 12.5 \cdot K_m \cdot C_{sk} \cdot m \quad (2-33)$$

In (2-33), K_m and C_{sk} is calculated from (2-47) and (2-17) respectively.

Rotor leakage reactance, X_2 , is obtained from subtracting the value of stator leakage reactance X_1 , from the total leakage reactance X in (2-34);

$$X_2 = X - X_1 \quad (2-34)$$

2.6.1.1 Flat Bottom Trapezoidal Slots

For the flat bottom trapezoidal slots shown in Figure 2-6-a, the slot constant is calculated as;

$$k_s = \phi_s \cdot \frac{b}{a_2} + \frac{d}{e} + \frac{2c}{e + a_1} \quad (2-35)$$

For the slot shown in Figure 2-6-b, the slot constant is;

$$k_s = \phi_s \cdot \frac{b}{a_2} + \frac{d}{e} + \frac{\pi}{4} \cdot \frac{\cos^{-1} \frac{e}{a_1}}{90} \quad (2-36)$$

where, ϕ_s is the factor for slot constant correction for the part of the slot which contains the conductors in it.

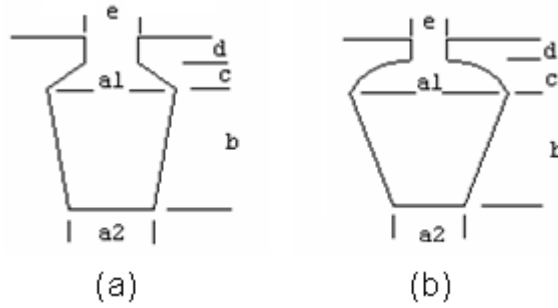


Figure 2-6 Flat Bottom Trapezoidal Slots

To determine slot constant, ϕ_s , a pre-defined curve is used. ([3]) This curve is used in TPCAD as a look-up table. The table entered to the program is given in Table 2-3. For the values exceeding the defined points, linear extrapolation is used to predict these points.

Table 2-3 Look-Up Table of Slot Constants for Flat Bottom Trapezoidal Slots

ϕ_s	$\frac{a_1}{a_2}$
0.5	0.630
0.7	0.470
0.8	0.410
1.1	0.300
1.3	0.250
1.6	0.200
2.1	0.150
3.1	0.100
3.9	0.075
4.4	0.065

2.6.1.2 Round Bottom Slots

Another shape of the slot is the slots with round bottoms as in Figure 2-7. The slot constant for this type of slot shape is;

$$k_s = F + \frac{d}{e} + \frac{2c}{e + a_1} \quad (2-37)$$

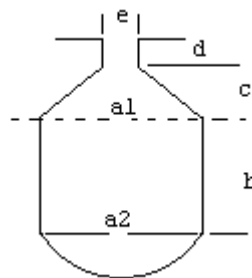


Figure 2-7 Round Bottom Slots

F is the slot constant corresponding to the bottom of the slot where the conductors are placed. To determine slot constant, F, a pre-defined curve is used shown in Figure 2-8. ([3]) This curve is used in TPCAD as a look-up table. The table entered to the program is given in Table 2-4. For the values exceeding the defined points, linear extrapolation is used to predict these points.

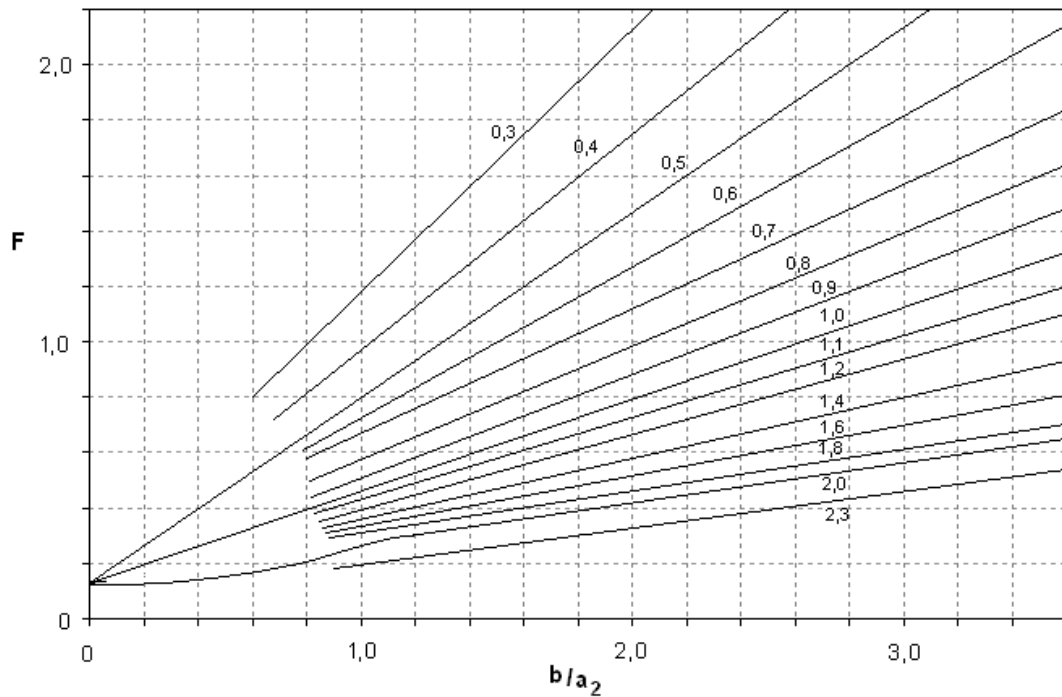


Figure 2-8 Slot Constants for Round Bottom Slots

Table 2-4 Look-Up Table of Slot Constants for Round Bottom Slots

$\frac{a_1}{a_2}$	Slope of Line	b
0.3	1.000	0.200
0.4	0.730	0.220

Table 2-4 (cont'd)

$\frac{a_1}{a_2}$	Slope of Line	b
0.5	0.667	0.133
0.6	0.570	0.142
0.7	0.500	0.100
0.8	0.400	0.200
0.9	0.375	0.125
1.0	0.333	0.133
1.1	0.285	0.171
1.2	0.272	0.127
1.4	0.250	0.050
1.6	0.200	0.080
1.8	0.166	0.100
2.0	0.166	0.030
2.3	0.125	0.075

2.6.1.3 Round Slots

For the round slots shown in Figure 2-9, the slot constant is;

$$k_s = \frac{d}{e} + 0.623 \quad (2-38)$$

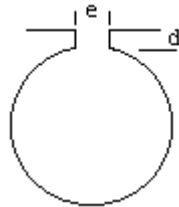


Figure 2-9 Round Slots

2.6.1.4 Closed Slots

Another slot type is the closed slot tops shown in Figure 2-10. Because of the permeability of the surrounding iron cannot be assumed infinite, the slot constant is assumed to be a function of saturation.

$$k_s = F + \text{Bridge Permeance} \quad (2-39)$$

In (2-39), F is the slot constant for bottom part (below the dashed line labeled A in Figure 2-10) which is same as round bottom slots and is found by using Table 2-4. However, finding the slot constant for the bridge part of the slot is not easy. The approach used is dividing the bridge of the slot (between the dashed lines labeled with A and B shown in Figure 2-10) to 7 equal strips with equal width. By finding the flux at each strip the total mmf drop through the bridge can be found. With this method a curve which gives the slot top permeance as a function of slot mmf is obtained for each geometry. The iterative method used in this work is explained in detail in [2].

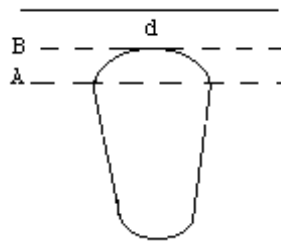


Figure 2-10 Closed Slot of Rotor

A sample of this curve used in TPCAD is shown in Table 2-5. For the values exceeding the defined points, extrapolation is used to predict these points.

Table 2-5 Look-Up Table of Bridge Permeance versus Bar Current

Bridge Permeance	Bar Current (A)
39.9	18.20106
139.5	8.055477
236.8	6.112758
335.4	5.185507
435.7	4.669307
541.9	4.323229
639.4	4.068949
736.5	3.831831
839.3	3.678564
937.9	3.554145
1036.9	3.432671
1435.2	3.15158
1835.3	2.965895
2242.9	2.857787
2636.2	2.772884
3044.9	2.718622
3442.6	2.669646
3840.3	2.630873
4237.9	2.599416
4635.6	2.573382
5044.3	2.556486
5441.9	2.537438
5839.6	2.520999
6237.3	2.506667
6640.5	2.495962
7038.1	2.484682
7435.8	2.474614
7844.5	2.468792
8242.2	2.460473
8639.8	2.452925

2.6.2 Zig – Zag Leakage Reactance

Another part of the leakage reactance is the zig-zag leakage reactance. The zig-zag leakage flux is the flux between the paths from one stator tooth to the next rotor tooth as shown in Figure 2-11. The value of the zig-zag leakage reactance, $X_{zig-zag}$, in TPCAD is found from (2-40);

$$X_{zig-zag} = \frac{42 \cdot K_x \cdot L_1 \cdot K_{zz} \cdot m}{S_1 \cdot g} \quad (2-40)$$

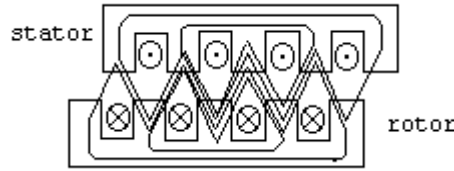


Figure 2-11 Stator and Rotor Zig-Zag Leakage Flux

where K_{zz} is the permeance related to zig-zag leakage reactance found from (2-41) and g is the air gap length entered to TPCAD by the user.

$$K_{zz} = \frac{(t_{10} + t_{20})}{4 \cdot (\lambda_1 + \lambda_2)} \quad (2-41)$$

In (2-41), λ_1 and λ_2 are stator and rotor tooth pitches, t_{10} and t_{20} are stator and rotor tooth faces respectively. These parameters are calculated in (2-42) and (2-43) respectively.

$$\lambda_1 = \frac{\pi \cdot D_1}{S_1}, \quad \lambda_2 = \frac{\pi \cdot D_2}{S_2} \quad (2-42)$$

$$t_{10} = \lambda_1 - w_{10}, \quad t_{20} = \lambda_2 - w_{20} \quad (2-43)$$

In (2-42), D_1 is stator bore diameter, D_2 is rotor outside diameter, w_{10} and w_{20} are stator and rotor slot openings respectively shown in Figure 2-4 and Figure 2-5. All these parameters are user defined parameters and entered to TPCAD by the user.

2.6.3 End Leakage Reactance

End leakage reactance is the reactance due to the flux which is built up around the end connections. (2-44) is used to determine end leakage reactance, X_{end} , in TPCAD;

$$X_{end} = K_x \cdot \left(\frac{62 \cdot D_e \cdot ACT \cdot m}{S_1 \cdot p} \right) \quad (2-44)$$

where, D_e is the diameter of the stator from center of the stator slots and calculated from the dimensions of the slots which is entered by the user, and ACT is the weighted average coil throw of stator windings and entered by the user.

2.6.4 Skew Leakage Reactance

When the rotor or the stator of the motor is skewed, this forms a new differential leakage reactance. This is called as skew leakage reactance, X_{skew} , and calculated from (2-45);

$$X_{skew} = 12.5 \cdot K_m \cdot K_{p1} \cdot Q \cdot m \quad (2-45)$$

where, K_{p1} is the primary flux factor and entered to TPCAD by the user. Q is skew leakage factor found from (2-46) and K_m is a constant found from (2-47).

$$Q = 1 - C_{sk}^2 \quad (2-46)$$

$$K_m = \frac{A_g}{L_g \cdot SF \cdot p} \quad (2-47)$$

In (2-47), A_g is the air gap area per pole and L_g is the effective length of air gap. SF is the saturation factor calculated in section 2.5.1.

2.7 Calculation of Losses

2.7.1 Calculation of Iron Losses

Iron losses in induction motors may be considered to have two components, which are fundamental frequency losses and high frequency losses. Fundamental frequency losses are assumed to be supplied directly by the stator from the line. High frequency losses are assumed to be supplied by mechanical power developed by the rotor. Calculations used in TPCAD are given in Figure E-6.

2.7.1.1 Fundamental Frequency Iron Losses

Fundamental frequency iron losses are assumed to exist only in the stator teeth and the stator core because the frequency in the rotor is too low. At the operating speeds the fundamental frequency losses in the rotor are negligible. Core losses are generally determined from curves based on tests of samples. These curves are entered to TPCAD for different operating frequencies by the user. A sample of these inputs is given in Table 2-6.

Table 2-6 Sample Core Loss Curve

B (T)	P (W/kg) (f : 25 Hz)	P (W/kg) (f : 50 Hz)	P (W/kg) (f : 75 Hz)	P (W/kg) (f : 100 Hz)	P (W/kg) (f : 150 Hz)	P (W/kg) (f : 200 Hz)
0.0	0.000	0.000	0.000	0.000	0.000	0.000
0.2	0.050	0.068	0.187	0.264	0.463	0.661
0.5	0.242	0.551	1.036	1.411	2.646	3.969
1.0	0.770	1.613	2.866	4.189	7.276	11.025
1.5	1.760	4.189	7.270	10.140	17.640	22.271
2.0	3.500	8.000	13.000	17.500	28.500	36.000
2.5	4.500	12.000	18.000	24.500	40.000	50.000

2.7.1.2 High Frequency Losses

Since there is no simple and reliable method for predicting the high frequency losses, the high frequency losses are calculated as ([4]);

$$F_{eloss}(hf) = 19.71 \cdot K_{hi} \cdot B_g^{2.3} \cdot \left(\frac{f}{p}\right)^{1.55} \cdot D_1^{2.05} \cdot \sqrt{S_1} \cdot \left(\frac{w_{10}}{g}\right)^{1.22} \cdot L_1 \quad (2-48)$$

In (2-48), K_{hi} is high frequency loss constant which depends on the material used and entered to TPCAD by the user, B_g is the air gap flux density and calculation of this is given in (2-24). K_{hi} is introduced to give flexibility to calculations and depending on the manufacturing methods and test results of similar motors. Its value can be adjusted to get more accurate calculation of the iron losses.

2.7.2 Friction and Windage Losses

On small induction motors, most of the windage loss is negligible. In this work, the value of the friction and windage loss at full speed is entered to TPCAD by the user. Windage loss is found from (2-49);

$$K_f = \frac{\text{Windage Loss At Full Load}}{n_{full\ load}^3} \quad (2-49)$$

The windage loss, $P_{windage}$, at any value of speed, n , then is found as given in (2-50);

$$P_{windage} = n^3 K_f \quad (2-50)$$

2.8 Performance Calculations

After the calculation of the machine parameters, user can calculate the performance of the motor. For the performance calculations, the equivalent circuit model shown in Figure 2-1 is used in TPCAD. Algorithms developed and implemented in TPCAD to determine the performance of the motor are described in the following sub sections.

2.8.1 Calculation of Current

Full load current is the current drawn by the motor when it is delivering its rated output power. To calculate the current of the motor, the equivalent impedance, Z_{th} , of the circuit of the machine (Figure 2-1) is used. Stator current of the motor, I_1 , is calculated from (2-51);

$$I_1 = \frac{V}{|Z_{th}|} \quad (2-51)$$

As seen from the equation, its value highly depends on the values of reactances. Calculations of reactances are given in section 2.6. To calculate the reactance of the rotor, rotor bar current has to be found. (Calculation of the bar current was given in (2-6)) This problem can be solved by an iterative method. The flowchart of the calculation is shown in APPENDIX E Figure E-4.

To calculate secondary current and slot leakage, first of all an estimation is made for the primary current. Using this primary current, secondary current and leakage reactances are calculated. Then, primary current is recalculated using the found values. After that primary current is compared with the old one. If the error between old and new values of the primary current is less than 0.005 Ampere, the iteration is stopped; else this iteration is repeated until the error is in acceptable range.

2.8.2 Calculation of Torque

Full load torque is the torque required to produce the rated power at the full-load speed of the motor. Rotor current, rotor resistance and synchronous speed, all depend on the torque on the shaft of the motor. Using the equivalent circuit of the motor, full load torque can be calculated from (2-52);

$$T = \frac{m \cdot i_2'^2 \cdot r_2'}{\omega_s \cdot s} = \frac{m \cdot i_2'^2 \cdot r_2'}{(n_s \cdot \frac{2\pi}{60}) \cdot s} \quad (2-52)$$

In (2-52), n_s is the synchronous speed of the motor and this value is entered to TPCAD by the user. s is the slip and calculated from (2-53) where n is the rotor speed and entered by the user.

$$s = \frac{n_s - n}{n_s} \quad (2-53)$$

2.8.3 Calculation of Output Power

Output power of an induction motor is the power dissipated on the resistance $\frac{r_2' (1-s)}{s}$ shown in Figure 2-1. Total net output power is calculated by subtracting the friction and windage losses from the power converted to mechanical form on the rotor resistance in (2-54);

$$P_{out} = m \cdot i_2'^2 \cdot r_2' \cdot \frac{(1-s)}{s} - P_{friction} - P_{windage} \quad (2-54)$$

Friction and windage losses are calculated as explained in section 2.7.2.

2.8.4 Calculation of Efficiency

In order to calculate the efficiency the following data are required; input power, total copper loss and iron loss. Stator and rotor copper losses can be found from (2-55) and (2-56) respectively;

$$P_{Stator\ Cu\ Losses} = m \cdot i_1^2 \cdot r_1 \quad (2-55)$$

$$P_{Rotor\ Cu\ Losses} = m \cdot i_2'^2 \cdot r_2' \quad (2-56)$$

Total iron loss calculation is explained in Section 2.7. The input power is found from (2-57);

$$P_{in} = P_{out} + P_{friction} + P_{windage} + P_{Stator\ Cu\ Losses} + P_{Rotor\ Cu\ Losses} + P_{Core\ Losses} \quad (2-57)$$

Then, the efficiency is calculated easily from (2-58);

$$\eta = \frac{P_{out}}{P_{in}} \quad (2-58)$$

2.8.5 Calculation of Power Factor

Using the equivalent circuit of the machine (Figure 2-1), the ratio of the equivalent circuit resistance to impedance gives the power factor of the machine as shown in (2-59);

$$PF = \frac{R_{th}}{|Z_{th}|} \quad (2-59)$$

2.8.6 Pull-Out Torque

Pull-out torque is the maximum torque available on the motor shaft that the motor can develop without stalling. For every slip value from 0 to 1 with 0.01 intervals, the torque of the motor is calculated. From the calculated torque values, the maximum torque is determined as pull-out torque. The flowchart of the calculation is shown in Figure 2-12. In the calculation, 0.999 is taken as the maximum slip value, since taking it as 1 will create problems in the calculations due to denominator becoming 0.

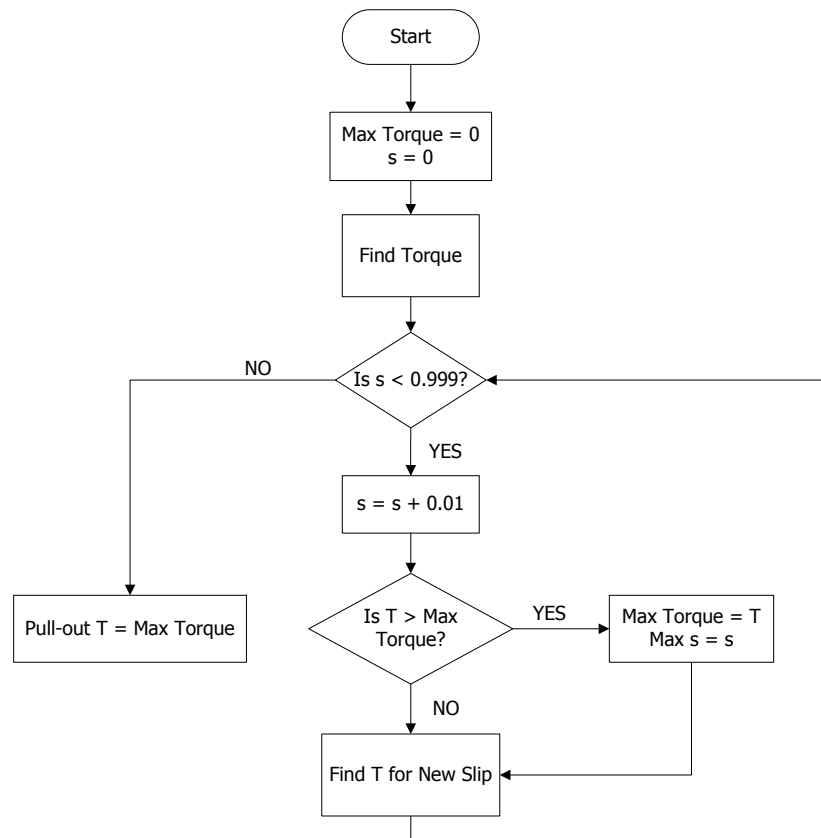


Figure 2-12 Flowchart of Pull-Out Torque Calculation

2.9 Double Cage Motor Calculations

In the previous sections, calculations of machine parameters for single cage motors are explained. However, to get high starting torque with a low starting current, double cage motors are preferred. To analyse this type of motors, a feature is added to TPCAD. The purpose of this part is to present an equivalent circuit for the double cage motor together with its describing equations and then to indicate how the parameters of this circuit may be found.

Double cage rotor contains two separate conductors, one above the other, located in the same slot. The two bars are placed in the same slot with thin

neck as shown in Figure 2-13. The slot close to the air gap will be called as upper cage shown as 3, and the other one will be lower cage shown as 4. These numbers will be used to represent upper and lower cage respectively to obtain equivalent circuit parameters in the following sections.

Behavior of the cages is different while the motor is in starting condition. When the rotor slip frequency is high, the current in the rotor bar is forced to flow primarily in the upper cage. When the motor is accelerated near its rated speed, the frequency of the rotor slip becomes low, so the lower cage defines the characteristics of the rotor circuit. ([5])

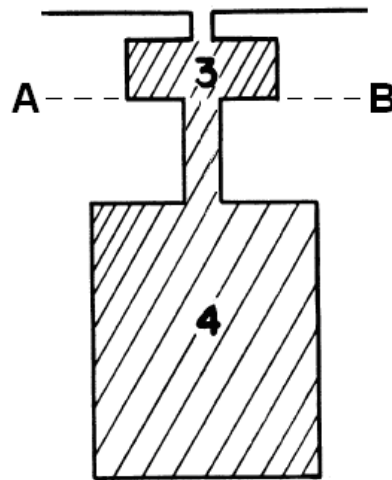


Figure 2-13 Double Cage Rotor Slot

The upper cage is small and has a high value of resistance when compared with lower cage. On the other hand, the lower cage is described as high reactance winding compared to upper cage. So, this type of rotor shows a high starting torque with a low starting current.

2.9.1 Derivation of Equivalent Circuit

Since there are two different cages in the rotor structure, the given equivalent circuit in section 2.2 cannot be used for double cage motors. For that reason it has to be modified. In the following part, the derivation of the equivalent circuit model for double cage motors is explained.

TPCAD uses the per phase equivalent circuit of a double cage induction motor given in Figure 2-14, to calculate the performance of the motor. Since there is a mutual reactance between upper and lower cage, the complex branch of the rotor circuit (as shown 1 and 2 in Figure 2-14) is replaced by the rotor circuit given in Figure 2-15. ([5])

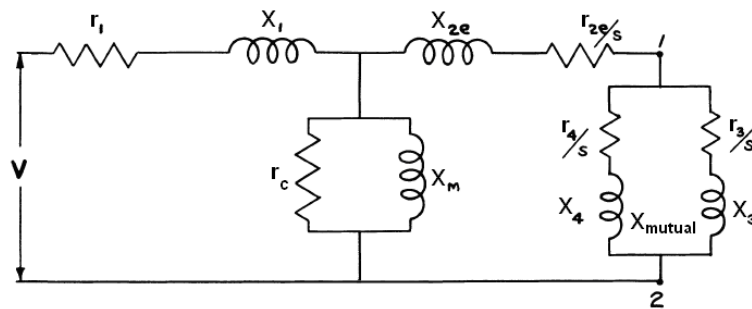


Figure 2-14 Equivalent Circuit of Double Cage Motor

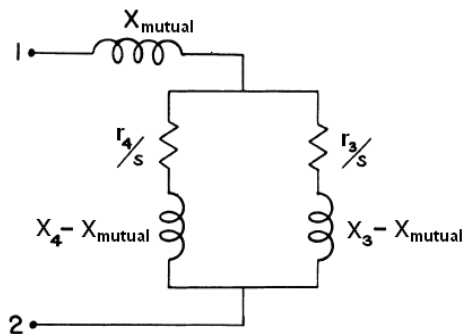


Figure 2-15 Exact Equivalent Circuit of Rotor Bars

However, in the usual double cage design, the value of $X_3 - X_{mutual}$ is nearly equal to zero. For that reason $X_3 - X_{mutual}$ can be assumed to be zero. ([5])

According to this assumption, the complex branch of the rotor circuit becomes the rotor circuit given in Figure 2-16.

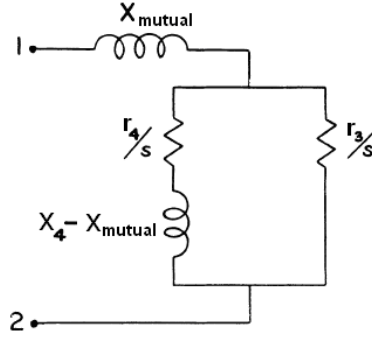


Figure 2-16 Approximate Equivalent Circuit of Rotor Bars

Using the equivalent circuit in Figure 2-16, the thevenin equivalent of points 1 and 2 is calculated as;

$$r_{12} = \frac{r_3 r_4 (r_3 + r_4) + r_3 (X_4 - X_{mutual})^2 s^2}{(r_3 + r_4)^2 + (X_4 - X_{mutual})^2 s^2} \quad (2-60)$$

$$X_{12} = \frac{r_3^2 (X_4 - X_{mutual})}{(r_3 + r_4)^2 + (X_4 - X_{mutual})^2 s^2} \quad (2-61)$$

where, r_3 and r_4 are the resistance values of the upper and lower cage respectively. X_4 is the leakage reactance value of the lower cage. X_{mutual} is the mutual reactance between upper and lower cage. Calculations used in TPCAD are given in Figure E-6.

2.9.2 Calculation of Resistances

In the previous section the equivalent circuit model of the double cage motors is described. According to this equivalent circuit, the only change is on the rotor side. Upper and lower cage resistances and end ring resistances are separated when we compare with the single cage rotor resistance described in section 2.4. In the following two sub-sections, the resistance calculation of upper and lower cage and end ring will be described.

2.9.2.1 Calculation of Upper and Lower Cage Resistances

To calculate upper and lower cage resistances, the equations defined in section 2.4 is used. However, according to the equivalent circuit given in Figure 2-14, end ring resistance is separated from upper and lower cage resistances. Taking out the end ring resistance calculation from (2-10), the equation given in (2-62) is used to calculate upper and lower cage resistances respectively. Parameters used in (2-62) are defined in section 2.4.

$$r_i = (C \cdot K_{wm})^2 \cdot \left(\frac{L_b \cdot \rho_b}{S_2 \cdot A_{b_i}} \right) \cdot m \quad (2-62)$$

2.9.2.2 Calculation of End Ring Resistance

End ring resistance, r_{2e} , is excluded from the equation (2-10) to calculate rotor cage resistance as mentioned before. For that reason end ring resistance is calculated from (2-63). Parameters used in equation (2-63) are defined in section 2.4.

$$r_{2e} = (C \cdot K_{wm})^2 \cdot \left(\frac{2 \cdot D_r \cdot \rho_r}{\pi \cdot p^2 \cdot A_r} \right) \cdot m \quad (2-63)$$

2.9.3 Calculation of Leakage Reactances

As mentioned in the previous section, the only change at the equivalent circuit of the motor is on the rotor side. Lower cage leakage and end ring leakage reactances are separated when we compare with the single cage rotor leakage reactances described in section 2.6. In the following two sub-sections, the leakage reactance calculation of lower cage and end ring will be described.

2.9.3.1 Calculation of Lower Cage Leakage Reactances

To calculate lower cage leakage reactance, the equations defined in section 2.6 can be used. However, according to the equivalent circuit given in Figure 2-14, end leakage reactance is separated from lower cage leakage reactance. Taking out the end leakage reactance from (2-30), the equation given in (2-64) is used to calculate lower cage leakage reactances. Parameters used to calculate leakage reactance in (2-64) are defined in section 2.6.

$$X_4 = K_x (X_{slot} + X_{skew} + Z_{zig-zag}) \quad (2-64)$$

2.9.3.2 Calculation of End Leakage Reactance

End leakage reactance is excluded from (2-30) to calculate rotor cage leakage reactance as mentioned before. For that reason end ring leakage reactance is calculated from (2-65). Parameters used in equation (2-65) are defined in section 2.6.

$$X_{2e} = K_x (X_{end}) \quad (2-65)$$

2.9.4 Calculation of Mutual Reactance

Since two currents path exist in the rotor circuit, these currents interacts each other because of the current change in coupled reactance. Because of this effect, a mutual reactance exists in the equivalent circuit and the value of this reactance is calculated from (2-66).

$$X_{mutual} = K_x \cdot P_{mutual} \quad (2-66)$$

In (2-66), K_x is the reactance constant and found from (2-16), P_{mutual} is a constant and determination of this constant is found using (2-67);

$$P_{mutual} = \frac{125.5 \cdot L_1 \cdot \left(\frac{\pi}{4} + \frac{d_{20}}{w_{20}} \right) \cdot m}{S_2} \quad (2-67)$$

In (2-67), L_1 is the stator stack length, m is number of phases and S_2 is the number of rotor bars. d_{20} and w_{20} are the mouth depth and slot opening of upper cage respectively.

2.9.5 Modifications in Program Structure

Double cage rotor contains two bars called upper and lower cage as given in the previous sections. In the program structure these two cages are entered to TPCAD with two separate rotor slots. Upper cage is the upper part of the A-B point and lower cage is the lower part of the A-B point as shown in Figure 2-13. There is no difference to enter slot dimensions and types. The only difference is, selecting and entering two slot data instead of one. Calculations are made according to these data entered by the user.

While doing performance calculations for double cage, magnetic circuit calculations are rearranged for upper and lower rotor cages. Flux densities for the rotor teeth are calculated from (2-68) and (2-69). Parameters used to calculate these flux densities are explained in section 2.5.1.

$$B_{rt_upper} = \frac{\phi \cdot K_{p1}}{0.637 \cdot A_{rt_upper}} \quad (2-68)$$

$$B_{rt_lower} = \frac{\phi \cdot K_{p1}}{0.637 \cdot A_{rt_lower}} \quad (2-69)$$

Since rotor teeth magnetic circuit composed of two components, saturation factor is also recalculated due to these modifications as given in (2-70).

$$SF = \frac{(AT_{sc} + AT_{st} + AT_{rc} + AT_{rt_upper} + AT_{rt_lower} + AT_g)}{AT_g} \quad (2-70)$$

AT_{rt_upper} and AT_{rt_lower} are the mmf drops on the rotor teeth upper and lower cage respectively. Calculations to determine these parameters are explained in section 2.5.1.

CHAPTER 3

OTHER FEATURES OF TPCAD

3.1 Introduction

TPCAD has other useful features which are;

- Parameter calculation from tests
- Analyze a motor using parameters
- Electrical power measurement with loss segregation

These features provide useful tools to the user as discussed below. Details of these tools are also described below. Note that in the calculations the procedures recommended by IEEE Standard 112 are adopted. ([6])

3.2 Parameter Calculation From Tests

User often wishes to determine the performance of the machine. To get the performance of the machine without actual load test, user needs the parameters of that machine so that the equivalent circuit of the machine can be used to predict the motor performance. The most common way to

determine the parameters of the machine is to test the machine under locked rotor and no load conditions. A tool is added to TPCAD to determine the machine parameters from locked rotor and no load test results. By using that tool, user can get the machine parameters from the test data, or the data can be exported to “Analyze a Motor Using Parameters” option to get the performance of the machine. User interface of that tool is described in 5.7.1.

In the following sub sections, the equations used in TPCAD to obtain the machine parameters from locked rotor and no load tests are mentioned.

3.2.1 Locked Rotor Test

The locked rotor test gives information about leakage impedances, X_1 and X_2 , and rotor resistance r_2 . The rotor of the machine is blocked and voltage is applied to stator terminals to circulate rated current. Current, voltage and power are measured at that point. ([6]) Since there is no rotation, slip is equal to 1 which gives the equivalent circuit shown in Figure 3-1.

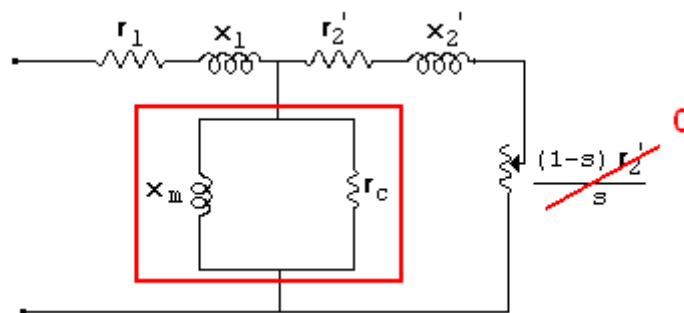


Figure 3-1 Equivalent Circuit for Locked Rotor Test

Since the slip of the machine is equal to 1, speed dependent equivalent resistance, $\frac{(1-s)r_2'}{s}$, goes to zero. Therefore, the resistance of the rotor branch becomes very small and the current on that branch is larger than the current on the magnetizing circuit. So the magnetizing branch can be neglected while evaluating the equivalent circuit of the machine.

The ratio of the locked rotor test voltage and current gives the locked rotor impedance in (3-1);

$$Z_{locked} = \frac{V_{locked}}{I_{locked}} \quad (3-1)$$

The locked rotor resistance, r_{locked} , is found from the locked rotor input power, P_{locked} , in (3-2);

$$r_{locked} = \frac{P_{locked}}{3I_{locked}^2} \quad (3-2)$$

The rotor winding resistance, r_2' , is determined from (3-3);

$$r_2' = r_{locked} - r_1 \quad (3-3)$$

Locked rotor reactance, X_{locked} , is found from (3-4);

$$X_{locked} = \sqrt{Z_{locked}^2 - r_{locked}^2} \quad (3-4)$$

Since stator and rotor leakage reactances are assumed to be equal, these reactances are equal to half of the locked rotor reactance shown in (3-5).

$$X_1 = X_2 = \frac{X_{locked}}{2} \quad (3-5)$$

It is not possible to make an additional test to determine X_1 and X_2 separately. The standard recommends an empirical distribution for these leakage reactances as shown in Table 3-1. ([6]) There is an option in that tool to select the class of the motor and make the calculations according to this selection.

Table 3-1 Empirical Distribution of Leakage Reactances

Motor Class	Description	Fraction of X_1+X_2	
		X_1	X_2
Class A	Normal starting torque, normal starting current	0.5	0.5
Class B	Normal starting torque, low starting current	0.4	0.6
Class C	High starting torque, low starting current	0.3	0.7
Class D	High starting torque, high slip	0.5	0.5
Wound Rotor	Performance varies with rotor resistance	0.5	0.5

3.2.2 No Load Test

The no load test gives information about exciting current and rotational losses. The test is performed by applying rated voltage to the stator terminals at the rated frequency without any load on the rotor. Current, voltage and power are measured at that point. ([6]) The measured power is due to core, friction and windage losses. The equivalent circuit for no load test is shown in Figure 3-2.

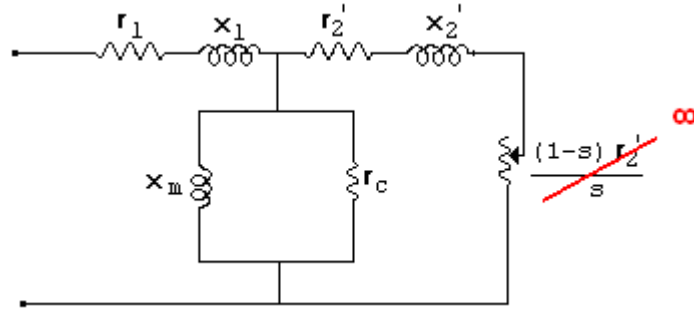


Figure 3-2 Equivalent Circuit for No Load Test

Machine rotates at almost synchronous speed which means slip is nearly equal to zero. The value of the equivalent resistance $\frac{(1-s)r_2'}{s}$ becomes very high. For that reason, no load current is small and the magnetizing branch can be neglected while evaluating the equivalent circuit of the machine.

To find the coreloss resistance, the power on the magnetizing branch is calculated. The power on that branch is found from (3-6);

$$P_{core} = P_{noload} - (P_{cu-stator} + P_{friction} + P_{windage}) \quad (3-6)$$

Stator copper loss, $P_{cu-stator}$, is found from (3-7),

$$P_{cu-stator} = 3 \cdot I_{noload}^2 \cdot r_1 \quad (3-7)$$

Coreloss resistance is found from (3-8),

$$r_c = \frac{3 \cdot V_{noload}^2}{P_{core}} \quad (3-8)$$

To find the magnetizing reactance, the reactive power on the magnetizing branch is calculated. (3-9)

$$Q_{noload} = \sqrt{S_{noload}^2 - P_{noload}^2} \quad (3-9)$$

Apparent power of no load test, S_{noload} , is found from (3-10);

$$S_{noload} = 3 \cdot V_{noload} \cdot I_{noload} \quad (3-10)$$

Magnetizing reactance, X_m , is determined from (3-11);

$$X_m = \frac{Q_{noload}}{3 \cdot I_{noload}} - X_1 \quad (3-11)$$

3.3 Analyze A Motor Using Parameters

It is mentioned that, user wants to get the performance of the machine. To get the performance of that machine, user needs the parameters of that machine. In the previous section, the calculation method to get the machine parameters from locked rotor and no load tests is explained. Alternately, the parameters may be calculated from the motor data. In any case a software tool is needed to calculate the motor performance using the equivalent circuit.

Performance calculation from the equivalent circuit can be tedious process. Also, calculations have to be repeated for any speed value. To ease that matter, a tool is added to TPCAD. Using that tool, user can enter the machine parameters or import these from the result of the calculated equivalent circuit parameters from locked rotor and no load tests. After entering parameters to the TPCAD, user can get the performance of the machine at any value of the rotor speed. User interface of that tool is described in 5.7.2. In the following part, the equations used in TPCAD to obtain the machine performance from parameters are mentioned. The outputs of that calculation are; output power, output torque, full load current,

no load current, efficiency, power factor, coreloss, stator and rotor copper loss.

To evaluate the performance of the machine, the model given in Figure 2-1 is used. Using that model, the currents on each branch are calculated respectively. Using these values, stator and rotor copper losses of the machine, $P_{cu-stator}$ and $P_{cu-rotor}$, is found from (2-55) and (2-56) respectively.

From the equivalent circuit of the machine shown in Figure 2-1, the total power transferred across the air gap from stator, P_{gap} , is calculated from (3-12);

$$P_{gap} = m \cdot I_2^2 \cdot \frac{r_2}{s} \quad (3-12)$$

Net output power taken on the shaft of the motor is calculated from (3-13);

$$P_{gap-net} = P_{gap} - P_{cu-rotor} - P_{friction} - P_{windage} - P_{stray} \quad (3-13)$$

Input power of the equivalent circuit is found from (3-14);

$$P_{in} = P_{gap} + P_{cu-stator} + P_{coreloss} \quad (3-14)$$

The electromechanical torque, T_{mech} , corresponding to the power P_{gap} , is obtained from (3-15);

$$T_{mech} = \frac{P_{gap}}{\omega_s} = \frac{m \cdot I_2^2 \cdot \frac{r_2}{s}}{\omega_s} \quad (3-15)$$

The efficiency of the test motor is calculated as the ratio of net output power taken on the shaft to the stator input power. Thus, efficiency is found from (3-16);

$$\eta = \frac{P_{out}}{P_{in}} = \frac{P_{gap-net}}{P_{in}} \quad (3-16)$$

Power factor of the machine is found from (3-17);

$$PF = \frac{\text{Re}(Z_{th})}{|Z_{th}|} \quad (3-17)$$

3.4 Electrical Power Measurement With Loss Segregation

In the previous two sections, calculation of machine parameters from locked rotor and no load tests, and calculation of performance from machine parameters are explained.

Often, users may not have an access to a proper test set up to measure the shaft torque and power output of a machine under a certain load. However, measurement of terminal voltage and input power is often possible. Also, the speed of the motor is relatively easy to measure. For that reason, a tool is added to TPCAD to obtain the machine performance only from no load test and load test measuring only motor terminal voltage, current, input power and motor speed. User interface of that tool is described in 5.7.3. In the following part, the equations used in TPCAD to obtain the machine performance from no load and load test data are mentioned. Calculations are made according to Method E1 of IEEE Standard 112. ([6]) The outputs of that calculation are; output power, output torque, efficiency, coreloss, stator and rotor copper loss.

Load test voltage, current, $\cos\phi$, rotor and synchronous speed, friction and windage losses and stray load percentage has to be entered to TPCAD by the user, hence no load test measurements and stator resistance.

In the standard, it is mentioned that, if the stray-load loss is not measured, the values shown in Table 3-2 can be used to find the stray-load loss according to the machine rating.

Table 3-2 Assumed Values for Stray-Load Loss

Machine Rating	Stray-Load Loss Percent of Rated Output
1 - 125 hp	1.8 %
126 - 500 hp	1.5 %
501 - 2499 hp	1.2 %
2500 hp and greater	0.9 %

Input power of the machine is found from (3-18);

$$P_{in} = 3 \cdot V_{test} \cdot I_{test} \cdot \cos \phi \quad (3-18)$$

(2-55) is used to find total stator copper loss $P_{cu-stator}$. Total power transferred across the air gap from stator is determined from (3-19);

$$P_{gap} = P_{in} - P_{cu-stator} - P_{core} \quad (3-19)$$

In (3-19), P_{core} is already determined from no load test in (3-6).

Total rotor copper loss, $P_{cu-rotor}$, is found from (3-20);

$$P_{cu-rotor} = P_{gap} \cdot s \quad (3-20)$$

Net output power of the machine, $P_{gap-net}$, is determined by subtracting the total losses from the input measurement in (3-21). Stator and rotor copper losses, core loss, stray loss and friction and windage loss form the total losses.

$$P_{gap-net} = P_{gap} - P_{cu-rotor} - P_{friction} - P_{windage} - P_{stray} \quad (3-21)$$

Net output torque, T_{net} , corresponding to net output power is obtained from (3-22);

$$T_{net} = \frac{P_{gap-net}}{\omega_r} \quad (3-22)$$

The efficiency of the induction motor is defined as in (3-23);

$$\eta = \frac{P_{out}}{P_{in}} = \frac{P_{gap-net}}{P_{in}} \quad (3-23)$$

CHAPTER 4

SINGLE PHASE INDUCTION MOTOR PARAMETER AND PERFORMANCE CALCULATIONS

4.1 Introduction

In this chapter, a software developed earlier for single phase induction motor design called SPCAD is improved. SPCAD is a design tool to analyze capacitor start or capacitor run type single phase induction motors. The original software is developed by Aftahi to operate in Dos. ([2])

The calculations given in the following sections are made for the capacitor type motors which are capacitor start and capacitor run type. In this section, the approach used is based on the Veinott's work. ([3])

4.2 Calculation of Machine Parameters

To calculate the performance of a motor, one needs the equivalent circuit of the motor. For design purposes, the equivalent circuit parameters need to be calculated from the dimensions of the motor and material properties. To obtain a correct model it is important to calculate the parameters accurately

and use them to calculate machine performance at any value of the slip. To meet these needs, SPCAD has a feature to calculate motor parameters from the entered motor data and the motor performance. User defined parameters entered to SPCAD for calculations are given in APPENDIX B. Units of these parameters are also given in APPENDIX B.

Capacitor type single phase induction motors have two modes of operation, which are starting and running conditions. Figure 4-1 represents a capacitor start single phase induction motor. ([3]) Starting switch is a centrifugally operated switch which takes the auxiliary winding and capacitor out of the circuit when the motor comes up to speed which is called “Switching Speed”.

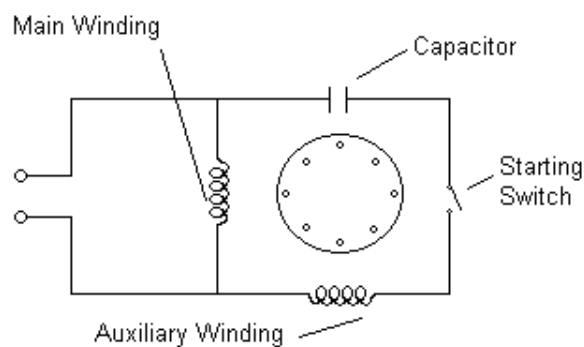


Figure 4-1 Schematic Representation of Capacitor Start Motor

SPCAD uses the per phase equivalent circuit of a single phase induction motor shown in Figure 4-2 and Figure 4-4, to calculate the performance of the motor.

In the following sections, methods used in the developed software for the calculation of parameters and performance of a given induction motor will be described.

4.3 Calculation of Main and Auxiliary Winding Resistances

The stator winding resistance in the equivalent circuit can be found from the same equations used for three phase motors. Therefore, the resistances of the main winding, r_1 , and the auxiliary winding, r_{1a} , are found using equation (2-1).

4.4 Calculation of Rotor Resistance

The rotor resistance of the equivalent circuit can be found from the bar cross section, core length, end ring dimensions and the cage materials. Since rotor cage of the single phase induction motor is similar with the three phase motors, the calculations described in section 2.4 are used in SPCAD to calculate the rotor resistance.

Calculations of equivalent circuit resistances are given in the previous sections. SPCAD can calculate performance of the motor for any given operating temperature value using these values. However, to calculate the performance of the motor for a given operating temperature, the calculated resistances have to be corrected. For that reason, to find the values at any operating temperature value, t_{main} , (2-12) is used. Operating temperature is entered to the program as final temperature by the user.

4.5 Calculation of Magnetizing Reactance

Magnetizing reactance is the ratio of the voltage induced by the fundamental component of flux to magnetizing current required to set up the flux. Calculation of magnetizing reactance is explained in section 2.5. Instead of using (2-15); (4-1) is used to calculate magnetizing reactance. This difference is coming from taking the number of phases, m , as 2 for the

single phase induction motors. ([3]) Variables used in the equation are explained in section 2.5.

$$X_m = K_x \cdot C_{sk} \cdot \frac{25 \cdot A_g}{L_g \cdot SF \cdot p} \quad (4-1)$$

4.6 Calculation of Leakage Reactance

Leakage reactance is the reactance due to the leakage flux. This value depends on the operating conditions of the motor. Main cause of this variation is the magnetic saturation of the leakage flux paths. Saturation increases with increasing current and decreases the leakage reactance. Here, leakage reactances are taken as independent of saturation except when the rotor side has closed slots. To calculate the correct value of the reactances, they must be computed at any slip. The components of the leakage reactance are; Slot leakage (stator and rotor) reactance, Zig-zag leakage reactance, End leakage reactance and Skew leakage reactance. The flowchart given in Figure F-8 explains how these calculations are done in the software.

Detailed information about methods to calculate these reactances are described in section 2.6. In the following sub sections, differences that exist in the equations are explained.

4.6.1 Slot Leakage Reactance

Determination of the slot leakage reactance is explained in section 2.6.1. The only difference in the calculations is, instead of using (2-29); (4-2) is used to calculate slot leakage reactance. This difference is coming from taking the number of phases, m , as 2 for the single phase induction motors. ([3])

$$X_{slot} = K_x \cdot 251 \cdot L_1 \cdot \frac{K_s}{S_1} \cdot \quad (4-2)$$

4.6.2 Zig – Zag Leakage Reactance

The zig-zag leakage flux is the flux between the paths from one stator tooth to the next rotor tooth as shown in Figure 2-11. The value of the zig-zag leakage reactance, $X_{zig-zag}$, in SPCAD is found from (4-3);

$$X_{zig-zag} = \frac{84 \cdot K_x \cdot L_1 \cdot K_{zz}}{S_1 \cdot g} \quad (4-3)$$

Using the number of phases, m , as 2, (2-40) becomes (4-3) to calculate the zig-zag leakage reactance for single phase induction motors. ([3]) Variables used in the equation are explained in section 2.6.2.

4.6.3 End Leakage Reactance

End leakage reactance is the reactance due to the flux which is built up around the end connections as mentioned in section 2.6.3. (4-4) is used to determine end leakage reactance, X_{end} , in SPCAD by using the number of phases, m , as 2, in (2-44). ([3]) Variables used in the equation are explained in section 2.6.3.

$$X_{end} = K_x \cdot \left(\frac{124 \cdot D_e \cdot ACT}{S_1 \cdot p} \right) \quad (4-4)$$

4.6.4 Skew Leakage Reactance

When the rotor or the stator of the motor is skewed, this forms a new differential leakage reactance which is called as skew leakage reactance,

X_{skew} , and is calculated from (4-5) by using the the number of phases, m , as 2, in (2-45). ([3])

$$X_{skew} = 25 \cdot K_m \cdot K_{p1} \cdot Q \quad (4-5)$$

4.7 Calculation of Losses

4.7.1 Calculation of Iron Losses

Iron losses in induction motors may be considered to have two components, which are fundamental frequency losses and high frequency losses. Fundamental frequency losses are assumed to be supplied directly by the stator from the line. High frequency losses are assumed to be supplied by mechanical power developed by the rotor. Calculations used in SPCAD are given in Figure F-8.

4.7.1.1 Fundamental Frequency Iron Losses

Fundamental frequency iron losses are assumed to exist only in the stator teeth and the stator core because the frequency in the rotor is too low. At the operating speeds the fundamental frequency losses in the rotor are negligible. Core losses are generally determined from curves based on tests of samples. These curves are entered to SPCAD by the user. A sample of these inputs is given in Table 4-1.

Table 4-1 Sample Core Loss Curve

B (T)	P (W/kg)
0.00	0.00
0.20	0.12
0.40	0.56
0.60	0.88
0.80	1.56
0.95	2.00
1.00	2.12
1.20	3.00
1.36	4.00
1.50	5.00
1.60	5.88
1.74	7.00
1.88	8.00

4.7.1.2 High Frequency Losses

Determination of high frequency losses is explained in section 2.7.1.2.

4.7.2 Friction and Windage Losses

Determination of friction and windage losses is explained in section 2.7.2.

4.8 Performance Calculations

After the calculation of the machine parameters, user can calculate the performance of the motor. For the performance calculations, the equivalent circuit models shown in Figure 4-2 and Figure 4-4 are used in SPCAD. Algorithms developed and implemented in SPCAD to determine the performance of the motor are described in the following sub sections.

4.8.1 Calculation of Full Load Performance

This section mentions about performance calculations of the single phase induction motor at full load condition when only the main winding is energized. To calculate the performance, equivalent circuit of the machine shown in Figure 4-2 is used. However, to simplify the calculations the equivalent circuit shown in Figure 4-3 is used.

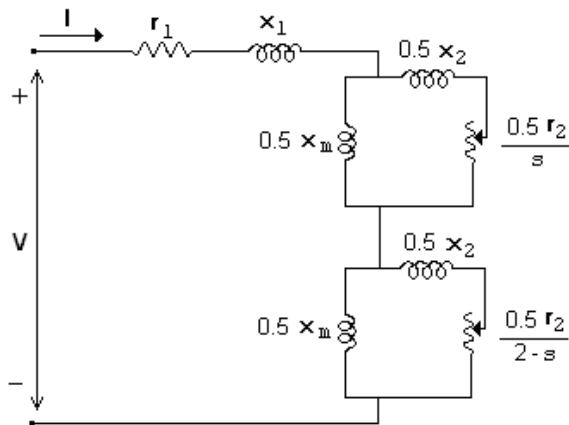


Figure 4-2 Equivalent Circuit of Single Phase Motor with Main Winding

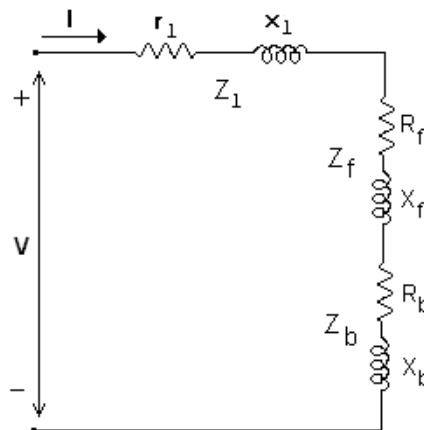


Figure 4-3 Simplified Equivalent Circuit Model of Main Winding

According to the Figure 4-3, R_f and R_b are the apparent resistance of forward and backward field respectively and X_f and X_b are the apparent reactance of forward and backward field respectively. Calculations used to find these parameters, the following equations are used in SPCAD.

$$R_f = \frac{0,5 \cdot K_r \cdot \frac{r_2}{s}}{\left[\left(\frac{r_2}{X_0} \right) / s \right]^2 + 1} \quad (4-6)$$

$$X_f = \frac{0,5 \cdot X_0 \cdot K_p \cdot \left[\left(\frac{r_2}{X_0} \right) / s \right]^2 + 0,5 \cdot K_p \cdot X_1}{\left[\left(\frac{r_2}{X_0} \right) / s \right]^2 + 1} \quad (4-7)$$

$$R_b = \frac{0,5 \cdot K_r \cdot \frac{r_2}{2-s}}{\left[\left(\frac{r_2}{X_0} \right) / (2-s) \right]^2 + 1} \quad (4-8)$$

$$X_b = \frac{0,5 \cdot X_0 \cdot K_p \cdot \left[\left(\frac{r_2}{X_0} \right) / (2-s) \right]^2 + 0,5 \cdot K_p \cdot X_1}{\left[\left(\frac{r_2}{X_0} \right) / (2-s) \right]^2 + 1} \quad (4-9)$$

Open circuit reactance of the main winding, X_0 , is found from (4-10);

$$X_0 = X_m + X_1 \quad (4-10)$$

In (4-7) and (4-9), a constant, K_p , is used to find forward and backward reactances. This value is found from (4-11);

$$K_p = \frac{X_m}{X_m + X_1} \quad (4-11)$$

In (4-6) and (4-8), a constant, K_r , is used to find forward and backward resistances. This value is found from (4-12);

$$K_r = K_p^2 \quad (4-12)$$

Total apparent resistance of the main winding is found from (4-13);

$$R_T = R_f + R_b + r_{1(hot)} \quad (4-13)$$

where, $r_{1(hot)}$ is the value of the primary resistance at operating temperature and is found from (2-12).

Total apparent reactance of the main winding is found from (4-14);

$$X_T = X_f + X_b + X_1 \quad (4-14)$$

Using (4-13) and (4-14), total impedance of the main winding is found from (4-15);

$$Z_T = \sqrt{R_T^2 + X_T^2} \quad (4-15)$$

The main winding current of the equivalent circuit shown in Figure 4-3, is found from (4-16);

$$I = \frac{V}{Z_T} \quad (4-16)$$

Input power of the equivalent circuit is found from the summation of the total power dissipated in the resistances and fundamental frequency loss, as given in (4-17);

$$P_{in} = I^2 \cdot r_{1(hot)} + I^2 \cdot (R_f + R_b) + Feloss(ff) \quad (4-17)$$

$F_{eloss}(ff)$ is the fundamental frequency loss of the motor and the calculation of that value is given in section 4.7.1.1.

Output power of the motor is found from the subtraction of the friction, windage and high frequency iron loss from power transferred to rotor as shown in (4-18);

$$P_{out} = I^2 \cdot (R_f - R_b) \cdot (1-s) - (F_{eloss}(hf) + friction + windage) \quad (4-18)$$

In (4-18), $F_{eloss}(hf)$ is the high frequency iron loss. (4.7.1) Friction and windage losses are determined in section 4.7.2.

Efficiency of the motor is found from the ratio of the output power to the input power as given in (4-19).

$$\eta = \frac{P_{out}}{P_{in}} \quad (4-19)$$

Power factor of the machine is found from the ratio of the input power to the apparent power.

$$PF = \frac{P_{in}}{V \cdot I} \quad (4-20)$$

Output torque of the machine at any speed value is found from (4-21);

$$T = \frac{60 \cdot P_{out}}{2 \cdot \pi \cdot n} \quad (4-21)$$

The flowchart given in Figure F-6 explains how these calculations are done in the software.

4.8.2 Combined Winding Performance

Capacitor type induction motors use an auxiliary winding to bring the motor up to speed. Most commercial capacitor type induction motors use windings which are quadrature in space with each other. Main winding of the motor sets up a magnetic field which is stationary in space but pulsating with respect to time. When the auxiliary winding is in the circuit, there are two single phase windings on the stator. These two windings set up forward and backward field which makes four revolving components. Figure 4-4 shows the equivalent circuit of the main and auxiliary winding with respective impedances and voltages. ([3])

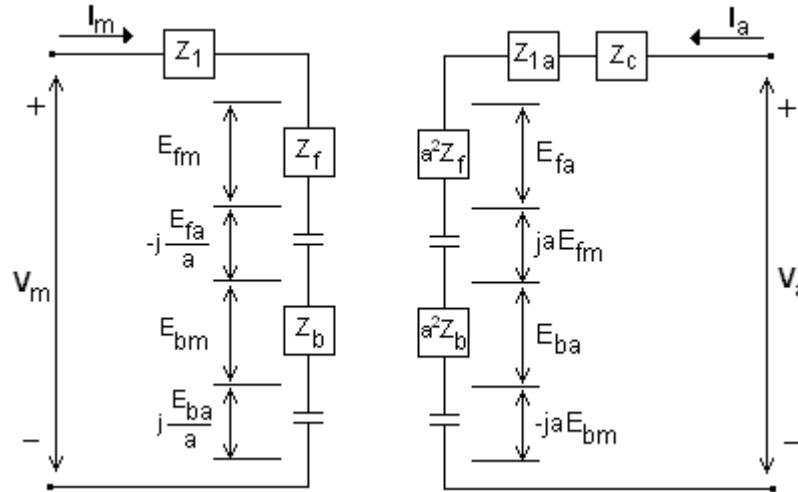


Figure 4-4 Main and Auxiliary Winding Equivalent Circuit

Voltages induced in the main winding by the two components of revolving fields are calculated from (4-22) and (4-23);

$$E_{fm} = I_m \cdot Z_f \quad (4-22)$$

$$E_{bm} = I_m \cdot Z_b \quad (4-23)$$

The field components set up by auxiliary winding, is calculated from (4-24) and (4-25);

$$E_{fa} = I_a \cdot a^2 \cdot Z_f \quad (4-24)$$

$$E_{ba} = I_a \cdot a^2 \cdot Z_b \quad (4-25)$$

where a is the ratio of effective turns in auxiliary winding to effective turns in main winding. That component is calculated from (4-26);

$$a = \frac{\text{No of Effective Conductors in Auxiliary Winding}}{\text{No of Effective Conductors in Main Winding}} = \frac{C_a \cdot K_{wa}}{C_m \cdot K_{wm}} \quad (4-26)$$

In (4-26), K_{wa} is the distribution factor for the auxiliary winding and found from (4-27);

$$K_{wa} = \frac{\sum_{i=1}^{N_{spa}} C_{ia} \cdot \sin\left(\frac{\pi \cdot T_{ia}}{2 \cdot S_{1p}}\right)}{\sum_{i=1}^{N_{spa}} C_{ia}} \quad (4-27)$$

In (4-27), N_{spa} is the number of slots used for auxiliary winding conductors in a pole, C_{ia} and T_{ia} are the number of conductors and throw of auxiliary winding coils in the i^{th} slot respectively. S_{1p} is the stator slot number per pole. All these parameters are entered to the SPCAD by the user. K_{wm} is the distribution factor for the main winding, and calculated from (4-28).

$$K_{wm} = \frac{\sum_{i=1}^{N_{spm}} C_{im} \cdot \sin\left(\frac{\pi \cdot T_{im}}{2 \cdot S_{1p}}\right)}{\sum_{i=1}^{N_{spm}} C_{im}} \quad (4-28)$$

Solving the equivalent circuit given in Figure 4-4, the currents of the main and auxiliary winding is obtained from (4-29) and (4-30) respectively;

$$I_m = \frac{V_m \cdot Z_{Ta} + j \cdot V_a \cdot a \cdot (Z_f - Z_b)}{Z_T \cdot Z_{Ta} - a^2 \cdot (Z_f - Z_b)^2} \quad (4-29)$$

$$I_a = \frac{V_a \cdot Z_T - j \cdot V_m \cdot a \cdot (Z_f - Z_b)}{Z_T \cdot Z_{Ta} - a^2 \cdot (Z_f - Z_b)^2} \quad (4-30)$$

where Z_T and Z_{Ta} are the impedances of the main and auxiliary windings, and calculated from (4-31) and (4-32);

$$Z_{Ta} = R_{Ta} + jX_{Ta} \quad (4-31)$$

$$Z_T = R_T + jX_T \quad (4-32)$$

In (4-31) R_{Ta} and X_{Ta} is obtained from (4-33) and (4-34) respectively.

$$R_{Ta} = r_{1a} + R_c + a^2 \cdot (R_f + R_b) \quad (4-33)$$

$$X_{Ta} = X_{1a} + X_c + a^2 \cdot (X_f + X_b) \quad (4-34)$$

R_c and X_c are the capacitor resistance and reactance respectively and entered to the program by the user.

Defining;

$$A = \text{Real part of } I_m$$

$$B = \text{Imaginary part of } I_m$$

$$C = \text{Real part of } I_a$$

D = Imaginary part of I_a

The magnitudes of the main and auxiliary winding currents are found from;

$$I_m = \sqrt{A^2 + B^2} \quad (4-35)$$

$$I_a = \sqrt{C^2 + D^2} \quad (4-36)$$

Power transferred to rotor from air gap is found from (4-37);

$$P_{gap} = (I_m^2 + (a \cdot I_a)^2) \cdot (R_f - R_b) + 2 \cdot a \cdot (A \cdot D - B \cdot C) \cdot (R_f + R_b) \quad (4-37)$$

Output power of the machine is calculated from (4-38);

$$P_{out} = (P_{gap} - (F_{loss}(hf) + bearing\ loss)) \cdot (1 - s) - windage \quad (4-38)$$

Input power of the machine is calculated from (4-39);

$$P_{in} = A \cdot V_m + C \cdot V_a \quad (4-39)$$

Efficiency of the motor is found from the ratio of the output power to the input power as given in (4-40);

$$\eta = \frac{P_{out}}{P_{in}} \quad (4-40)$$

Power factor of the machine is found from the ratio of the input power to the apparent power and calculated from (4-41);

$$PF = \frac{P_{in}}{V_m \cdot I_{line}} \quad (4-41)$$

Output torque of the machine at any speed value is calculated from (4-42);

$$T = (I_m^2 + (a \cdot I_a)^2) \cdot (R_f - R_b) + \frac{2 \cdot a \cdot I_m \cdot I_a \cdot \sin(\phi_a - \phi_m) \cdot (R_f + R_b)}{\omega_s} \quad (4-42)$$

In (4-42), ϕ_m and ϕ_a are the phase angles of the main and auxiliary winding currents and are found from (4-43) and (4-44) respectively. ω_s is the synchronous speed in rad/sec and found from (4-45);

$$\phi_m = \tan^{-1} \frac{A}{B} \quad (4-43)$$

$$\phi_a = \tan^{-1} \frac{C}{D} \quad (4-44)$$

$$\omega_s = \frac{2 \cdot \pi \cdot n}{60} \quad (4-45)$$

Capacitor voltage is found from (4-46);

$$V_c = I_a \cdot \sqrt{R_c^2 + X_c^2} \quad (4-46)$$

The flowchart given in Figure F-7 explains how these calculations are done in the software.

CHAPTER 5

USER INTERFACE AND SOFTWARE

5.1 Introduction

In the previous chapters the calculation methods to find machine parameters and performance are given. To show these calculated results to the user, some interfaces are designed and implemented to both TPCAD and SPCAD program.

In addition to the calculated results, user may want to see the performance output of the machine on a graphical chart, may want to calculate the performance of the machine with respect to desired speed or power, and may want to get the performance output of the machine in a brief or detailed summary, and so on. To meet these user needs, some interfaces are developed. In the following sections the interfaces developed and implemented to the programs will be explained in detail. Since the same interfaces used in TPCAD and SPCAD, user interfaces implemented in TPCAD will be given.

5.2 Technical Features of TPCAD

TPCAD is a user friendly windows application software product designed for design of three phase induction motors. The features of TPCAD are;

- Performance analysis of three phase squirrel cage induction motor according to the user defined motor such as geometry and materials used data
- Graphical performance analysis
 - Torque versus speed
 - Current versus speed
 - Power factor versus speed
 - Output power versus speed
 - Efficiency versus speed
- Performance calculation of any set of user defined parameter (at a speed, at a power)
- Machine parameters calculation from geometry
- Detailed design information such as; flux density in various sections of the magnetic circuit, current densities in the conductors, coreloss distribution
- Drawing lamination of the motor
- Ability to change Coreloss and B-H curves
- Calculating parameters from No Load and Locked Rotor tests

- Analyzing the performance of the motor from parameters
- Calculating the performance of the motor from Load test according to IEEE Standard 112
- Print option for the calculation results

TPCAD, while satisfying these features, also has a user friendly graphical user interface. To create these user interfaces, the object oriented programming language called C++ Microsoft Visual Studio .Net software development environment is used. ([8]) This programming environment helps the programmer to develop interfaces in a fast way by supplying all necessary design tools such as windows forms, buttons, group box, list view, etc. C++ programming language is one of the most powerful compilers with its object oriented programming logic.

5.3 Structure of TPCAD

The form shown in Figure 5-1 forms the main user interface of TPCAD. Using this main form, user can reach all the facilities of TPCAD. Menu structure of TPCAD is given in Figure 5-2. Detailed information about the functions of TPCAD is given in the following sections.

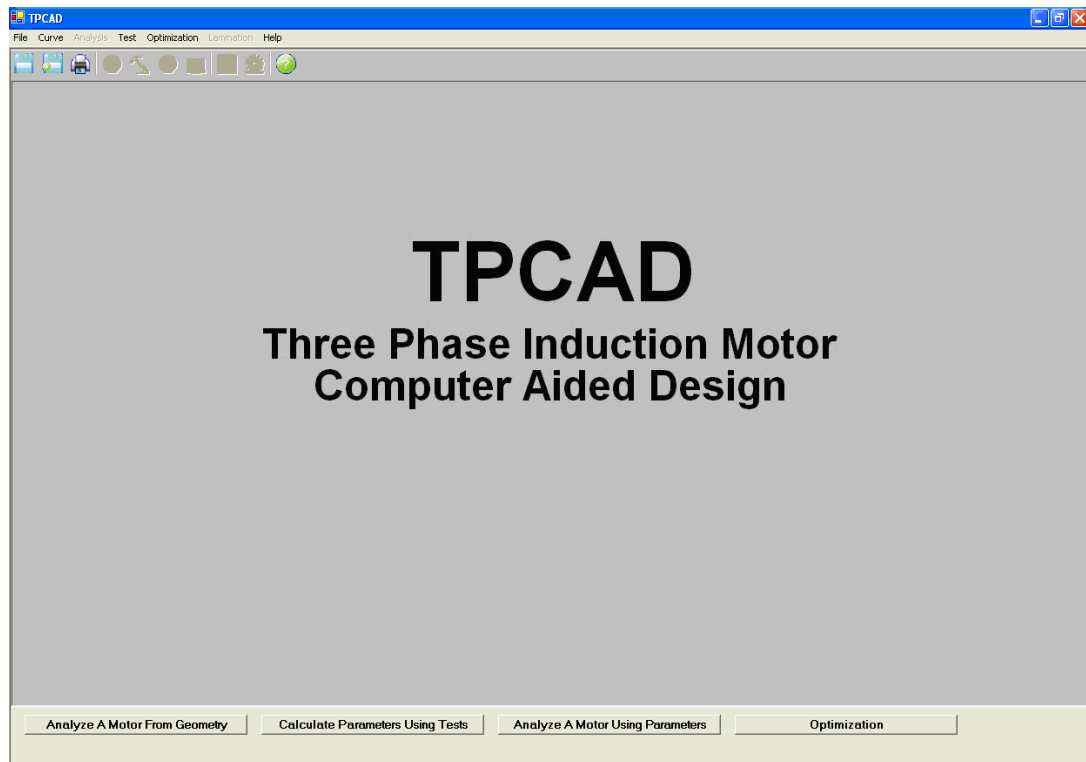


Figure 5-1 Main Form of TPCAD

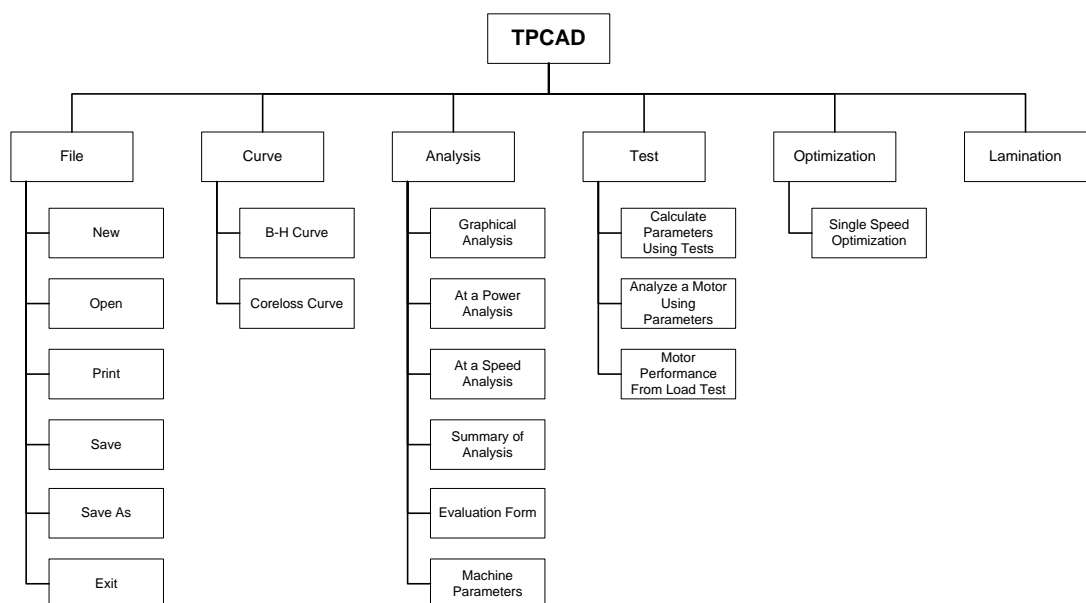


Figure 5-2 Menu Structure of TPCAD

5.4 File Menu

Using that menu, user can enter a new or load an existing motor data. Also, the motor data can be saved or can be printed out from the sub items of that menu.

5.4.1 New

This menu is used to enter a new motor data file. When the user selects that item, a form shown in Figure 5-3 is opened to enter the data of a motor.

The information about a motor which composed of winding, stator and rotor data can be entered on that form by selecting the tab pages. To change or enter the data, user should “double click” the related value on the list view. After the data entry, user can save that information by using the “Save” or “Save As” button. User can also take printout of the entered motor data by using “Print” button. Function of that feature is explained in section 5.4.3.

New Motor Form

Double Click To Change Values!

This Menu is Used Only to Create a New Motor Data File. To Analyze the Motor With the Data Created, Save and Exit This Menu and Open the File You Created from "File >> Open" Menu!

Selected Motor Data File :

Winding | Stator | Rotor

Motor Information	Values	Units
Description	Enter Data	
Title	Enter Data	
Date	Enter Data	
Phase Number	Enter Data	
Impressed Voltage	Enter Data	Volt
Frequency	Enter Data	Hz
Number of Poles	Enter Data	
Number of Conductor	Enter Data	
Per unit Pitch	Enter Data	
Stacking Factor	Enter Data	
Reactance Voltage Drop Factor	Enter Data	
Total Flux Factor	Enter Data	
Primary Flux Factor	Enter Data	
Throw of Coil (Number of Slot Pitches)	Enter Data	
Number of Parallel Paths in Stator Winding	Enter Data	
Cross-sectional Area of Conductor	Enter Data	m ²
Resistivity of Copper	Enter Data	ohm/m
Resistivity of Aluminium	Enter Data	ohm/m
Copper Resistivity Measured At	Enter Data	°C
Aluminium Resistivity Measuring Temperature	Enter Data	°C
Cross-Sectional Area of End Ring	Enter Data	m ²
Mean Diameter of End Ring	Enter Data	m
Synchronous Speed	Enter Data	rpm
Rotor Speed	Enter Data	rpm
Friction Loss	Enter Data	W
Windage Loss	Enter Data	W
Extension of Coil From Core	Enter Data	
Temperature at which Performance to be Calculated	Enter Data	°C
Rated Output Power	Enter Data	W
High Frequency Loss Constant	Enter Data	
Ab - Bar Cross Sectional Area	Enter Data	m ²
RhoFe - Density of Iron	Enter Data	kg/m ³
Ar2 - Cross Sectional Area of End Rings	Enter Data	m ²
Dr2 - End Ring Diameters	Enter Data	m ²

Save

Save As

Print

Close

Figure 5-3 New Motor Form

5.4.2 Open

This menu is used to load an existing motor data to use that for analysis as shown in Figure 5-4. So, user can perform a performance analysis and can see the lamination for that motor. To perform a performance analysis, user has to leave this form open to reach the analysis functions.

User can change the data of the loaded motor by double clicking the related value on the list view. Changed motor data can be saved from the "Save" and "Save As" buttons. As mentioned before, user can also take printout of the motor data by using "Print" button.

Motor Parameters

Leave This Form Open To Perform Motor Analysis
Double Click To Change Values!

Selected Motor Data File : C:\tpcad\mtr\15HP.MTR

Winding | Stator | Rotor

Motor Information	Values	Units
Description	12nisop1	
Title	ALARKO 11kW	
Date	13/4/1998	
Phase Number	3	
Impressed Voltage	220	Volt
Frequency	50	Hz
Number of Poles	2	
Number of Conductor	136	
Per unit Pitch	1	
Stacking Factor	0.96	
Reactance Voltage Drop Factor	0.94	
Total Flux Factor	0.96	
Primary Flux Factor	0.98	
Throw of Coil (Number of Slot Pitches)	12	
Number of Parallel Paths in Stator Winding	1	
Cross-sectional Area of Conductor	1.5393E-06	m ²
Resistivity of Copper	1.75E-08	ohm/m
Resistivity of Aluminium	1.75E-08	ohm/m
Copper Resistivity Measured At	25	°C
Aluminium Resistivity Measuring Temperature	25	°C
Cross-Sectional Area of End Ring	0.0001734857	m ²
Mean Diameter of End Ring	0.05714	m
Synchronous Speed	3000	rpm
Rotor Speed	2854.45	rpm
Friction Loss	250	W
Windage Loss	150	W
Extension of Coil from Core	0.256	
Temperature at which Performance to be Calculated	40.38241	°C
Rated Output Power	11000	W
High Frequency Loss Constant	2.45	
Ab - Bar Cross Sectional Area	4.226946E-05	m ²
RhoFe - Density of Iron	7750	kg/m ³
Ar2 - Cross Sectional Area of End Rings	0.0001734857	m ²
Dr2 - End Ring Diameters	0.05714	m

Save

Save As

Print

Close

Figure 5-4 Loaded Motor Data Form

5.4.3 Print

In the previous sections it is mentioned that, user can take printout of the motor data by using "Print" button. TPCAD can use any printer which is defined to the windows operating system. Thus, there is no limitation to use a specific printer with TPCAD. User can take the printouts by using the form shown in Figure 5-5. Up to this point, it is mentioned that motor data can be printed. In addition, the graphs, performance results, etc. can also be printed. These functions will be explained in the following sections.

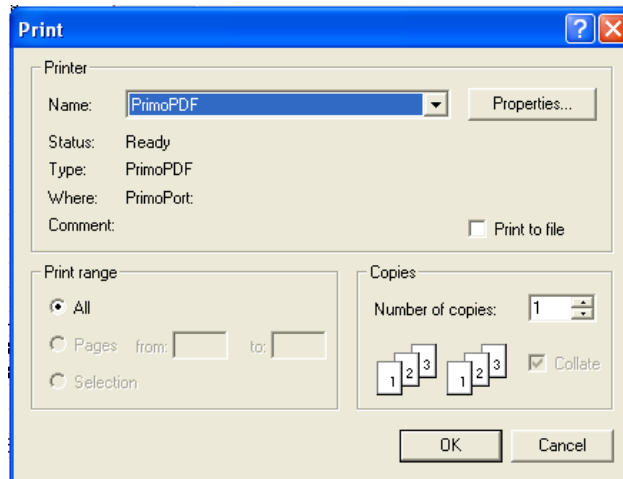


Figure 5-5 Print Form

5.5 Curve Menu

The characteristic of the material used in manufacturing of the motor is introduced to TPCAD by means of some user defined curves. In performance calculations, B-H and coreloss curves are needed. For that reason the interfaces implemented to TPCAD to enter B-H and Coreloss curve data respectively.

5.5.1 B-H Curve Menu

For the mmf drop calculations, user defined curves are used in TPCAD as mentioned in section 2.5.1. These curves can be entered to the program by the user from the interface shown in Figure 5-6.

When the user opens that form, the B-H curve used in the calculations is loaded. User can define a new curve by using “New” button or can change the values of the existing curve. User can save the changed data to the existing B-H curve using “Save” button. User can also save the changed data to a new file using “Save As” button. After changing the values from the

list view, the graph of the entered data is plotted using “Change” button. The plotted B-H data can be saved as a bitmap picture file from the “Save to BMP” button.

B-H curve data can also be printed from the “Print” button. In addition to these features, the B-H data can be defined to TPCAD for use in the calculations. This is done by using “Use This Curve for Analysis” button.

B-H curve is not linear and it is not possible to represent it by a simple nonlinear function. Therefore, to represent the material characteristics linear interpolation is used in TPCAD. Values between points that the user entered are calculated by linear interpolation of the two end points.

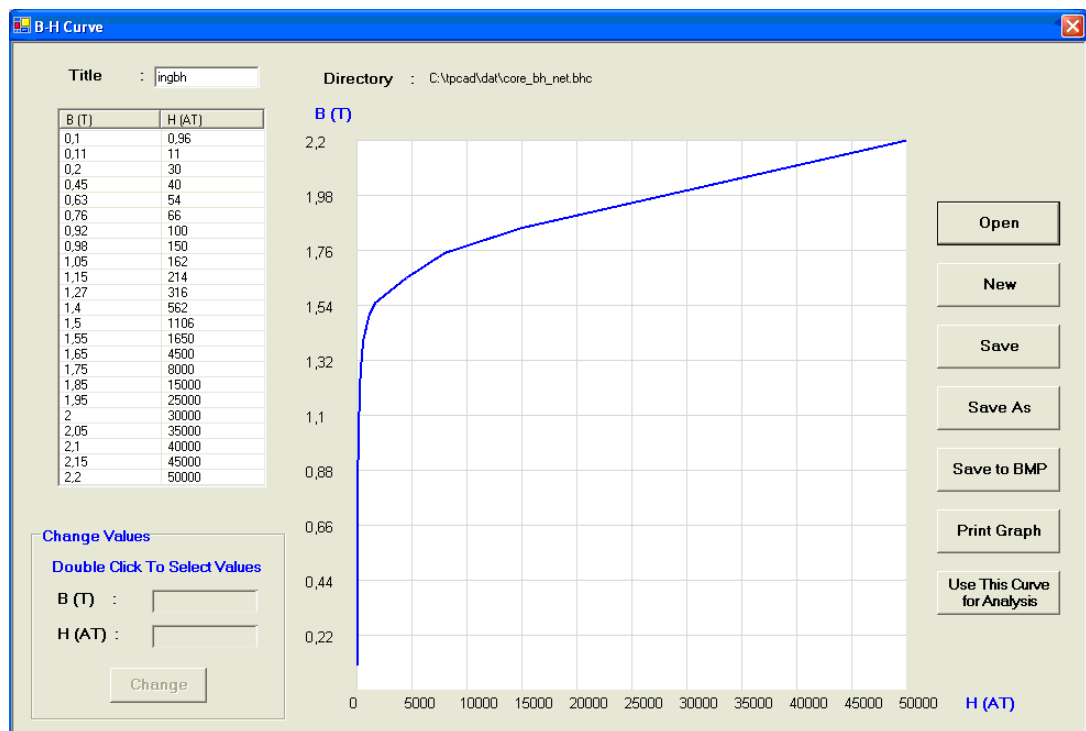


Figure 5-6 B-H Curve Menu

5.5.2 Coreloss Curve Menu

For the fundamental frequency iron loss calculation, the user defined curves are used in TPCAD as mentioned in section 2.7.1.1. These curves can be entered to the program by the user using the interface shown in Figure 5-7.

When the user opens that form, the coreloss curve used in the calculations is loaded. User can define a new curve using “New” button given in that form. User can save the changed data to the existing coreloss curve using “Save” button. User can also save the changed data to a new file using “Save As” button. After changing the values from the list view, user can see the graph of the entered data using the “Plot” button. The plotted coreloss data can be saved as a bitmap picture file from the “Save to BMP” button.

Coreloss curve data can also be printed from the “Print” button. In addition to these features, the coreloss data can be defined to TPCAD for use this in the calculations. This is done by using “Use This Curve for Analysis” button.

User can enter the coreloss data up to six different frequencies. This is implemented to use these data for variable speed applications in the future.

Coreloss curve is not linear and it is not possible to represent it by a simple nonlinear function. Therefore, to represent the material characteristics linear interpolation is used in TPCAD. Values between points that the user entered are calculated by linear interpolation of the two end points.

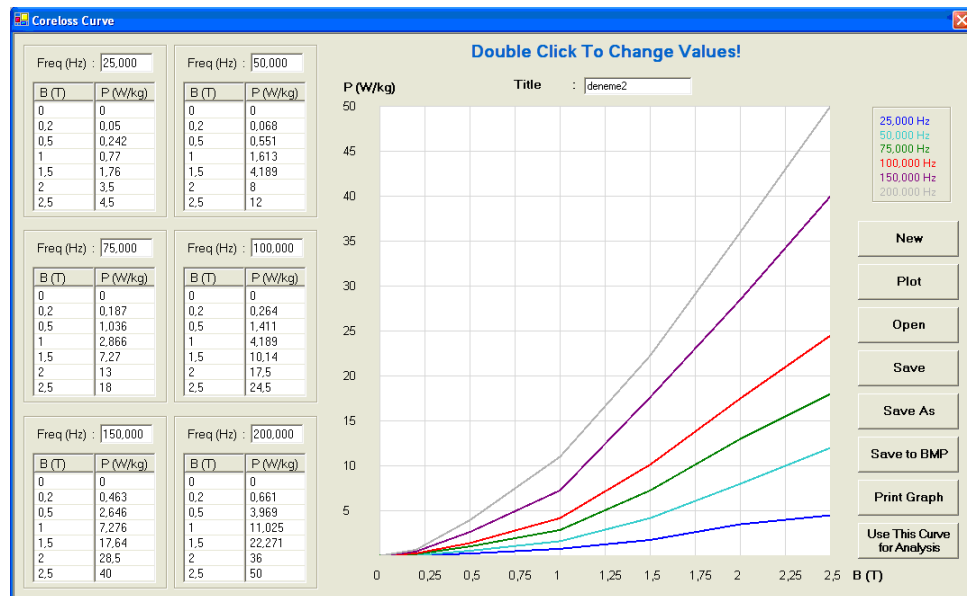


Figure 5-7 Coreloss Curve Menu

5.6 Analysis Menu

As mentioned before, the performance of the motor is calculated for the entered motor data. When the user requires to observe a certain output of a motor, the performance of the motor is calculated with an interval 0.008 in the slip range 1.0 to 0.0. (The flowchart given in Figure E-2 explains how these calculations are done in the software) During these calculations, the calculated results are saved in a temporary file. As it can be observed in the flowchart, the performance of the motor is calculated for slip intervals of 0.008. To get the performance of the motor at a desired slip, it is enough to find the interval that the slip falls in, and use that performance data to find the performance record of the motor by linear interpolation. The feature of the analysis menu can be used when the existing motor data is loaded. Loading that motor data is explained in section 5.4.2.

Using the results saved in the temporary file, the performance of the motor is shown to the user with five different formats as mentioned in the following sections.

5.6.1 Graphical Performance Analysis

Calculated performance of the motor is shown in a graphical representation as shown in Figure 5-8. Performance of the motor covers torque, current, power factor, output power and efficiency calculations. These outputs are shown to user in a graphical representation versus to speed. User can monitor the performance output variables of the motor by moving the mouse on the graphical chart. Values can also be picked by clicking the mouse on the chart. With this feature user can compare the picked results and the attained results by moving the mouse on the chart.

Plotted performance output can be saved as a bitmap picture file using the “Save to BMP” button. The graph and the picked values can also be printed from the “Print Graph” button.

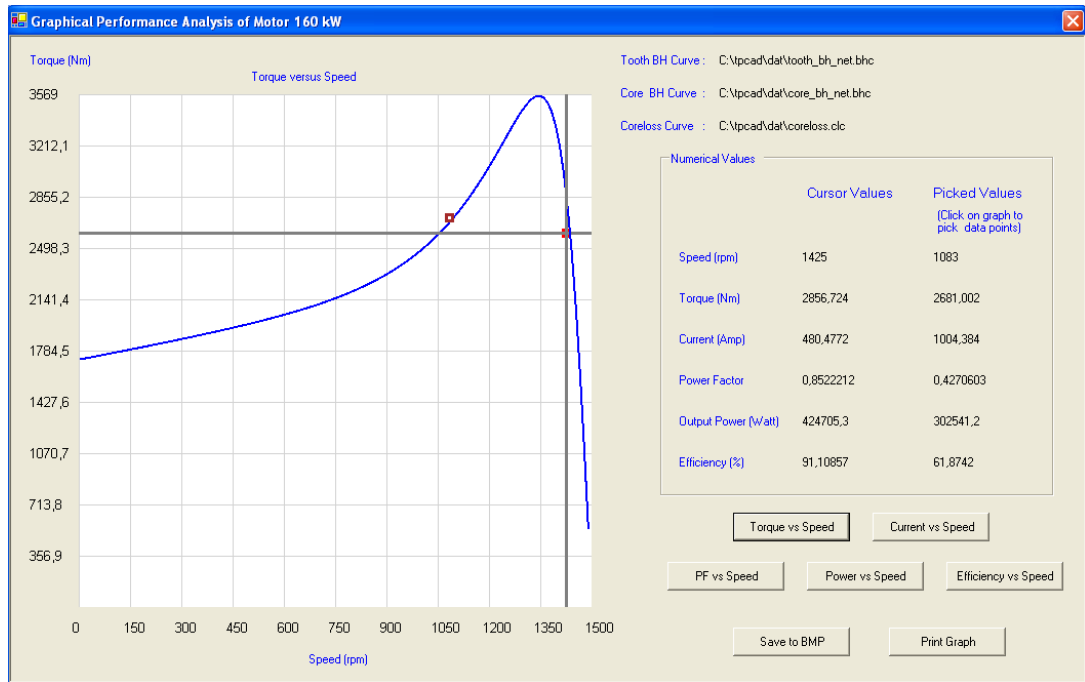


Figure 5-8 Graphical Performance Analysis Menu

5.6.2 At a Power Analysis

According to this feature of TPCAD, the performance of the motor is calculated with respect to the desired output power entered by the user. To obtain the performance record to the desired power, TPCAD searches the power interval where the performance that it falls in. After determining the power interval, TPCAD gets the performance record to the desired power by linear interpolation as mentioned in section 5.6.

After performing the performance calculation for the desired power; speed, torque, current, power factor and efficiency are shown in an interface to inform the user with the performance record as shown in Figure 5-9.

Rated Performance at Power

Tooth BH Curve : C:\tpcad\data\tooth_bh_net.bhc

Core BH Curve : C:\tpcad\data\core_bh_net.bhc

Coreloss Curve : C:\tpcad\data\coreloss.clc

The Entered Value Should Be Less Than Maximum Power!

Maximum Power: 503192 Watts

Power Watt

SPEED (rpm)	1478.417
TORQUE (Nm)	1043.289
EFFICIENCY	94.95994
POWER FACTOR	0.8840991
PHASE CURRENT(A)	167.2534

Figure 5-9 At a Power Analysis Menu

5.6.3 At a Speed Analysis

According to this feature of TPCAD, the performance of the motor is calculated with respect to the desired speed entered by the user. Calculation methodology is similar with the “At a Power Analysis”.

After performing the performance calculation for the desired speed; output power, torque, current, power factor and efficiency are shown in an interface to inform the user with the performance record as shown in Figure 5-10.

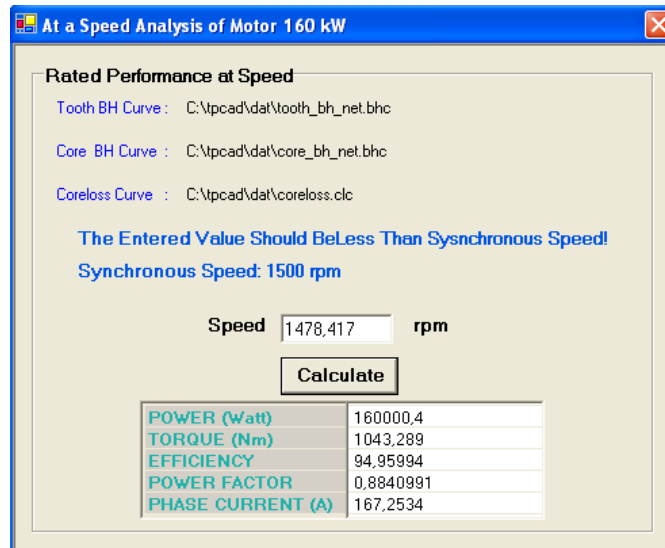


Figure 5-10 At a Speed Analysis Menu

5.6.4 Summary of the Analysis

In that feature, TPCAD shows the performance record of the motor according to the entered motor data. The outputs of that analysis; current, output power, power factor, efficiency, full load torque, pull out torque, starting torque, starting current and no load current are shown in an interface to inform the user with the performance record as shown in Figure 5-11.

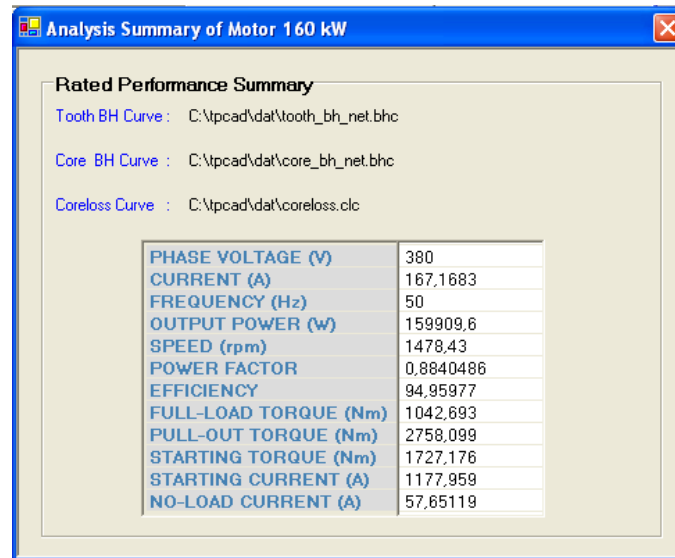
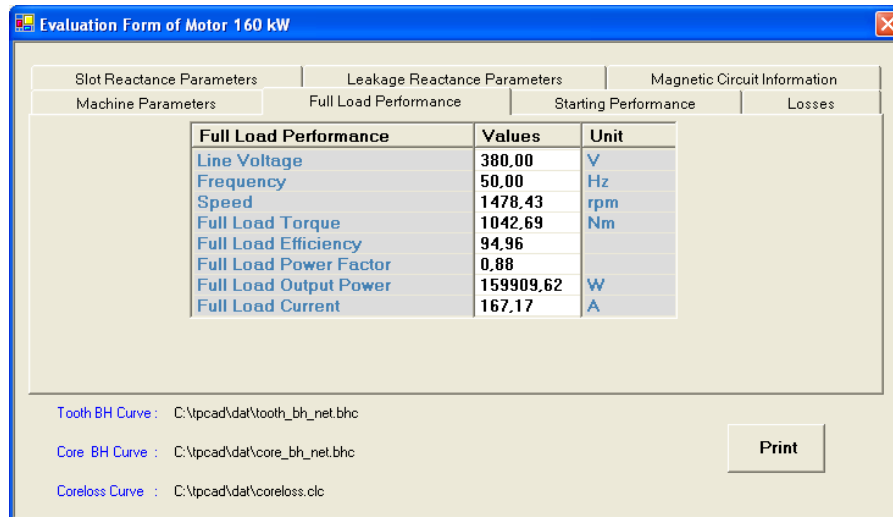


Figure 5-11 Summary of Analysis Menu

5.6.5 Evaluation Form of the Analysis

In that feature, detailed analysis record of the motor data according to the performance calculation is given with an interface as shown in Figure 5-12. Designer can get detailed information about their designs and can improve their designs according to the data obtained from this menu.

The results can be classified as; machine parameters, full load performance, starting performance, losses, slot reactance component values, leakage reactance parameters, flux densities, mmf drops and current densities information. User can reach the related function using the tab pages. Detailed analysis record can also be printed from the “Print” button.



The screenshot shows a software window titled "Evaluation Form of Motor 160 kW". It contains several tabs: "Slot Reactance Parameters", "Leakage Reactance Parameters", "Magnetic Circuit Information", "Machine Parameters", "Full Load Performance", "Starting Performance", and "Losses". The "Full Load Performance" tab is active, displaying a table of motor parameters.

Full Load Performance	Values	Unit
Line Voltage	380.00	V
Frequency	50.00	Hz
Speed	1478.43	rpm
Full Load Torque	1042.69	Nm
Full Load Efficiency	94.96	
Full Load Power Factor	0.88	
Full Load Output Power	159909.62	W
Full Load Current	167.17	A

Below the table, there are file paths for the curves used in the calculation:

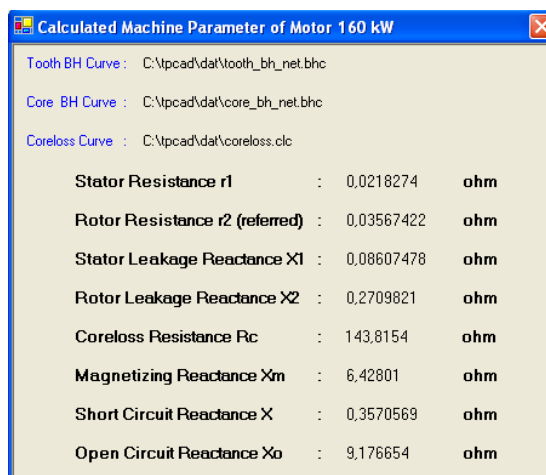
- Tooth BH Curve : C:\mpcad\data\tooth_bh_net.bhc
- Core BH Curve : C:\mpcad\data\core_bh_net.bhc
- Coreloss Curve : C:\mpcad\data\coreloss.clc

A "Print" button is located at the bottom right of the window.

Figure 5-12 Evaluation Form of the Analysis Menu

5.6.6 Parameter Calculation

User may want to see the parameters of the motor according to the motor data. Parameter calculation according to the motor data is explained in the previous chapters. Calculated motor parameters for the entered motor data are shown with an interface to user as shown in Figure 5-13.



The screenshot shows a software window titled "Calculated Machine Parameter of Motor 160 kW". It displays the same file paths for the curves as Figure 5-12. Below these, it lists the calculated machine parameters:

Stator Resistance r1	:	0.0218274	ohm
Rotor Resistance r2 (referred)	:	0.03567422	ohm
Stator Leakage Reactance X1	:	0.08607478	ohm
Rotor Leakage Reactance X2	:	0.2709821	ohm
Coreloss Resistance Rc	:	143.8154	ohm
Magnetizing Reactance Xm	:	6.42801	ohm
Short Circuit Reactance X	:	0.3570569	ohm
Open Circuit Reactance Xo	:	9.176654	ohm

Figure 5-13 Calculated Machine Parameters Menu

5.7 Test Menu

As mentioned before user may want to obtain machine parameters from tests, and use these parameters to get the performance record of the machine for any speed value. Also, user may want to get the performance record according to the measurements taken under a certain load. In the following sections the user interfaces developed to meet these user needs are explained.

5.7.1 Calculate Parameters Using Tests

The most common way to determine the parameters of the machine is to test the machine under locked rotor and no load conditions. To perform calculations, a tool is added to TPCAD to determine the machine parameters from locked rotor and no load test results. By using that tool, user can get the machine parameters from the test data as shown in Figure 5-14.

After entering the related test data, user can get the machine parameters using “Calculate Motor Parameters” button. The equations used for the calculations are mentioned in section 3.2. Stator and rotor reactances are calculated according to the selected motor class data. Information about the motor classes is given in section 3.2. Moreover, user can also export the calculated machine parameters to use them for the performance calculations using “Export Parameters for Analysis” button.

Calculate Parameters Using No Load And Locked Rotor Tests

No Load Test Data

Voltage (line) : Volt

Current (line) : Ampere

Power : Watt

Friction Loss : Watt

Windage Loss : Watt

Locked Rotor Test Data

Voltage (line) : Volt

Current (line) : Ampere

Power : Watt

Machine Parameters

Connection Type :

Motor Class :

Stator Resistance : Ohm (measured)

Rotor Resistance : Ohm

Stator Reactance : Ohm

Rotor Reactance : Ohm

Magnetizing Reactance : Ohm

Core Loss Resistance : Ohm

Calculate Motor Parameters **Export Parameters For Analysis**

Figure 5-14 Calculate Parameters Using Tests Menu

5.7.2 Analyze A Motor Using Parameters

It is mentioned that, user may want to get the performance of the machine. For that reason, user needs the parameters of that machine. In the previous section, a feature to get the machine parameters from locked rotor and no load tests is explained. Alternately, the parameters may be calculated from the motor data. In any case, to calculate the motor performance using these parameters, a tool is added to TPCAD as shown in Figure 5-15.

User has to enter the related machine parameters to perform performance analysis. In addition, user can also enter the machine parameters using “Import Machine Parameters” button from the calculated results of “Calculate Parameters Using Tests Menu” as mentioned in the previous section.

When the parameters of the machine are entered, the results are shown to user after using “Performance Analysis” button. Calculations done to get performance record are explained in section 3.3.

Analyze A Motor Using Parameters

Enter Machine Parameters

Stator Resistance : Ohm

Rotor Resistance : Ohm

Stator Reactance : Ohm

Rotor Reactance : Ohm

Magnetizing Reactance : Ohm

Core Loss Resistance : Ohm

Measured Temperature : °C

Test Temperature : °C

Calculate Performance at Following Data

Test Voltage (phase) : Volt

Rotor Speed : rpm

Synchronous Speed : rpm

Friction Loss : Watt

Windage Loss : Watt

Stray Loss : Watt

Import Machine Parameters

**Import Machine Parameters From "Calculate Parameters Using Tests" Menu
Or Enter Machine Parameters and Test Data**

Performance From Parameters

Voltage (phase)	Volt	Efficiency	%
Current Full - Load	Ampere	Power Factor	
Output Power	Watt	Torque Full - Load	Nm
Stator Copper Loss	Watt	Coreloss	Watt
Rotor Copper Loss	Watt	Starting Torque	Nm
No Load Current	Ampere	Starting Current	Ampere

Performance Analysis

Figure 5-15 Analyze a Motor Using Parameters Menu

5.7.3 Motor Performance From Load Test

As mentioned before, users may not have an access to a proper test set up to measure the shaft torque and power output of a machine under a certain load. However, measurement of terminal voltage and input power is often possible. Also, the speed of the motor is relatively easy to measure. For that reason, a tool is added to TPCAD as shown in Figure 5-16 to obtain the machine performance only from no load test and load test measuring only motor terminal voltage, current, input power and motor speed.

When the related data is entered, the results are shown to user after using “Calculate” button. Calculations done to get performance record are explained in section 3.4.

Enter Machine Parameters				Calculate Performance at Following Data			
R1 (measured)	:	<input type="text"/>	Ohm	Test Voltage (line)	:	<input type="text"/>	Volt
Temp at R1 Measured	:	<input type="text"/>	°C	Test Current (line)	:	<input type="text"/>	A
Load Test Temp	:	<input type="text"/>	°C	Cos Phi	:	<input type="text"/>	
No Load Test Voltage (line)	:	<input type="text"/>	Volt	Rotor Speed	:	<input type="text"/>	rpm
No Load Test Current (line)	:	<input type="text"/>	A	Synchronous Speed	:	<input type="text"/>	rpm
No Load Test Power	:	<input type="text"/>	Watt	Friction Loss	:	<input type="text"/>	Watt
Stray Load Percentage	:	<input type="text"/>	%	Windage Loss	:	<input type="text"/>	Watt
Connection Type	:	Delta		Calculate			

Result							
Efficiency	:		%	Stator Copper Lost	:		W
Net Torque	:		Nm	Rotor Copper Lost	:		W
Output Power	:		W	Coreloss	:		W

Figure 5-16 Motor Performance From Load Test Menu

5.8 Lamination Menu

Motor designer often wishes to see the final motor design in drawing form. Furthermore, it is desirable to transfer the lamination design into another drawing or design analysis software for further processing. For this reason, a tool is added to TPCAD, to draw lamination of the designed motor and export that lamination data as a dxf drawing format. (Figure 5-17) This format is a well known Computer Aided Design (CAD) data file format which is used to enable data interoperability between professional design programs.

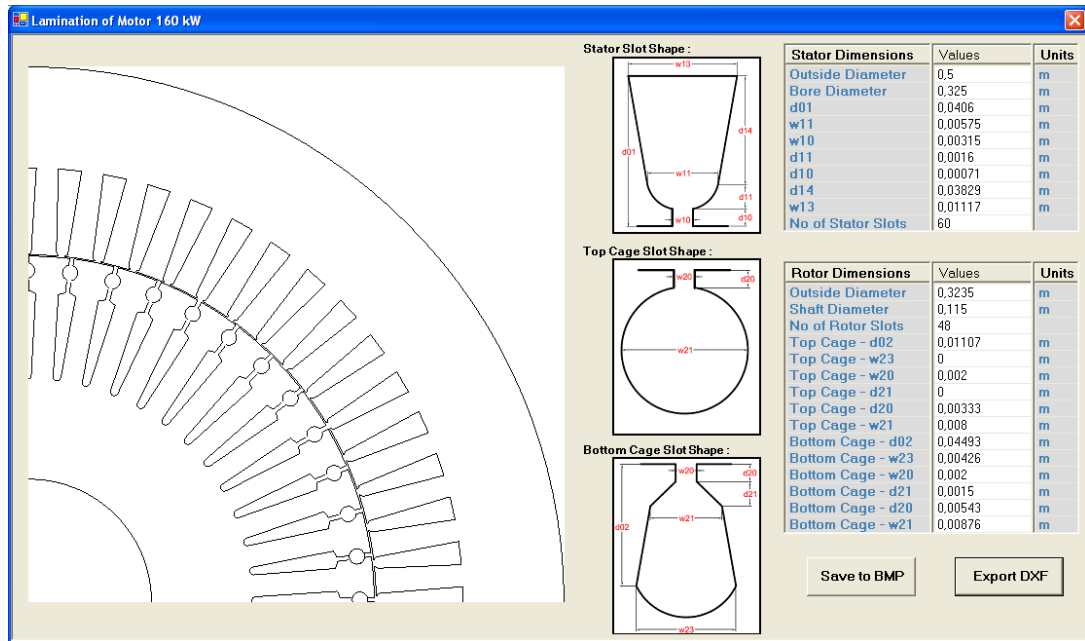


Figure 5-17 Lamination Menu

A sample motor lamination is shown in Figure 5-18. Lamination drawing algorithm is based on the observation that a lamination is simply a repetition of a slot pitch of stator and rotor. All calculations are made for polar coordinate system. However, to draw lamination of the motor, TPCAD drawing functions accept cartesian coordinate system. This condition occurs because of the functions defined to draw ellipse, circle and line in software development environment. In the following sections, the algorithm developed to draw lamination of the motor is explained.

The base point to calculate coordinates of each point on the stator or rotor slot is the center of the motor lamination as shown as point “O” in Figure 5-18. However to draw lamination using functions in TPCAD, base point is taken as point “S”. Therefore, the description here concentrates on describing how a stator slot pitch drawing is prepared.

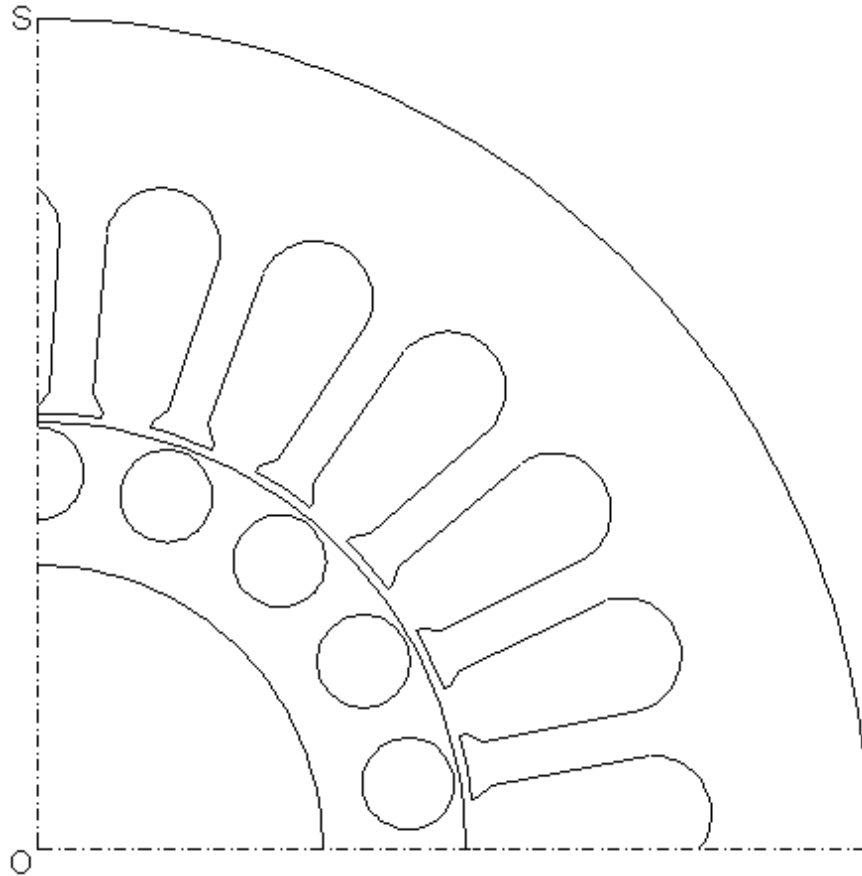


Figure 5-18 Sample Motor Lamination

5.8.1 Creation of Repeating Stator Portion

As mentioned before, one stator slot is drawn after that all the stator side drawing is completed by repeating that portion by stator slot number. In TPCAD three different stator slot types can be selected as shown in Figure 2-4. Algorithm of stator side drawing is given in Figure 5-22. Calculations made in that algorithm are explained in detail in the following part. To understand the calculations of the algorithm, a sample stator slot drawing is given in Figure 5-19.

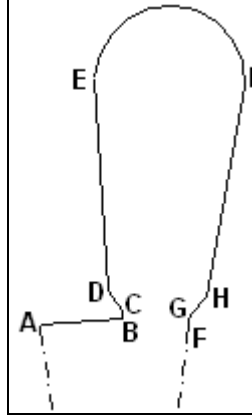


Figure 5-19 Sample Stator Slot Drawing

To draw the stator tooth width (“A – B”), the angle of tooth width, *alfa* should be calculated first. This is the angle of “A – B” portion to the center of the motor. Stator tooth width is calculated from subtracting stator slot width from stator tooth pitch as shown in (5-2). Stator tooth pitch can be found by using stator bore diameter, D_1 and stator slot number, S_1 from (5-1).

$$\text{Tooth Pitch} = \frac{\pi \cdot \text{Bore Diameter}}{\text{Stator Slot Number}} \quad (5-1)$$

$$\text{Tooth Width} = \text{Tooth Pitch} - w_{10} \quad (5-2)$$

Stator tooth width angle, *alfa*, can be calculated from (5-3). To use angles at drawing functions defined in TPCAD, these angles must be in radians. For that reason all angles are converted to radians.

$$\text{alfa} = \frac{\text{Tooth Width} \cdot 360^\circ}{\pi \cdot D_1} \quad (5-3)$$

Coordinates of A and B points can be found using stator tooth width angle and stator bore diameter from (5-4) to (5-7). Using these points “A – B” portion of the stator slot is drawn.

$$A_x = D_1 \quad (5-4)$$

$$A_y = D - D_1 \quad (5-5)$$

$$B_x = D_1 \cdot \sin(\alpha) \quad (5-6)$$

$$B_y = D - (D_1 \cdot \cos(\alpha)) \quad (5-7)$$

After completion of drawing stator tooth width, “B – C” portion is drawn using coordinates of point B and C. Using the length of stator mouth depth, d_{10} , coordinates of point C can be found from (5-8) and (5-9).

$$C_x = (D_1 + d_{10}) \cdot \sin(\alpha) \quad (5-8)$$

$$C_y = D - ((D_1 + d_{10}) \cdot \cos(\alpha)) \quad (5-9)$$

To draw “C – D” portion of the stator slot, the angle of the point D, δ , is required. To understand the angles used to draw that portion, Figure 5-20 is used to show angles. The half of the angle of stator slot bottom width, δ , is calculated from (5-10).

$$\delta = \tan^{-1}\left(\frac{\frac{w_{11}}{2}}{D_1 + d_{10} + d_{11}}\right) \quad (5-10)$$

$$D_x = \sqrt{\left(\frac{w_{11}}{2}\right)^2 + (D_1 + d_{10} + d_{11})^2 \sin(tetal)} \quad (5-13)$$

$$D_y = D - \sqrt{\left(\frac{w_{11}}{2}\right)^2 + (D_1 + d_{10} + d_{11})^2 \cos(tetal)} \quad (5-14)$$

To draw “D – E” portion of the stator slot, same algorithm defined to draw “C – D” portion is used to find the coordinates of point E. The only difference is, *delta* and *tetal* angles are now measured from point E.

$$delta = A \tan\left(\frac{\frac{w_{13}}{2}}{D_1 + d_{10} + d_{11} + d_{14}}\right) \quad (5-15)$$

$$tetal = alfa + \frac{delta}{2} - delta \quad (5-16)$$

$$E_x = \sqrt{\left(\frac{w_{13}}{2}\right)^2 + (D_1 + d_{10} + d_{11} + d_{14})^2 \sin(tetal)} \quad (5-17)$$

$$E_y = D - \sqrt{\left(\frac{w_{11}}{2}\right)^2 + (D_1 + d_{10} + d_{11})^2 \cos(tetal)} \quad (5-18)$$

For the “F – G” portion of the stator slot, angle of point F is required. This angle is the sum of stator tooth width and slot width. So coordinates of these points can be calculated from;

$$F_x = D_1 \cdot \sin(alfa + delta) \quad (5-19)$$

$$F_y = D - (D_1 \cdot \cos(alfa + delta)) \quad (5-20)$$

$$G_x = (D_1 + d_{10}) \cdot \sin(alfa + delta) \quad (5-21)$$

$$G_y = D - ((D_1 + d_{10}) \cdot \cos(alfa + delta)) \quad (5-22)$$

For the drawing of “G – H” portion of the stator slot, the angle of point H, $teta1$, is required. To understand the angles used to draw that portion, Figure 5-21 is used to show angles. The half of the angle of the stator slot bottom width, $delta$, is already calculated at (5-10).

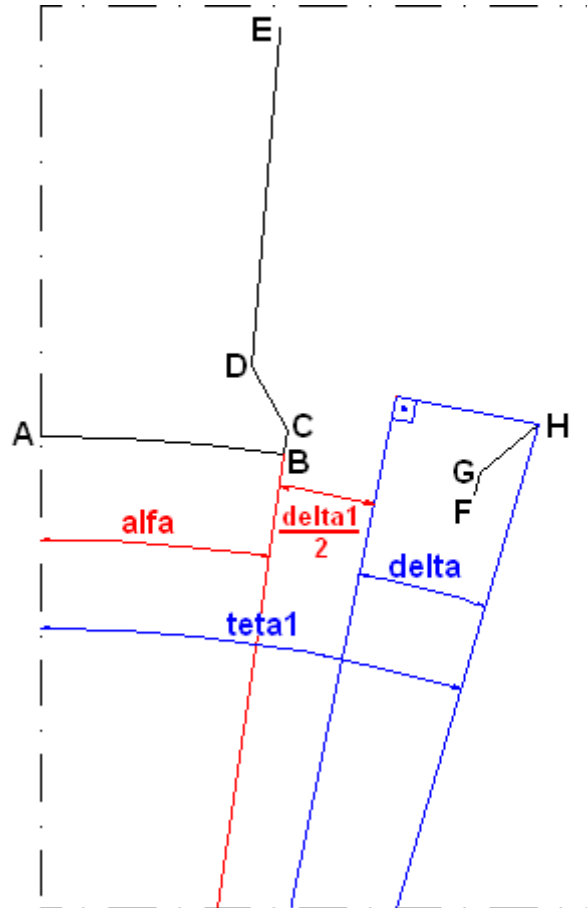


Figure 5-21 “G - H” Drawing

Sum of angle $alfa$, $delta$ and $\frac{delta1}{2}$ is equal to angle $teta1$ as shown in Figure 5-21. So using that equality $teta1$ can be found from (5-23).

$$teta1 = alfa + \frac{delta1}{2} + delta \quad (5-23)$$

Coordinates of point H can be found from (5-24) and (5-25).

$$H_x = \sqrt{\left(\frac{w_{11}}{2}\right)^2 + (D_1 + d_{10} + d_{11})^2} \sin(tetal) \quad (5-24)$$

$$H_y = D - \sqrt{\left(\frac{w_{11}}{2}\right)^2 + (D_1 + d_{10} + d_{11})^2} \cos(tetal) \quad (5-25)$$

To draw “H – I” portion of the stator slot, same algorithm defined to draw “G – H” portion is used to find the coordinates of point I. The only difference is, *delta* and *tetal* angles are now measured from point I.

$$delta = A \tan\left(\frac{\frac{w_{13}}{2}}{D_1 + d_{10} + d_{11} + d_{14}}\right) \quad (5-26)$$

$$tetal = alfa + \frac{delta}{2} + delta \quad (5-27)$$

$$I_x = \sqrt{\left(\frac{w_{11}}{2}\right)^2 + (D_1 + d_{10} + d_{11} + d_{14})^2} \sin(tetal) \quad (5-28)$$

$$I_y = D - \sqrt{\left(\frac{w_{11}}{2}\right)^2 + (D_1 + d_{10} + d_{11} + d_{14})^2} \cos(tetal) \quad (5-29)$$

After calculation of all coordinates, drawing of the stator slot portion can be done by the drawing functions defined in TPCAD as shown in the flowchart given in Figure 5-22.

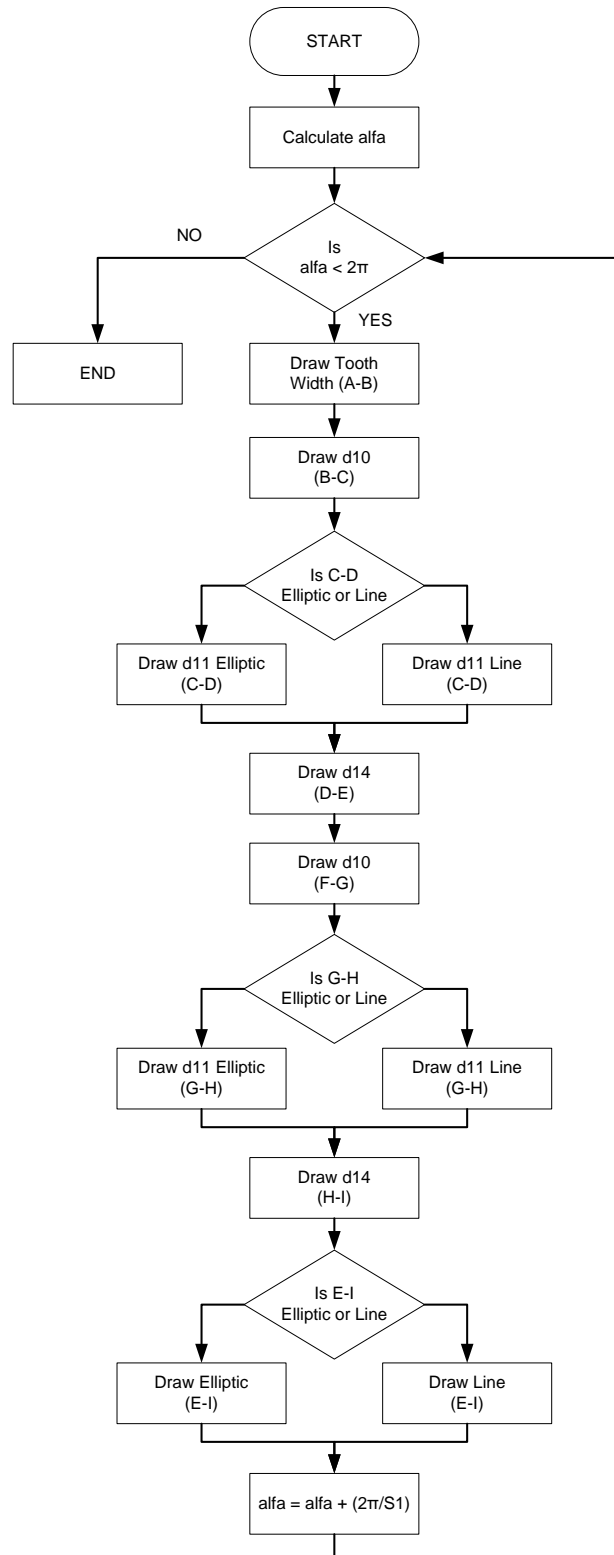


Figure 5-22 Algorithm of Drawing Stator Slot Portion

5.8.2 Creation of Repeating Rotor Portions

As mentioned before, one slot is drawn after that all the other drawing is completed by repeating that portion by slot number. This is also valid for rotor slots. In that section only the flowchart of the drawing steps defined in TPCAD will be given to understand the drawing of the rotor lamination.

In TPCAD six different rotor slot types can be selected as shown in Figure 2-5. Algorithm of rotor side drawing is given in Figure 5-23. Sample rotor slot drawing is given in Figure 5-24 to clarify the coordinates.

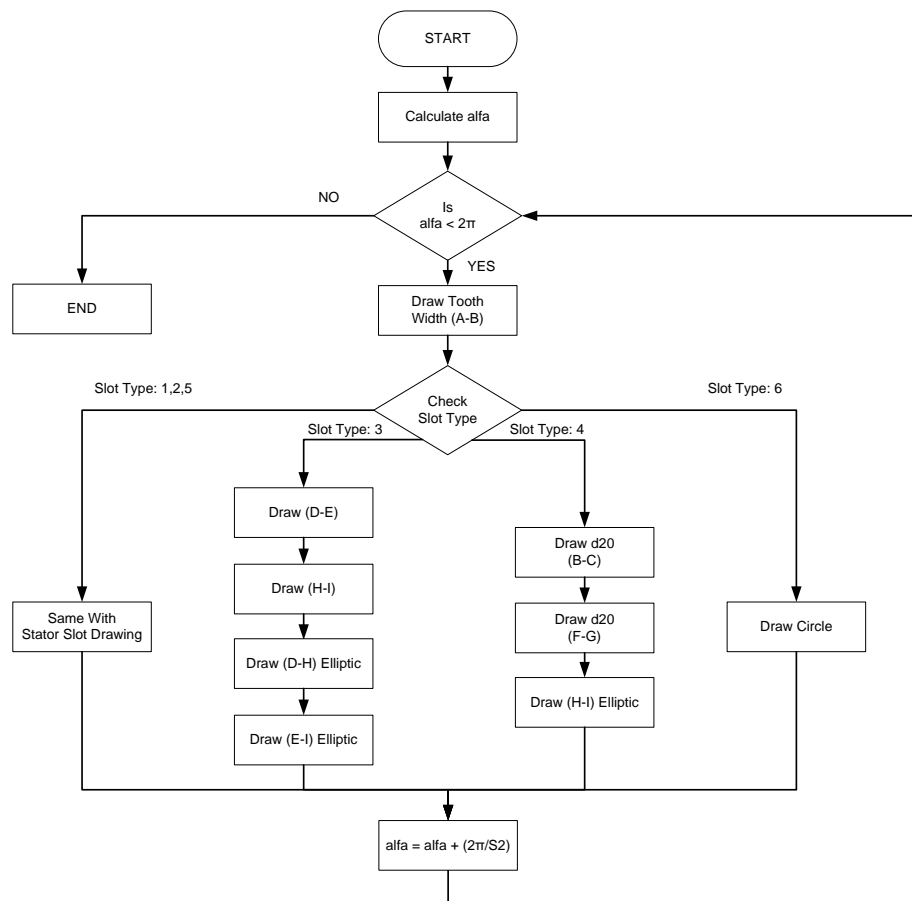


Figure 5-23 Algorithm of Drawing Rotor Slot Portion

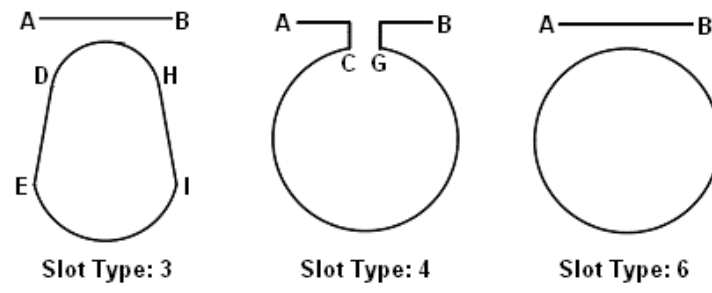


Figure 5-24 Types of Rotor Slots

CHAPTER 6

TEST RESULTS AND VERIFICATION

6.1 Introduction

In this chapter, the methods used to calculate machine parameters and performance calculation methods given in the previous chapters will be verified. To verify these calculations, TPCAD and SPCAD outputs will be compared with test results.

6.2 Verification of TPCAD Results

The purpose of this section is;

- To assess the accuracy of parameter calculation by TPCAD.
- To assess the accuracy of TPCAD performance calculations, when measured parameters are used for performance calculation via TPCAD. Note that, this study indicates the limits of the models used in TPCAD for performance calculation. This statement assumes that the tests on the motor give the most realistic values for parameters.

- Finally, the test motor performance is calculated using TPCAD calculated parameters and compared with test results. In this manner an idea of the accuracy that may be expected from TPCAD when a new design is made.

6.2.1 Test Motors

It is worthwhile to find out whether the accuracy of predictions depends on the size of the motor, number of poles or cage type. However, it was not possible to access enough motors of different sizes with pole numbers other than 4. The motors tested are listed in Table 6-1. The motors manufactured by Elsan A.Ş. are tested in the factory motor performance test laboratory by the author. Other test results are taken from the verifications done in reference [1]. Motor data of these motors are given in APPENDIX C.

Table 6-1 Three Phase Test Motors

Pole Number	Power	Cage Type	Slot Type	Model No	Manufacturer
4 pole	1.5 kW	Single Cage	Closed	90L4A	TEE A.Ş.
6 pole	2.2 kW	Single Cage	Open	NM 112M-6	Elsan A.Ş.
4 pole	4 kW	Single Cage	Open	NM 112M-4	Elsan A.Ş.
4 pole	5.5 kW	Single Cage	Closed	132S4C	TEE A.Ş.
4 pole	7.5 kW	Single Cage	Closed	132M4B	TEE A.Ş.
2 pole	7.5 kW	Single Cage	Closed	132S2C	TEE A.Ş.
4 pole	15 kW	Single Cage	Closed	160L4A	TEE A.Ş.
4 pole	18.5 kW	Single Cage	Closed	180M4B	TEE A.Ş.
4 pole	55 kW	Double Cage	Open	NM 250M-4	Elsan A.Ş.
4 pole	160 kW	Double Cage	Open	NM 315Ma-4	Elsan A.Ş.

Tests are done in accordance with TS3025 (IEC 60034-1/Rating and Performance) and TS6848 (IEC 60034-12/Starting Performance of Single-

Speed Three-Phase Cage Induction Motors) standards. Tests are performed in the order;

- No load test
- Locked rotor test
- Starting performance tests
- Load tests

Before starting to the mentioned tests, the ambient temperature is recorded as start temp. Before and after each test, the value of the stator resistance is measured to find the temperature of the motor. In Table 6-2, measured temperatures of the tested motor after starting and load tests are given respectively. These values are used in TPCAD to calculate related performance of the motor.

Table 6-2 Performance Calculation Temperature for Three Phase Motors

Motor Model	Start Temp	Starting Test	Load Test
90L4A (1.5 kW-4pole)	20	45	45
NM 112M-6 (2.2 kW-6pole)	20	40	55
NM 112M-4 (4 kW-4pole)	20	33	43
132S4C (5.5 kW-4pole)	20	25	25
132M4B (7.5 kW-4pole)	25	35	35
132S2C (7.5 kW-2pole)	20	30	30
160L4A (15 kW-4pole)	20	35	35
180M4B (18.5 kW-4pole)	25	35	35
NM 250M-4 (55 kW-4pole)	18.4	30	37.6
NM 315Ma-4 (160 kW-4pole)	20	50	59

The capacity of test setup is not suitable for direct measurement of starting torque of motors named NM 250M-4 (55 kW-4pole) and NM 315Ma-4 (160

kW-4pole) at rated voltage. For that reason starting performance test for these motors is performed at lower terminal voltages. The measured torque and current values are rearranged according to the equations given in (6-1) and (6-2) respectively.

$$T_{starting} = T_{measured} \cdot \left(\frac{V_{rated}}{V_{test}}\right)^2 \quad (6-1)$$

$$I_{starting} = I_{measured} \cdot \left(\frac{V_{rated}}{V_{test}}\right) \quad (6-2)$$

6.2.2 Verification of Parameter Calculation Algorithm

In this part, the parameter calculation algorithm is verified by comparing the parameters obtained from No Load and Locked Rotor tests and the parameters obtained from the motor geometry.

Motor parameters of the test motors named NM 315Ma - 4 (160 kW - 4pole), NM 250M - 4 (55 kW - 4pole), NM 112M - 4 (4 kW - 4pole), NM 112M - 6 (2.2 kW - 6pole), 180M4B (18.5 kW - 4pole) and 160L4A (15 kW - 4pole) are calculated. Results of the double cage motors are given in Table 6-3 and results of the single cage motors are given in Table 6-4 and Table 6-5 respectively. Since test results of the other test motors are not available, parameters of these motors are not calculated.

In these tables, the first column "Test Results" shows the calculated parameters according to No Load and Locked Rotor tests; the second column "TPCAD Results" shows the calculated parameters from the motor geometry and the third column "Error Percent" shows the error percentage of these two calculations.

Error percentage is defined as the difference between the test and TPCAD results. Error percentage is calculated from the equation given in (6-3).

$$\% \text{ Error} = \frac{\text{Test Result} - \text{TPCAD Result}}{\text{Test Result}} \cdot 100 \quad (6-3)$$

Table 6-3 Double Cage Motors Parameter Calculations

	NM 315Ma - 4 (160 kW - 4pole)			NM 250M - 4 (55 kW - 4pole)		
	Test Results	TPCAD Results	Error Percent	Test Results	TPCAD Results	Error Percent
r_1 (ohm)	0.0220	0.0218	1.03	0.1210	0.1205	0.45
r_2' (ohm)	0.0426	0.0356	16.34	0.1602	0.1417	11.52
x_1 (ohm)	0.1019	0.0860	15.62	0.2763	0.2257	18.31
x_2' (ohm)	0.2776	0.2709	2.43	0.8539	0.8094	5.21
r_c (ohm)	143.67	143.81	-0.10	283.40	283.18	0.08
x_m (ohm)	6.38	6.42	-0.63	17.77	16.67	6.21
$x_1 + x_2'$ (ohm)	0.3795	0.3569	5.97	1.1302	1.0351	8.41

Table 6-4 Single Cage Motors Parameter Calculations - 1

	NM 112M - 4 (4 kW - 4pole)			NM 112M - 6 (2.2 kW - 6pole)		
	Test Results	TPCAD Results	Error Percent	Test Results	TPCAD Results	Error Percent
r_1 (ohm)	3.598	3.569	0.79	2.4855	2.426	2.38
r_2' (ohm)	3.925	3.711	5.45	3.1028	2.507	19.20
x_1 (ohm)	4.135	2.046	50.52	1.9494	1.159	40.50
x_2' (ohm)	4.135	5.436	-31.46	1.9494	2.917	-49.67
r_c (ohm)	1721.28	1721.39	-0.01	789.20	789.65	-0.06
x_m (ohm)	120.85	113.52	6.07	53.58	53.73	-0.28
$x_1 + x_2'$ (ohm)	8.270	7.482	9.53	3.898	4.077	-4.58

Table 6-5 Single Cage Motors Parameter Calculations - 2

	180M4B (18.5 kW - 4pole)			160L4A (15 kW - 4pole)		
	Test Results	TPCAD Results	Error Percent	Test Results	TPCAD Results	Error Percent
r_1 (ohm)	0.4765	0.4608	3.30	0.5681	0.5540	2.48
r_2' (ohm)	0.7518	0.6828	9.18	0.8246	0.7220	12.44
x_1 (ohm)	1.721	0.945	45.08	1.434	0.895	37.61
x_2' (ohm)	1.721	2.063	-19.92	1.434	2.275	-58.62
r_c (ohm)	1313.04	1351.2	-2.91	747.60	745.8	0.23
x_m (ohm)	47.51	47.50	0.01	37.86	39.22	-3.58
$x_1 + x_2'$ (ohm)	3.44	3.009	12.58	2.869	3.17	-10.51

As it can be observed from the results, TPCAD calculates stator resistance with a small error percentage when it is compared with the measured stator resistance. It can be seen that measured stator resistance is higher than the calculated stator resistance by TPCAD. This error is coming from the length of the conductor used on the motor. Used stator stack length and coil extension values are the exact values taken from the drawings. It is also possible to change the coil extension value to make these equal. However no correction is made on that value for the calculations here.

Coreloss resistance models the resistance of the coreloss of the magnetic circuit. B-H curve differs according to the material used for motor lamination. For that reason, material B-H curve data should be used to evaluate related motor performance. However for the calculations in this work the B-H curve data given in APPENDIX G is used by TPCAD.

Calculation of coreloss resistance in the motors, the calculated corelosses of the motor are on the bases of the average flux density in various parts of

the magnetic circuit. (In the calculations coreloss is only calculated for stator teeth and back core) In the calculations it is assumed that a uniform flux density exists in the two regions. In reality distribution of the flux density is non uniform. However, in the coreloss curves provided by the manufacturers are obtained with a uniform distribution in the material. Therefore very good accuracy cannot be expected when these curves are used for coreloss calculation. TPCAD solves this problem by introducing a correction factor. Table 6-6 shows that correction factor values shows considerable dispersion from motor to motor. It is thought that the designer has access to coreloss data for motors of various sizes. And therefore one can choose a good estimate for coreloss correction factor for a new motor design. When such correction is made naturally the error in calculation of coreloss resistance becomes very small.

Table 6-6 Coreloss Resistance Correction Factors

Motor Name	Correction Factor
NM 315Ma - 4 (160 kW - 4pole)	0.673
NM 250M - 4 (55 kW - 4pole)	1.028
NM 112M - 4 (4 kW - 4pole)	1.495
NM 112M - 6 (2.2 kW - 6pole)	1.397
180M4B (18.5 kW - 4pole)	0.970
160L4A (15 kW - 4pole)	1.0158

According to this information, comparison of the machine parameters will be done for the rotor resistance, stator and rotor leakage reactance and magnetizing reactance.

For the double cage motors it can be observed that larger error occurs for r_2' . It can be observed that the measured rotor resistance value is greater

than the calculated values. This is understandable as there may be bubbles in the actual rotor bars because of the aluminum casting process. In addition the resistivity of the aluminum may be different than what is used in the simulation. During the casting process the aluminum may be contaminated causing higher resistivity value. Another reason for measuring higher resistance values may be performing the locked rotor test at 50 Hz at stand still. Due to this, the measured resistance value is likely to be higher than the resistance at operating conditions where the rotor frequency is very low. In TPCAD the DC resistance values are calculated.

It is not possible to make an additional test to determine X_1 and X_2' separately. However, the standard recommends an empirical distribution for these leakage reactances as given in Table 3-1. ([6]) For double cage motors the class of the motor is taken as “Class C” which means “High starting torque, low starting current”. Since there is some uncertainty here, the comparison is based on the total leakage reactance $X_1 + X_2'$. The error percentage for this value is changing from 6 to 8. This is an acceptable result as saturation effect and local distribution of the magnetic field is not considered in TPCAD calculations.

Furthermore, the variation of the air gap size is very important for calculation of magnetizing reactance. Now, air gap length of the double cage motors will be increased and decreased with 10% of the actual gap length. New air gap length values are given in Table 6-7. According to the new air gap length values, magnetizing reactance of these motors will be recalculated. New magnetizing reactance values are given in Table 6-8.

Table 6-7 New Air Gap Length Values of Double Cage Motors

	Airgap length + 10%		Air gap length - 10%	
	Actual Value (mm)	New Value (mm)	Actual Value (mm)	New Value (mm)
NM 315Ma - 4 (160 kW - 4pole)	1.1	1.21	1.1	0.99
NM 250M - 4 (55 kW - 4pole)	0.75	0.825	0.75	0.675

As given in (2-15), the value of the magnetizing reactance has an inverse relation with the air gap length. For example, when the actual air gap length is increased, the new value of the magnetizing reactance becomes less when it is compared with the actual magnetizing reactance value. In addition, saturation affects the value of the magnetizing reactance. The calculated value of the magnetizing reactances for the actual and the modified air gap length are given in Table 6-8. It can be stated that any error in air gap size, almost proportionally affects the calculated magnetizing reactance. Therefore, the difference in measured and predicted values of magnetizing reactance may be attributed to the difference between actual air gap size of a test motor and its design value.

Table 6-8 Comparison of Magnetizing Reactance for Double Cage Motors

	Air gap length + 10%			Air gap length - 10%		
	TPCAD Result (ohm)	New Result (ohm)	Error Percent	TPCAD Result (ohm)	New Result (ohm)	Error Percent
NM 315Ma - 4 (160 kW - 4pole)	6.42	6.07	5.45	6.42	6.83	-6.83
NM 250M - 4 (55 kW - 4pole)	15.77	14.59	7.48	15.77	17.16	-8.81

Up to here, the comparison is done for double cage motors. From now on, same comparison of the machine parameters for single cage motors will be done for the rotor resistance, stator and rotor leakage reactance and magnetizing reactance.

For the single cage motors it is also observed that larger error occurs for r_2' . It can be observed that the measured rotor resistance value is greater than the calculated values. As mentioned for double cage motors, bubbles exist in the actual rotor bars coming from the alluminium casting process causes this difference. Since the rotor slot area is smaller for single cage rotors when it is compared with double cage rotors, more bubbles exist in the cage. Another reason for measuring higher resistance values may be performing the locked rotor test at 50 Hz at stand still. Due to this, the measured resistance value is likely to be higher than the resistance at operating conditions where the rotor frequency is very low. In TPCAD the DC resistance values are calculated.

As mentioned before, it is not possible to make an additional test to determine X_1 and X_2' separately. Using the empirical distribution for leakage reactances given in Table 3-1 ([6]), the class of the single cage motors is taken as "Class A" which means "Normal starting torque, normal starting current". Since there is some uncertainty here, the comparison is based on the total leakage reactance $X_1 + X_2'$. The error percentage for this value is changing from 4 to 12. This is an acceptable result as saturation effect and local distribution of the magnetic field is not considered in TPCAD calculations.

As stated before, the variation of the air gap size is very important for calculation of magnetizing reactance. Now, air gap length of the single cage motors will be increased and decreased with 10% of the actual gap length. New air gap length values are given in Table 6-9. According to the new air

gap length values, magnetizing reactance of these motors will be recalculated. New magnetizing reactance values are given in Table 6-10.

Table 6-9 New Air Gap Length Values of Single Cage Motors

	Airgap length + 10%		Air gap length - 10%	
	Actual Value (mm)	New Value (mm)	Actual Value (mm)	New Value (mm)
NM 112M – 4 (4 kW - 4pole)	0.425	0.4675	0.425	0.3825
NM 112M – 6 (2.2 kW - 6pole)	0.325	0.3575	0.325	0.2925
180M4B (18.5 kW - 4pole)	0.75	0.825	0.75	0.675
160L4A (15 kW - 4pole)	0.8	0.88	0.8	0.72

According to the (2-15), the value of the magnetizing reactance has an inverse relation with the air gap length. In addition, saturation affects the value of the magnetizing reactance. The calculated value of the magnetizing reactances for the actual and the modified air gap length are given in Table 6-10. It can be stated that any error in air gap size, almost proportionally affects the calculated magnetizing reactance. Therefore, the difference in measured and predicted values of magnetizing reactance may be attributed to the difference between actual air gap size of a test motor and its design value.

Table 6-10 Comparison of Magnetizing Reactance for Single Cage Motors

	Air gap length + 10%			Air gap length - 10%		
	TPCAD Result (ohm)	New Result (ohm)	Error Percent	TPCAD Result (ohm)	New Result (ohm)	Error Percent
NM 112M – 4 (4 kW - 4pole)	113.5200	105.5178	7.05	113.5200	122.9213	-8.28
NM 112M – 6 (2.2 kW - 6pole)	53.7326	49.7353	7.43	53.7326	57.4804	-6.97
180M4B (18.5 kW - 4pole)	47.507	43.726	7.95	47.507	52.019	-9.49
160L4A (15 kW - 4pole)	39.22	36.34	7.34	39.22	42.62	-8.66

6.2.3 Sensitivity of Performance Calculations to Equivalent Circuit Parameters

To evaluate the accuracy of TPCAD performance calculations it is worthwhile to assess how sensitive the performance calculations are to the parameters of the equivalent circuit. Sensitivity of performance calculations will be done for one double and one single cage motor respectively. For each motor; rotor resistance, stator and rotor leakage reactance and magnetizing reactance values will be changed by $\pm 10\%$ of their actual values and so the change of the performance calculations will be examined. Stator and core loss resistance values will not be changed for this verification. This is because, these values can be adjusted to make them equal with the stator and core loss parameters obtained from tests as mentioned in section 6.2.2. Comparison of the performance results will be done at the motor rated output power.

The performance comparison for double cage motors will be done for the motors named NM 315Ma - 4 (160 kW - 4pole) to check performance variation, when mentioned parameters are changed.

Note that, full load rotor resistance of the double cage motor is calculated by using the ratio of starting and full load rotor resistances of the motor found from TPCAD with starting rotor resistance of the motor calculated from No Load and Locked Rotor tests.

Effect of Rotor Resistance Change:

Actual value of the rotor resistance of the motor is 0.0426, and the modified values of that resistance with $\pm 10\%$ change are 0.04686 and 0.03834 respectively. Performance calculation of the motor according to the rotor resistance variation is given in Table 6-11.

Table 6-11 Performance Variation of Double Cage Motor for Rotor Resistance

NM 315Ma - 4 (160 kW - 4pole)	Rotor Resistance Value + 10%			Rotor Resistance Value - 10%		
	Test Results	New Results	Error Percent	Test Results	New Results	Error Percent
Output Power (W)	159904	159904	0.00	159904	159904	0.00
Power Factor	0.880	0.88	0.00	0.880	0.879	0.11
Efficiency	94.67	94.5	0.18	94.67	94.84	-0.18
Full-load Torque (Nm)	1045.82	1047.71	-0.18	1045.82	1043.95	0.18
Full-load Current (A)	168.42	168.7	-0.17	168.42	168.15	0.16
Speed (rpm)	1474	1471.3	0.18	1474	1476.6	-0.18
Starting Torque (Nm)	1768.40	1918.14	-8.47	1768.40	1612.54	8.81
Starting Current (A)	1098.40	1090.8	0.69	1098.40	1105.54	-0.65
No Load Current (A)	57.79	57.79	0.00	57.79	57.8	-0.02

Effect of Leakage Reactance Change:

Since the class of the motor is taken as “Class C” which means “High starting torque, low starting current” at parameter calculations, the stator and rotor leakage reactance values are different. For that reason these two values are changed with $\pm 10\%$ of their actual values. Actual value of the stator leakage reactance of the motor is 0.086, and the modified values of that resistance with $\pm 10\%$ change are 0.0946 and 0.0774 respectively. Actual value of the rotor leakage reactance of the motor is 0.2709, and the modified values of that resistance with $\pm 10\%$ change are 0.29799 and 0.24381 respectively. Performance calculation of the motor with mentioned leakage reactance variation is given in Table 6-12.

Table 6-12 Performance Variation of Double Cage Motor for Leakage Reactance

NM 315Ma - 4 (160 kW - 4pole)	Total Leakage Reactance Value + 10%			Total Leakage Reactance Value - 10%		
	Test Results	New Results	Error Percent	Test Results	New Results	Error Percent
Output Power (W)	159904	159904	0.00	159904	159904	0.00
Power Factor	0.880	0.874	0.68	0.880	0.885	-0.57
Efficiency	94.67	94.66	0.01	94.67	94.68	-0.01
Full-load Torque (Nm)	1045.82	1045.99	-0.02	1045.82	1045.68	0.01
Full-load Current (A)	168.42	169.58	-0.69	168.42	167.32	0.65
Speed (rpm)	1474	1473.7	0.02	1474	1474.15	-0.01
Starting Torque (Nm)	1768.40	1479.89	16.31	1768.40	2145.6	-21.33
Starting Current (A)	1098.40	1008.42	8.19	1098.40	1205.55	-9.76
No Load Current (A)	57.79	57.63	0.28	57.79	57.95	-0.28

Effect of Magnetizing Reactance Change:

Actual value of the magnetizing reactance of the motor is 6.38, and the modified values of that resistance with $\pm 10\%$ change are 7.018 and 5.742 respectively. Performance calculation of the motor for the mentioned magnetizing reactance variation is given in Table 6-13.

Table 6-13 Performance Variation of Double Cage Motor for Magnetizing Reactance

NM 315Ma - 4 (160 kW - 4pole)	Magnetizing Reactance Value + 10%			Magnetizing Reactance Value - 10%		
	Test Results	New Results	Error Percent	Test Results	New Results	Error Percent
Output Power (W)	159904	159904	0.00	159904	159904	0.00
Power Factor	0.880	0.892	-1.36	0.880	0.864	1.82
Efficiency	94.67	94.71	-0.04	94.67	94.63	0.04
Full-load Torque (Nm)	1045.82	1045.76	0.01	1045.82	1045.89	-0.01
Full-load Current (A)	168.42	165.97	1.45	168.42	171.59	-1.88
Speed (rpm)	1474	1474.02	0.00	1474	1473.85	0.01
Starting Torque (Nm)	1768.40	1771.95	-0.20	1768.40	1764.02	0.25
Starting Current (A)	1098.40	1095.9	0.23	1098.40	1101.43	-0.28
No Load Current (A)	57.79	52.63	8.93	57.79	64.09	-10.90

Performance calculation of the double cage motor named NM 315Ma - 4 (160 kW - 4pole) according to the $\pm 10\%$ variation on the actual values of rotor resistance, leakage reactances and magnetizing reactance are examined in Table 6-11, Table 6-12 and Table 6-13 respectively. According to these results, error percentages change only for starting conditions and no load current. The remaining performance is not affected. The summary of the performance variation of that motor is given in Table 6-14.

Table 6-14 Summary of Performance Variation for Double Cage Motor

NM 315Ma - 4 (160 kW - 4pole)	Rotor Resistance		Total Leakage Reactance		Magnetizing Reactance	
	Value + 10%	Value - 10%	Value + 10%	Value - 10%	Value + 10%	Value - 10%
Starting Torque % Error	-8.47	8.81	16.31	-21.33	-	-
Starting Current % Error	-	-	8.19	-9.76	-	-
No Load Current % Error	-	-	-	-	8.93	-10.90

According to the results given in Table 6-14, the change on the rotor resistance value of the motor has an almost directly proportional effect on the starting torque of the motor. That is why; the change of the rotor resistance affects the starting torque of the motor according to the equation (2-52). So, it shows that this is an expected result.

The change of the leakage reactance has an effect on the starting performance only as given in Table 6-14. According to the equation (2-51), leakage reactance has an inverse relation with the current. So when the leakage reactance is increased, the stator current decreased. The change on the current also affects the starting torque of the motor with the square of the error percent of the starting current according to equation (2-52).

The change of the magnetizing reactance has an effect on the no load current. According to the results it can be observed that, the change on the magnetizing reactance value of the motor has an almost directly proportional effect on the no load current of the motor.

Up to here, the performance comparison of double cage motors according to the variation of rotor resistance, stator and rotor leakage reactance and magnetizing reactance is examined. From now on, same comparison will be

done for the single cage motor named NM 112M – 4 (4 kW - 4pole) to check performance variation, when mentioned parameters are changed.

Effect of Rotor Resistance Change:

Actual value of the rotor resistance of the motor is 3.925, and the modified values of that resistance with $\pm 10\%$ change are 4.3175 and 3.5325 respectively. Performance calculation of the motor according to the rotor resistance variation is given in Table 6-15.

Table 6-15 Performance Variation of Single Cage Motor for Rotor Resistance

NM 112M - 4 (4 kW - 4pole)	Rotor Resistance Value + 10%			Rotor Resistance Value - 10%		
	Test Results	New Results	Error Percent	Test Results	New Results	Error Percent
Output Power (W)	4001	4001	0.00	4001	4001	0.00
Power Factor	0.793	0.794	-0.13	0.793	0.792	0.13
Efficiency	84.93	84.52	0.48	84.93	85.33	-0.47
Full-load Torque (Nm)	26.75	26.89	-0.52	26.75	26.62	0.49
Full-load Current (A)	5.20	5.22	-0.38	5.20	5.19	0.19
Speed (rpm)	1433	1426.24	0.47	1433	1440.3	-0.51
Starting Torque (Nm)	83.21	87.44	-5.08	83.21	78.36	5.83
Starting Current (A)	35.17	34.38	2.25	35.17	35.96	-2.25
No Load Current (A)	2.92	2.919	0.03	2.92	2.921	-0.03

Effect of Leakage Reactance Change:

Since the class of the motor is taken as “Class A” which means “Normal starting torque, normal starting current” at parameter calculations, the stator and rotor leakage reactance values are equal. For that reason these two

values are changed with $\pm 10\%$ of their actual values. Actual value of the stator and rotor leakage reactance of the motor is 4.135, and the modified values of that resistance with $\pm 10\%$ change are 4.5485 and 3.7215 respectively. Performance calculation of the motor with mentioned leakage reactance variation is given in Table 6-16.

Table 6-16 Performance Variation of Single Cage Motor for Leakage Reactance

NM 112M - 4 (4 kW - 4pole)	Total Leakage Reactance Value + 10%			Total Leakage Reactance Value - 10%		
	Test Results	New Results	Error Percent	Test Results	New Results	Error Percent
Output Power (W)	4001	4001	0.00	4001	4001	0.00
Power Factor	0.793	0.791	0.25	0.793	0.796	-0.38
Efficiency	84.93	84.89	0.05	84.93	84.96	-0.04
Full-load Torque (Nm)	26.75	26.77	-0.07	26.75	26.74	0.04
Full-load Current (A)	5.20	5.22	-0.38	5.20	5.18	0.38
Speed (rpm)	1433	1432.69	0.02	1433	1433.89	-0.06
Starting Torque (Nm)	83.21	74.13	10.91	83.21	93.53	-12.40
Starting Current (A)	35.17	33.3	5.32	35.17	37.16	-5.66
No Load Current (A)	2.92	2.908	0.41	2.92	2.932	-0.41

Effect of Magnetizing Reactance Change:

Actual value of the magnetizing reactance of the motor is 120.85, and the modified values of that resistance with $\pm 10\%$ change are 132.935 and 108.765 respectively. Performance calculation of the motor for the mentioned magnetizing reactance variation is given in Table 6-17.

Table 6-17 Performance Variation of Single Cage Motor for Magnetizing Reactance

NM 112M - 4 (4 kW - 4pole)	Magnetizing Reactance Value + 10%			Magnetizing Reactance Value - 10%		
	Test Results	New Results	Error Percent	Test Results	New Results	Error Percent
Output Power (W)	4001	4001	0.00	4001	4001	0.00
Power Factor	0.793	0.815	-2.77	0.793	0.767	3.28
Efficiency	84.93	85.25	-0.38	84.93	84.5	0.51
Full-load Torque (Nm)	26.75	26.75	0.00	26.75	26.76	-0.04
Full-load Current (A)	5.20	5.04	3.08	5.20	5.41	-4.04
Speed (rpm)	1433	1433.74	-0.05	1433	1432.77	0.02
Starting Torque (Nm)	83.21	83.47	-0.31	83.21	82.89	0.38
Starting Current (A)	35.17	35.11	0.17	35.17	35.23	-0.17
No Load Current (A)	2.92	2.66	8.90	2.92	3.23	-10.62

Performance calculation of the single cage motor named NM 112M – 4 (4 kW - 4pole) according to the $\pm 10\%$ variation on the actual values of rotor resistance, leakage reactances and magnetizing reactance are examined in Table 6-15, Table 6-16 and Table 6-17 respectively. According to these results, error percentages change only for starting conditions and no load current. The remaining performance is not affected. The summary of the performance variation of that motor is given in Table 6-18.

Table 6-18 Summary of Performance Variation for Single Cage Motor

NM 112M - 4 (4 kW - 4pole)	Rotor Resistance		Total Leakage Reactance		Magnetizing Reactance	
	Value + 10%	Value - 10%	Value + 10%	Value - 10%	Value + 10%	Value - 10%
Starting Torque % Error	-5.08	5.83	10.91	-12.40	-	-
Starting Current % Error	2.25	-2.25	5.32	-5.66	-	-
No Load Current % Error	-	-	-	-	8.90	-10.62

According to the results given in Table 6-18, the change on the rotor resistance value of the motor has an effect on the starting performance of the motor. Rotor resistance has an inverse relation with the current according to the equation (2-51). So when the rotor resistance is increased, the stator current decreased. The change on the current also affects the starting torque of the motor according to the equation (2-52). Since the current and rotor resistance are both affected, the starting torque is not directly proportional effected according to the change on the rotor resistance.

To clarify this, the effect of the equivalent circuit impedance according to the +10% change on the rotor resistance is examined. Since total resistance is too small for the motor named NM 315Ma - 4 (160 kW - 4pole) when it is compared with the total leakage reactance, the change on the rotor resistance has a negligible effect on the total impedance as given in Table 6-19. However, this effect is higher for the motor named NM 112M - 4 (4 kW - 4pole). So, when the total impedance is increased the current becomes lower. As observed from the starting current given in Table 6-11, the change of the rotor resistance has a small effect on the current. For that reason, the change on the rotor resistance has an almost directly proportional effect on the starting torque of the motor according to the equation (2-52). However,

the change on the rotor resistance has an effect on the total impedance which affects both starting current and torque. As a result of that, the starting torque is not directly proportional affected according to the change on the rotor resistance when it is compared with other motor.

Table 6-19 Effect of Impedance on Current

	NM 315Ma - 4 (160 kW - 4pole)			NM 112M - 4 (4 kW - 4pole)		
	Actual Value	New Value	Error Percent	Actual Value	New Value	Error Percent
$R = r_1 + r_2' \text{ (ohm)}$	0.0646	0.0688	6.10	7.523	7.883	4.56
$X = x_1 + x_2' \text{ (ohm)}$	0.3796	0.3796	0.00	8.270	8.270	0.00
$Z = \sqrt{R^2 + X^2}$	0.3850	0.3857	0.18	11.180	11.425	2.14

The change of the leakage reactance has an effect on the starting performance as given in Table 6-18. According to the equation (2-51), leakage reactance has an inverse relation with the current. So when the leakage reactance is increased, the stator current decreased. The change on the current also affects the starting torque of the motor with the square of the error percent of the starting current according to the equation (2-52). Mentioned condition expressed above for rotor resistance is also valid for leakage reactances.

The change of the magnetizing reactance has an effect on the no load current. According to the results it can be observed that, the change on the magnetizing reactance value of the motor has an almost directly proportional effect on the no load current of the motor.

6.2.4 Performance Calculation from Test Parameters and Evaluation of Model Accuracy

In this part, performance of the test motors calculated using the parameters obtained from No Load and Locked Rotor tests will be compared with the performance tests results. By comparing these performance results, verification of the equivalent circuit model accuracy will be done. Comparison of the performance results will be done at the motor rated output power.

Motor performance of the test motors named NM 315Ma - 4 (160 kW - 4pole), NM 250M - 4 (55 kW - 4pole), NM 112M - 4 (4 kW - 4pole), NM 112M - 6 (2.2 kW - 6pole), 180M4B (18.5 kW - 4pole) and 160L4A (15 kW - 4pole) are calculated. Results of the double cage motors are given in Table 6-20 and results of the single cage motors are given in Table 6-21 and Table 6-22 respectively.

In these tables, the first column "Test Results" shows the performance results obtained from test measurement; the second column "From Test Params" shows the calculated performance from the motor parameters and the third column "Error Percent" shows the error percentage of these two calculations. Error percentage calculation is made according to the equation given in (6-3).

Table 6-20 Double Cage Motors Performance Analysis (measured parameters)

	NM 315Ma - 4 (160 kW - 4pole)			NM 250M - 4 (55 kW - 4pole)		
	Test Results	From Test Params	Error Percent	Test Results	From Test Params	Error Percent
Output Power (W)	159904	159904	0.00	54799	54799	0.00
Power Factor	0.866	0.880	-1.62	0.883	0.877	0.68
Efficiency	95.29	94.67	0.65	92.71	92.03	0.73
Full-load Torque (Nm)	1025.50	1045.82	-1.98	355.4	362.03	-1.87
Full-load Current (A)	170.72	168.42	1.35	60.10	59.53	0.95
Speed (rpm)	1489	1474	1.01	1473	1466	0.48
Starting Torque (Nm)	1692.22	1768.40	-3.50	799.65	794.90	0.59
Starting Current (A)	1138.70	1098.40	3.54	394.27	387.87	1.62
No Load Current (A)	58.49	57.79	1.20	21.66	20.62	3.80

Table 6-21 Single Cage Motors Performance Analysis - 1 (measured parameters)

	NM 112M - 4 (4 kW - 4pole)			NM 112M - 6 (2.2 kW - 6pole)		
	Test Results	From Test Params	Error Percent	Test Results	From Test Params	Error Percent
Output Power (W)	4001	4001	0.00	2216	2216	0.00
Power Factor	0.811	0.793	2.22	0.751	0.734	2.26
Efficiency	82.96	84.93	-2.37	77.65	79.86	-2.85
Full-load Torque (Nm)	26.78	26.75	0.11	22.40	22.67	-1.21
Full-load Current (A)	5.34	5.20	2.62	5.60	5.72	-2.14
Speed (rpm)	1427	1433	-0.42	945	940	0.53

Table 6-21 (cont'd)

	NM 112M - 4 (4 kW - 4pole)			NM 112M - 6 (2.2 kW - 6pole)		
	Test Results	From Test Params	Error Percent	Test Results	From Test Params	Error Percent
Starting Torque (Nm)	84.62	83.21	1.67	88.60	90.57	-2.22
Starting Current (A)	34.36	35.17	-2.36	32.92	34.12	-3.65
No Load Current (A)	2.97	2.92	1.68	3.79	3.77	0.53

Table 6-22 Single Cage Motors Performance Analysis - 2 (measured parameters)

	180M4B (18.5 kW - 4pole)			160L4A (15 kW - 4pole)		
	Test Results	From Test Params	Error Percent	Test Results	From Test Params	Error Percent
Output Power (W)	18500	18500	0.00	15089	15089	0.00
Power Factor	0.88	0.86	2.27	0.8	0.8	0.00
Efficiency	91.6	91.2	0.44	89.2	89.81	-0.68
Full-load Torque (Nm)	124.97	123.54	1.14	98.99	100.15	-1.17
Full-load Current (A)	20.78	20.62	0.77	18.47	18.34	0.70
Speed (rpm)	1450	1442	0.55	1455	1449	0.41
Starting Torque (Nm)	260.4	259.74	0.25	259.96	255.18	1.84
Starting Current (A)	139.9	135.85	2.89	135.8	131.43	3.22
No Load Current (A)	7.67	7.46	2.74	9.64	9.42	2.28

According to the overall performance results, it can be concluded that full load performance results obtained from test parameters are within 2.5% error when it is compared with the performance test results. That means the

used model for the performance calculations gives reasonable results for full load conditions. On the other hand, error percentages for starting conditions are within 3.5% error.

Parameters of the motor are obtained from No Load and Locked Rotor tests. Locked rotor test is performed at 50 Hz at stand still. Due to this, the measured rotor resistance value is likely to be higher than the resistance at operating conditions where the rotor frequency is very low. In addition, no additional test is possible to obtain stator and rotor leakage reactance separately. For that reason, an empirical distribution for these leakage reactances is used according to the standard as given in Table 3-1. Effect of the rotor resistance and leakage reactances on the performance of the motor is examined in section 6.2.3. According to these, the error percentages are in acceptable range. So, the model used in TPCAD can be used for the performance calculations.

6.2.5 Performance Calculation from Motor Geometry Using TPCAD and Accuracy of TPCAD Calculation

In this part, performance result of the test motors obtained from motor geometry using TPCAD will be compared with the performance test results to verify the accuracy of the TPCAD calculation. Comparison of the performance results will be done at the motor rated output power.

Motor performances of the test motors given in Table 6-1 are calculated. Results of the double cage motors are given in Table 6-23 and results of the single cage motors are given in Table 6-24, Table 6-25, Table 6-26 and Table 6-27 respectively.

In these tables, the first column "Test Results" shows the performance results obtained from test measurement; the second column "TPCAD Results" shows the calculated performance from motor geometry and the

third column “Error Percent” shows the error percentage of these two calculations. Error percentage calculation is made according to the equation given in (6-3).

Table 6-23 Double Cage Motors Performance Analysis (calculated performance)

	NM 315Ma - 4 (160 kW - 4pole)			NM 250M - 4 (55 kW - 4pole)		
	Test Results	TPCAD Results	Error Percent	Test Results	TPCAD Results	Error Percent
Output Power (W)	159904	159904	0.00	54799	54799	0.00
Power Factor	0.866	0.884	-2.08	0.883	0.873	1.13
Efficiency	95.29	94.95	0.36	92.71	92.25	0.50
Full-load Torque (Nm)	1025.50	1042.70	-1.68	355.4	360.97	-1.57
Full-load Current (A)	170.72	167.16	2.09	60.10	59.70	-0.67
Speed (rpm)	1489	1479	0.67	1473	1470	0.20
Starting Torque (Nm)	1692.22	1682.04	0.60	799.65	843.3	-5.46
Starting Current (A)	1138.70	1180.69	-3.69	394.27	424.6	-7.69
No Load Current (A)	58.49	57.65	1.44	21.66	22.05	-1.80

Table 6-24 Single Cage Motors Performance Analysis - 1 (calculated performance)

	NM 112M - 4 (4 kW - 4pole)			NM 112M - 6 (2.2 kW - 6pole)		
	Test Results	TPCAD Results	Error Percent	Test Results	TPCAD Results	Error Percent
Output Power (W)	4001	4001	0.00	2216	2216	0.00
Power Factor	0.811	0.777	4.19	0.751	0.731	2.66
Efficiency	82.96	84.91	-2.35	77.65	80.94	-4.24
Full-load Torque (Nm)	26.78	26.64	0.52	22.40	22.37	0.13

Table 6-24 (cont'd)

	NM 112M - 4 (4 kW - 4pole)			NM 112M - 6 (2.2 kW - 6pole)		
	Test Results	TPCAD Results	Error Percent	Test Results	TPCAD Results	Error Percent
Full-load Current (A)	5.34	5.32	0.37	5.60	5.72	-2.14
Speed (rpm)	1427	1439	-0.84	945	952	-0.74
Starting Torque (Nm)	84.62	90.90	-7.42	88.60	80.95	8.63
Starting Current (A)	34.36	38.29	-11.44	32.92	36.46	-10.75
No Load Current (A)	2.97	3.16	-6.40	3.79	3.79	0.00

Table 6-25 Single Cage Motors Performance Analysis - 2 (calculated performance)

	180M4B (18.5 kW - 4pole)			160L4A (15 kW - 4pole)		
	Test Results	TPCAD Results	Error Percent	Test Results	TPCAD Results	Error Percent
Output Power (W)	18500	18500	0.00	15089	15089	0.00
Power Factor	0.88	0.87	1.14	0.8	0.8	0.00
Efficiency	91.6	91.76	-0.17	89.2	90.22	-1.14
Full-load Torque (Nm)	124.97	122.88	1.67	98.99	99.6	-0.62
Full-load Current (A)	20.78	20.33	2.17	18.47	18.24	1.25
Speed (rpm)	1450	1449	0.07	1455	1456	-0.07
Starting Torque (Nm)	260.4	279.85	-7.47	259.96	276.36	-6.31
Starting Current (A)	139.9	150.66	-7.69	135.8	146.65	-7.99
No Load Current (A)	7.67	7.63	0.52	9.64	9.24	4.15

Table 6-26 Single Cage Motors Performance Analysis - 3 (calculated performance)

	132S2C (7.5 kW - 2pole)			132M4B (7.5 kW - 4pole)		
	Test Results	TPCAD Results	Error Percent	Test Results	TPCAD Results	Error Percent
Output Power (W)	7623	7623	0.00	7629	7629	0.00
Power Factor	0.91	0.91	0.00	0.81	0.82	-1.23
Efficiency	86.9	87.35	-0.52	89.9	89.43	0.52
Full-load Torque (Nm)	24.94	25.77	-3.33	49.4	50	-1.21
Full-load Current (A)	8.44	8.35	1.07	9.1	9.08	0.22
Speed (rpm)	2917	2921	-0.14	1474	1459	1.02
Starting Torque (Nm)	54.05	57.25	-5.92	114.35	106.58	6.79
Starting Current (A)	65.7	70.78	-7.73	65.87	67.12	-1.90
No Load Current (A)	2.78	2.55	8.27	4.22	4.19	0.71

Table 6-27 Single Cage Motors Performance Analysis - 4 (calculated performance)

	132S4C (5.5 kW - 4pole)			90L4A (1.5 kW - 4pole)		
	Test Results	TPCAD Results	Error Percent	Test Results	TPCAD Results	Error Percent
Output Power (W)	5573	5573	0.00	1500	1500	-0.00
Power Factor	0.79	0.81	-2.53	0.80	0.77	3.75
Efficiency	87.7	87.11	0.67	79	82.26	-4.13
Full-load Torque (Nm)	36.28	37.31	-2.84	10.32	10.04	2.71
Full-load Current (A)	7.07	6.92	2.12	3.45	3.59	-0.42
Speed (rpm)	1466	1448	1.23	1442	1436	0.42
Starting Torque (Nm)	87.28	85.77	1.73	27.48	27.46	0.07

Table 6-27 (cont'd)

	132S4C (5.5 kW - 4pole)			90L4A (1.5 kW - 4pole)		
	Test Results	TPCAD Results	Error Percent	Test Results	TPCAD Results	Error Percent
Starting Current (A)	49.1	47.01	4.26	20.46	21.89	-6.99
No Load Current (A)	3.52	3.39	3.69	2.35	2.24	4.68

According to the overall performance results, it can be concluded that the performance calculations generated from TPCAD give reasonable results for full load conditions within 5% error. On the other hand, error percentages increase for starting conditions.

Error percentages for starting torque and current are within 10% error. This is because the current reaches higher than the full load condition and saturation become dominant for starting. The saturating parts affect the reactances with increasing their actual values. This is why, calculated leakage reactance values from tests are higher than the values obtained from motor geometry using TPCAD as given in section 6.2.2. Effect of the leakage reactances on the starting performance is examined in section 6.2.3. In that part, actual values of the leakage reactances are modified with $\pm 10\%$ change. As a result of that, the starting current of the motor is changed with 10% error which is an expected variation. The change on the current also changes the starting torque of the motor with the square of the error percent of the starting current according to the equation (2-52).

Error percentages for no load current are within 5%. However, for the motor named NM 112M-4 (4 kW - 4 pole) and 132S2C (7.5 kW - 2pole), error value becomes higher. This is coming from the differences at the magnetizing reactance. Machining tolerances make the air gap different which changes magnetic properties of this part of the machine. For that

reason, magnetizing reactance and thus no load current become different. Effect of the magnetizing reactance on the no load current is examined in section 6.2.3. In that part, actual value of the magnetizing reactance of that motor is modified with $\pm 10\%$ change. As a result of that, the no load current of the motor is changed with 10% error which is an expected variation.

Air gap length of these motors is decreased for NM 112M-4 (4 kW - 4 pole) and increased for 132S2C (7.5 kW - 2pole) with 0.075 mm which is the machining tolerance given in the drawings of these motors. (Table 6-28) Using new values, the performance of these motors are recalculated and the no load currents values are given in Table 6-29.

Table 6-28 Machining Tolerances of the Motors

	NM 112M - 4 (4 kW - 4pole)			132S2C (7.5 kW - 2pole)		
	Air gap Length	Tolerance	Percent	Air gap Length	Tolerance	Percent
Length (mm)	0.425	0.075	17.64	0.5	0.075	15.00

Table 6-29 No Load Current Verification

	NM 112M - 4 (4 kW - 4pole)			132S2C (7.5 kW - 2pole)		
	Test Results	New TPCAD Results	Error Percent	Test Results	New TPCAD Results	Error Percent
No Load Current (A)	2.97	2.95	0.67	2.78	2.71	2.51

According to the results, it can be concluded that machining tolerances make the air gap different which has an effect on magnetizing reactance and thus no load current.

6.3 Verification of SPCAD Results

The purpose of this section is;

- To assess the accuracy of parameter calculation by SPCAD.
- To assess the accuracy of SPCAD performance calculations, when measured parameters are used for performance calculation via SPCAD. Note that, this study indicates the limits of the models used in SPCAD for performance calculation. This statement assumes that the tests on the motor give the most realistic values for parameters.
- Finally, the test motor performance is calculated using SPCAD calculated parameters and compared with test results. In this manner an idea of the accuracy that may be expected from SPCAD when a new design is made.

6.3.1 Test Motors

It is worthwhile to find out whether the accuracy of predictions may depend on the size of the motor or number of poles. Furthermore, this software is capable of simulating capacitor start or capacitor run motors. However, it was not possible to find test motors other than capacitor start types. Also, it was not possible to access enough motors of different sizes with pole numbers other than 4. The motors tested are listed in Table 6-30. Test results are taken from the verifications done in reference [2]. Motor data of these motors are given in APPENDIX D.

Table 6-30 Single Phase Test Motors

Pole Number	Power	Motor Type	Capacitor Value (μF)	Slot Type	Model No	Manufacturer
4 pole	180 W	Cap. Start	49.4	Closed	77C014	TEE A.Ş.
4 pole	370 W	Cap. Start	71.2	Closed	87C012	TEE A.Ş.
2 pole	550 W	Cap. Start	72.7	Closed	87A0345B	TEE A.Ş.
4 pole	750 W	Cap. Start	149.8	Closed	97C100	TEE A.Ş.
2 pole	750 W	Cap. Start	151	Closed	97A1005B	TEE A.Ş.

Performed tests are;

- No load test
- Locked rotor test
- Starting performance tests
- Speed - Torque tests

In Table 6-31, temperatures of the test motors after starting and load tests are given respectively. These values are used in SPCAD to calculate related performance of the motor.

Table 6-31 Performance Calculation Temperature for Single Phase Motors

Motor Model	Start Temp	Starting Test	Load Test
77C014 (180 W-4pole)	25	35	35
87C012 (370 W-4pole)	25	35	35
87A0345B (550 W-4pole)	20	68	68
97C100 (750 W-4pole)	20	45	45
97A1005B (750 W-2pole)	20	65	65

6.3.2 Verification of Parameter Calculation Algorithm

In this part, the parameter calculation algorithm is verified by comparing the parameters obtained from tests and the parameters obtained from the motor geometry.

Motor parameters of the test motors named 77C014 (180 W-4pole), 87C012 (370 W-4pole) and 97C100 (750 W-4pole) are calculated. Results of these motors are given in Table 6-32 and Table 6-33 respectively. Since test results of the other test motors are not available, parameters of these motors are not calculated.

In these tables, the first column "Test Results" shows the calculated parameters according to tests; the second column "SPCAD Results" shows the calculated parameters from the motor geometry and the third column "Error Percent" shows the error percentage of these two calculations.

Error percentage is defined as the difference between the test and SPCAD results. Error percentage is calculated from the equation given in (6-3).

Table 6-32 Single Phase Motor Parameter Calculations - 1

	77C014 (180 W-4pole)			87C012 (370 W-4pole)		
	Test Results	SPCAD Results	Error Percent	Test Results	SPCAD Results	Error Percent
r_1 (ohm)	15.33	15.50	-1.11	6.62	6.64	-0.30
r_2' (ohm)	7.62	7.50	1.57	4.69	4.59	2.13
x_1 (ohm)	11.92	9.99	14.19	6.77	5.86	13.44
x_m (ohm)	156.90	162.42	-3.52	104.60	110.24	-5.39
r_a (ohm)	40.47	39.99	1.19	25.06	25.52	-1.84
x_a (ohm)	13.44	15.63	-14.29	12.51	13.44	-7.43

Table 6-33 Single Phase Motor Parameter Calculations - 2

	97C100 (750 W-4pole)		
	Test Results	SPCAD Results	Error Percent
r_1 (ohm)	2.43	2.44	-0.41
r_2' (ohm)	2.82	2.62	7.09
x_1 (ohm)	3.45	3.38	2.03
x_m (ohm)	70.0	67.69	3.30
r_a (ohm)	8.88	8.88	0.00
x_a (ohm)	4.39	4.69	6.83

As it can be observed from the results, SPCAD calculates main and auxiliary winding resistances with a small error percentage when it is compared with the measured main and auxiliary winding resistances. This error is coming from the length of the conductor used on the motor. Used stator stack length and coil extension values are the exact values taken from the drawings. It is also possible to change the coil extension value to make these equal. However no correction is made on that value for the calculations here.

According to this information, comparison of the machine parameters will be done for the rotor resistance, main and auxiliary winding leakage reactance and magnetizing reactance.

For the single phase motors it is observed that smaller calculation error occurs for r_2' when it is compared with the results obtained from three phase motors. As mentioned before, errors may come from the resistivity of aluminum used for production and existing bubbles in the actual rotor bars.

The error percentage for main winding leakage reactance is changing from 2 to 14. This is an acceptable result as saturation effect and local distribution of the magnetic field is not considered in SPCAD calculations. To have a more accurate reactance calculation, advanced methods to calculate the flux distribution in the lamination can be used. (eg. using finite element methods to find exact flux distribution) The effect of the errors in predicting motor performance is discussed in section 6.3.3.

Furthermore, calculated magnetizing reactances are higher than the test results. However, the differences are not much. Any difference may be attributed to machining tolerances. The variation of the air gap size is important for calculation of magnetizing reactance. Now, air gap length of the single phase motors will be increased and decreased with 10% of the actual gap length. New air gap length values are given in Table 6-34. According to the new air gap length values, magnetizing reactance of these motors will be recalculated. New magnetizing reactance values are given in Table 6-35.

Table 6-34 New Air Gap Length Values of Single Phase Motors

	Airgap length + 10%		Air gap length - 10%	
	Actual Value (mm)	New Value (mm)	Actual Value (mm)	New Value (mm)
77C014 (180 W-4pole)	0.3	0.33	0.3	0.27
87C012 (370 W-4pole)	0.3	0.33	0.3	0.27
97C100 (750 W-4pole)	0.25	0.275	0.25	0.225

As given in (4-1), the value of the magnetizing reactance has an inverse relation with the air gap length. For example, when the actual air gap length is increased, the new value of the magnetizing reactance becomes less

when it is compared with the actual magnetizing reactance value. In addition, saturation affects the value of the magnetizing reactance. The calculated value of the magnetizing reactances for the actual and the modified air gap length are given in Table 6-35. It can be stated that any error in air gap size, almost proportionally affects the calculated magnetizing reactance. Therefore, the difference in measured and predicted values of magnetizing reactance may be attributed to the difference between actual air gap size of a test motor and its design value.

Table 6-35 Comparison of Magnetizing Reactance for Single Phase Motors

	Air gap length + 10%			Air gap length - 10%		
	SPCAD Result (ohm)	New Result (ohm)	Error Percent	SPCAD Result (ohm)	New Result (ohm)	Error Percent
77C014 (180 W-4pole)	162.42	152.39	6.06	162.42	173.98	-7.11
87C012 (370 W-4pole)	110.24	103.19	6.39	110.24	118.40	-7.40
97C100 (750 W-4pole)	67.7	63.43	6.30	67.7	72.17	-6.60

6.3.3 Sensitivity of Performance Calculations to Equivalent Circuit Parameters

To evaluate the accuracy of SPCAD performance calculations it is worthwhile to assess how sensitive the performance calculations are to the parameters of the equivalent circuit. Sensitivity of performance calculations will be done for one single phase motor. For the motor; rotor resistance, main and auxiliary winding leakage reactance and magnetizing reactance values will be changed by $\pm 10\%$ of their actual values and so the change of the performance calculations will be examined. Main and auxiliary winding resistance values will not be changed for this study. This is because, these

values can be adjusted to make them equal with the main and auxiliary winding parameters obtained from tests as mentioned in section 6.3.2. Comparison of the performance results will be done at the motor rated output power.

The performance comparison for single phase motors will be done for the motors named 87C012 (370 W-4pole) to check performance variation, when mentioned parameters are changed.

Effect of Rotor Resistance Change:

Actual value of the rotor resistance of the motor is 4.69, and the modified values of that resistance with $\pm 10\%$ change are 5.159 and 4.221 respectively. Performance calculation of the motor according to the rotor resistance variation is given in Table 6-36.

Table 6-36 Performance Variation of Single Phase Motor for Rotor Resistance

87C012 (370 W-4pole)	Rotor Resistance Value + 10%			Rotor Resistance Value - 10%		
	Test Results	New Results	Error Percent	Test Results	New Results	Error Percent
Output Power (W)	370	370	0.00	370	370	0.00
Power Factor	0.65	0.66	-1.54	0.65	0.65	0.00
Efficiency	57.69	56.94	1.30	57.69	58.42	-1.27
Full-load Torque (Nm)	2.46	2.47	-0.41	2.46	2.45	0.41
Full-load Current (A)	4.45	4.47	-0.45	4.45	4.43	0.45
Speed (rpm)	1438	1430.2	0.51	1438	1444.7	-0.50
Starting Torque (Nm)	6.00	6.25	-4.17	6.00	5.71	4.83
Starting Current (A)	17.93	17.62	1.73	17.93	18.24	-1.73
No Load Current (A)	3.64	3.65	-0.27	3.64	3.63	0.27

Effect of Main Winding Leakage Reactance Change:

Actual value of the main winding leakage reactance of the motor is 6.77, and the modified values of that resistance with $\pm 10\%$ change are 7.447 and 6.053 respectively. Performance calculation of the motor with mentioned leakage reactance variation is given in Table 6-37.

Table 6-37 Performance Variation of Single Phase Motor for Main Winding Leakage Reactance

87C012 (370 W-4pole)	Main Winding Leakage Reactance Value + 10%			Main Winding Leakage Reactance Value - 10%		
	Test Results	New Results	Error Percent	Test Results	New Results	Error Percent
Output Power (W)	370	370	0.00	370	370	0.00
Power Factor	0.65	0.65	0.00	0.65	0.65	0.00
Efficiency	57.69	57.51	0.31	57.69	57.81	-0.21
Full-load Torque (Nm)	2.46	2.46	0.00	2.46	2.45	0.41
Full-load Current (A)	4.45	4.46	-0.22	4.45	4.43	0.45
Speed (rpm)	1438	1434.7	0.19	1438	1440.2	-0.19
Starting Torque (Nm)	6.00	5.87	2.17	6.00	6.12	-2.00
Starting Current (A)	17.93	17.3	3.51	17.93	18.58	-3.63
No Load Current (A)	3.64	3.63	0.27	3.64	3.65	-0.27

Effect of Auxiliary Winding Leakage Reactance Change:

Actual value of the auxiliary winding leakage reactance of the motor is 12.51, and the modified values of that resistance with $\pm 10\%$ change are 13.761 and 11.259 respectively. Performance calculation of the motor with mentioned leakage reactance variation is given in Table 6-38.

Table 6-38 Performance Variation of Single Phase Motor for Auxiliary Winding Leakage Reactance

87C012 (370 W-4pole)	Auxiliary Winding Leakage Reactance Value + 10%			Auxiliary Winding Leakage Reactance Value - 10%		
	Test Results	New Results	Error Percent	Test Results	New Results	Error Percent
Output Power (W)	370	370	0.00	370	370	0.00
Power Factor	0.65	0.65	0.00	0.65	0.65	0.00
Efficiency	57.69	57.69	0.00	57.69	57.69	0.00
Full-load Torque (Nm)	2.46	2.46	0.00	2.46	2.46	0.00
Full-load Current (A)	4.45	4.45	0.00	4.45	4.45	0.00
Speed (rpm)	1438	1437.5	0.00	1438	1437.5	0.00
Starting Torque (Nm)	6.00	6.03	-0.50	6.00	5.97	0.50
Starting Current (A)	17.93	18.07	-0.78	17.93	17.79	0.78
No Load Current (A)	3.64	3.64	0.00	3.64	3.64	0.00

Effect of Magnetizing Reactance Change:

Actual value of the magnetizing reactance of the motor is 104.6, and the modified values of that resistance with $\pm 10\%$ change are 115.06 and 94.14 respectively. Performance calculation of the motor for the mentioned magnetizing reactance variation is given in Table 6-39.

Table 6-39 Performance Variation of Single Phase Motor for Magnetizing Reactance

87C012 (370 W-4pole)	Magnetizing Reactance Value + 10%			Magnetizing Reactance Value - 10%		
	Test Results	New Results	Error Percent	Test Results	New Results	Error Percent
Output Power (W)	370	370	0.00	370	370	0.00
Power Factor	0.65	0.66	-1.54	0.65	0.64	1.54
Efficiency	57.69	59.31	-2.81	57.69	55.73	3.40
Full-load Torque (Nm)	2.46	2.45	0.41	2.46	2.46	0.00
Full-load Current (A)	4.45	4.32	2.92	4.45	4.62	-3.82
Speed (rpm)	1438	1440	-0.17	1438	1434.5	0.21
Starting Torque (Nm)	6.00	6.02	-0.33	6.00	5.97	0.50
Starting Current (A)	17.93	17.9	0.17	17.93	17.95	-0.11
No Load Current (A)	3.64	3.38	7.14	3.64	3.95	-8.52

Performance calculation of the single phase motor named 87C012 (370 W-4pole) according to the $\pm 10\%$ variation on the actual values of rotor resistance, main and auxiliary winding leakage reactances and magnetizing reactance are examined in Table 6-36, Table 6-37 and Table 6-39 respectively. According to these results, error percentages change only for starting conditions and no load current. However, the change in starting current and torque is negligible small. The remaining performance is not affected. The summary of the performance variation of that motor is given in Table 6-40.

Table 6-40 Summary of Performance Variation for Single Phase Motor

87C012 (370 W-4pole)	Rotor Resistance		Main Winding Reactance		Magnetizing Reactance		Aux Winding Reactance	
	Value + 10%	Value - 10%	Value + 10%	Value - 10%	Value + 10%	Value - 10%	Value + 10%	Value - 10%
Starting Torque % Error	-4.17	4.83	2.17	-2.00	-	-	-0.50	0.50
Starting Current % Error	1.73	-1.73	3.51	-3.63	-	-	-0.78	0.78
No Load Current % Error	-	-	-	-	7.14	-8.52	-	-

According to the results given in Table 6-40, the change on the rotor resistance value of the motor has an effect on the starting performance of the motor. Rotor resistance affects the apparent resistance and reactance of the forward and backward field of the equivalent circuit given in section 4.8. For that reason rotor resistance has an effect on the current according to the equation (4-29) and (4-30). So when the rotor resistance is increased, the stator current decreased. The change on the current also affects the starting torque of the motor according to the equation (4-42). Since the current and rotor resistance are both affected, the starting torque is not directly proportional effected according to the change on the rotor resistance.

The change of the main winding leakage reactance has an effect on the starting performance as given in Table 6-37. The change on that value affects the apparent resistance and reactance of the forward and backward field of the equivalent circuit given in section 4.8. For that reason main winding reactance has an effect on the current according to the equation (4-29) and (4-30). Since the change on the apparent resistance and reactance of the forward and backward field is larger than the current, the change on the starting torque becomes less than the change on the current.

The change on the auxiliary winding leakage reactance only affects the starting performance of the motor since the tested motors are capacitor start type. The results given in Table 6-38 show that the idea is valid, because there is no change on the full load performance of the motor. Since the effect of the variation of auxiliary winding leakage reactance on the equivalent circuit impedance is low, the change on the starting torque and current and so the error percent becomes low.

The change of the magnetizing reactance has an effect on the no load current. According to the results it can be observed that, the change on the magnetizing reactance value of the motor has an almost directly proportional effect on the no load current of the motor.

6.3.4 Performance Calculation from Test Parameters and Evaluation of Model Accuracy

In this part, performance of the test motors calculated using the parameters will be compared with the performance tests results. By comparing these performance results, verification of the equivalent circuit model accuracy will be done. Comparison of the performance results will be done at the motor rated output power.

Motor performance of the test motors named 77C014 (180 W-4pole), 87C012 (370 W-4pole) and 97C100 (750 W-4pole) are calculated. Results of the single phase motors are given in Table 6-41 and Table 6-42 respectively.

In these tables, the first column "Test Results" shows the performance results obtained from test measurement; the second column "From Test Params" shows the calculated performance from the motor parameters and the third column "Error Percent" shows the error percentage of these two

calculations. Error percentage calculation is made according to the equation given in (6-3).

Table 6-41 Single Phase Motors Performance Analysis - 1 (measured parameters)

	77C014 (180 W-4pole)			87C012 (370 W-4pole)		
	Test Results	From Test Params	Error Percent	Test Results	From Test Params	Error Percent
Output Power (W)	180	180	0.00	370	370	0.00
Power Factor	0.62	0.64	-3.23	0.66	0.65	1.52
Efficiency	50.44	49.06	2.74	59.79	57.69	3.51
Full-load Torque (Nm)	1.17	1.19	-1.71	2.45	2.46	-0.41
Full-load Current (A)	2.57	2.64	-2.72	4.30	4.45	-3.49
Speed (rpm)	1446	1442	0.31	1438	1438	0.00
Starting Torque (Nm)	2.97	2.82	4.05	5.75	6.00	-4.15
Starting Current (A)	9.32	9.52	-2.15	17.20	17.93	-4.14
No Load Current (A)	2.32	2.38	-2.59	3.57	3.64	1.96

Table 6-42 Single Phase Motors Performance Analysis - 2 (measured parameters)

	97C100 (750 W-4pole)		
	Test Results	From Test Params	Error Percent
Output Power (W)	750	750	0.00
Power Factor	0.65	0.66	-1.54
Efficiency	70.07	69.81	0.37
Full-load Torque (Nm)	5.00	4.97	0.60
Full-load Current (A)	7.10	7.36	-3.66
Speed (rpm)	1440	1440	0.00
Starting Torque (Nm)	14.76	15.04	-1.90
Starting Current (A)	34.35	34.19	0.47
No Load Current (A)	5.47	5.57	-1.83

According to the overall performance results, it can be concluded that full load and starting performance results obtained from test parameters are within 4% error when it is compared with the performance test results. That means the used model for the performance calculations gives reasonable results for full load and starting conditions. According to these, the error percentages are in acceptable range. So, the model used in SPCAD can be used for the performance calculations.

6.3.5 Performance Calculation from Motor Geometry Using SPCAD and Accuracy of SPCAD Calculation

In this part, performance result of the test motors obtained from motor geometry using SPCAD will be compared with the performance test results

to verify the accuracy of the SPCAD calculation. Comparison of the performance results will be done at the motor rated output power.

Motor performances of the test motors given in Table 6-30 are calculated. Results of the motors are given in Table 6-43, Table 6-44 and Table 6-45 respectively.

In these tables, the first column “Test Results” shows the performance results obtained from test measurement; the second column “SPCAD Results” shows the calculated performance from motor geometry and the third column “Error Percent” shows the error percentage of these two calculations. Error percentage calculation is made according to the equation given in (6-3).

Table 6-43 Single Phase Motors Performance Analysis - 1 (calculated performance)

	77C014 (180 W-4pole)			87C012 (370 W-4pole)		
	Test Results	SPCAD Results	Error Percent	Test Results	SPCAD Results	Error Percent
Output Power (W)	180	180	0.00	370	370	0.00
Power Factor	0.62	0.64	-3.23	0.66	0.66	0.00
Efficiency	50.44	48.47	3.91	59.79	58.91	1.47
Full-load Torque (Nm)	1.17	1.18	-0.85	2.45	2.45	0.00
Full-load Current (A)	2.57	2.60	-1.17	4.30	4.30	0.00
Speed (rpm)	1446	1447	-0.07	1438	1444	-0.42
Starting Torque (Nm)	2.97	2.82	5.05	5.75	6.00	-4.35
Starting Current (A)	9.32	9.65	-3.54	17.20	17.67	-2.73
No Load Current (A)	2.32	2.30	0.86	3.57	3.45	3.36

Table 6-44 Single Phase Motors Performance Analysis - 2 (calculated performance)

	87A0345B (550 W-4pole)			97C100 (750 W-4pole)		
	Test Results	SPCAD Results	Error Percent	Test Results	SPCAD Results	Error Percent
Output Power (W)	550	550	0.00	750	750	0.00
Power Factor	0.71	0.69	2.82	0.65	0.64	1.54
Efficiency	70.50	68.66	3.97	70.07	67.45	3.74
Full-load Torque (Nm)	1.78	1.82	-3.41	5.00	4.97	0.60
Full-load Current (A)	4.98	5.22	-4.82	7.10	7.16	-0.85
Speed (rpm)	2888	2888	0.00	1440	1441	-0.07
Starting Torque (Nm)	3.77	3.77	0.00	14.76	14.70	0.41
Starting Current (A)	24.60	22.73	7.60	34.35	32.53	5.30
No Load Current (A)	3.67	3.82	-4.09	5.47	5.79	-5.85

Table 6-45 Single Phase Motors Performance Analysis - 3 (calculated performance)

	97A1005B (750 W-2pole)		
	Test Results	SPCAD Results	Error Percent
Output Power (W)	750	750	0.00
Power Factor	0.77	0.80	-3.90
Efficiency	74.62	76.60	-2.65
Full-load Torque (Nm)	2.45	2.45	0.00
Full-load Current (A)	6.25	6.09	2.56
Speed (rpm)	2936	2923	0.44
Starting Torque (Nm)	5.38	5.02	6.69
Starting Current (A)	38.80	36.41	6.16
No Load Current (A)	3.30	3.21	2.73

According to the overall performance results, it can be concluded that the performance calculations generated from TPCAD give reasonable results for full load conditions within 5% error.

Error percentages for starting torque and current are within 8% error. This is because in the actual motors the current reaches higher than the full load condition and saturation become dominant for starting. The saturating parts affect the reactances. Effect of the main and auxiliary winding leakage reactances on the starting performance is examined in section 6.3.3.

Error percentages for no load current are within 6%. This is coming from the differences at the magnetizing reactance. Machining tolerances make the air gap different which changes magnetic properties of this part of the machine. For that reason, magnetizing reactance and thus no load current become different. Effect of the magnetizing reactance on the no load current

is examined in section 6.3.3. In that part, actual value of the magnetizing reactance of that motor is modified with $\pm 10\%$ change. As a result of that, the no load current of the motor is changed with 10% error which is an expected variation.

CHAPTER 7

CONCLUSION

In the Electrical and Electronics Engineering department, two computer aided design programs TPCAD and SPCAD have been developed by Hamarat and Aftahi respectively which operate in DOS environment. These programs are used to design and analyze performance of three phase and single phase (capacitor start or capacitor run) induction motors respectively. The purpose of this study is to rewrite these programs using C++ Microsoft Visual Studio .Net programming language to run in windows environment. These software modifications have been further developed to have the features as below:

- Implementation of a module to analyze and design double cage motors,
- Drawing the lamination of the motor to monitor the final design,
- Implementation of an option to provide the data interoperability for lamination of the designed motor with other professional design programs for the purpose of finite element analysis, thermal analysis etc.,

- Implementation of a tool that calculates the machine performance only from no load test and load test which measures only motor terminal voltage, current, input power and motor speed,
- Additional features to support program with user friendly interface, graphical performance analysis, printing capability and detailed design information are the other features that are mentioned in CHAPTER 3 and CHAPTER 5,
- Software is also tested with double cage motors which was not done before.

To verify the calculations used, TPCAD and SPCAD are tested respectively with three methods which are; assessing the accuracy of parameter calculation, assessing the accuracy of the equivalent circuit model for performance calculation and comparing the performance calculation results of the programs with the results taken from the tests.

For assessing the accuracy of the parameter calculation of TPCAD, the comparison is done according to the rotor resistance, stator and rotor leakage reactance and magnetizing reactance. Comparisons of stator and coreloss resistances are not done since these two parameters can be adjusted by changing the coil extension length and correction factor of coreloss resistance respectively.

It is observed that larger error occurs for rotor resistance for both double and single cage motors. Bubbles in the actual rotor coming from casting process, differences coming from the resistivity of the aluminium and performing the locked rotor test at 50 Hz at stand still cause this difference on the actual rotor value. Instead of comparing stator and rotor leakage reactances, comparison of total leakage reactance is done since it is not possible to make an additional test to determine these reactances separately. Error percentage for total leakage reactance is changing from 6

to 8 for double cage, from 4 to 12 for single cage motors. It is concluded that, this is an acceptable result since the saturation effect and local distribution of the magnetic field is not considered in calculations. Also, the error percentage for the magnetizing reactance is within 10% for both double and single cage motors. This is an acceptable result that, the effect of the machining tolerances makes the air gap different which changes magnetic properties of this part and thus the magnetizing reactance of the machine.

After observation of the parameter calculation accuracy, verification of the equivalent circuit model accuracy is examined by comparing the performance results obtained from machine parameters with the performance test results. It is observed that, full load performance results are within 2.5%, starting performance results are within 3.5% error for both double and single cage motors when it is compared with performance test results. According to these results, it is concluded that the equivalent circuit model used by TPCAD gives reasonable results for performance conditions.

In the end, the performance prediction accuracy of TPCAD using only geometry of the motor winding data and material information is verified with test results. According to the performance results, it is observed that TPCAD gives reasonable results for full load conditions within 5% and for starting performance conditions within 10% error for both double and single cage motors. These errors are coming from the differences between the parameters obtained from TPCAD and from no load and locked rotor tests. The effect of the parameters on the performance results are examined by changing the actual value of the parameters by $\pm 10\%$. The change on the rotor resistance has an effect on the starting performance of the motor. This is also valid for leakage reactances. It is observed that, the change on the magnetizing reactance has an almost directly proportional effect on the no load current of the motor. It is concluded that the magnetizing current error

in TPCAD is likely to result from machining tolerances. From the study here it is concluded that, TPCAD can be used for the design and analysis of three phase induction machines, and gives reliable and acceptable accurate results.

The methods of verification used for TPCAD are also repeated for SPCAD. The parameter comparison is done according to the rotor resistance, main winding leakage reactance and magnetizing reactance. Comparisons of main and auxiliary winding resistances are not done since these two parameters can be adjusted by changing the coil extension lengths respectively.

It is observed that smaller error occurs in the prediction of rotor resistance as compared to three phase motor resistance predictions. The findings mentioned for TPCAD are also valid for the rotor resistance error.

In SPCAD the error percentage for main and auxiliary winding reactances is within 14%. Since the saturation effect and local distribution of the magnetic field is not considered in calculations, the error percentage is higher for reactance values. The error percentage for the magnetizing reactance is found to be within 5%. As mentioned earlier this error is likely to be due to the machining tolerances.

After verification of the parameter calculation accuracy, the equivalent circuit model that is used for performance calculations by SPCAD is examined. As a result it is observed that, performance results obtained for full load and starting conditions are within 4% error when compared with laboratory test results. As a consequence, it is concluded that the equivalent circuit model used by SPCAD gives reasonable results for performance conditions.

Performance prediction accuracy of SPCAD is verified with test results. According to the performance results, it is observed that SPCAD gives reasonable results for full load conditions within 5% and for starting

performance conditions within 8% error. These errors are coming from the differences between the parameters calculated by SPCAD and from tests.

The effect of the parameters on the performance results are examined by changing the actual value of the parameters by $\pm 10\%$. The change on the rotor resistance has an effect on the starting performance of the motor. This is also valid for main winding leakage reactance. The change on the auxiliary winding leakage reactance only affects the starting performance of the motor since the tested motors are capacitor start type. It is observed that, the change on the magnetizing reactance has an almost directly proportional effect on the no load current of the motor. As a result of these verifications it is concluded that, SPCAD can be used for the design and analysis of single phase induction machines, and reliable designs can be obtained.

Effect of the double layer winding on the reactance values is not examined here in detail. This issue needs to be examined. Both softwares have an optimization facility. However, this issue is not examined in this work. Further research is needed to determine how well this facility of the software works. Design and performance analysis for double speed and variable speed applications can also be the future work of this study.

REFERENCES

- [1]: Hamarat, S., "Design Optimization of Three-Phase Induction Motors", M.Sc. Thesis, Middle East Technical University, January 1997.
- [2]: Aftahi, M., "Computer Aided Design of Single-Phase Capacitor Type Induction Motors", M.Sc. Thesis, Middle East Technical University, January 1993.
- [3]: Veinott, C. G., "Theory and Design of Small Induction Motors", McGraw-Hill Book Company, 1959.
- [4]: Spooner, T., Kinnard, I.F., "Surface Iron Losses with Reference to Laminated Materials", Trans. AIEE, 1924, pp.262-280.
- [5]: Alger, P. L., "The Nature of Induction Machines", Gordon and Breach Science Publishers, 1965.
- [6]: IEEE Standard Test Procedure for Polyphase Induction Motors and Generator, IEEE Std 112, 1991.
- [7]: Fitzgerald, A. E., Kingsley, C., Umans, S., "Electric Machinery", McGraw-Hill Book Company, 2003, pp. 330-335.
- [8]: Microsoft Developers Network Library, <http://msdn.microsoft.com/en-us/default>, last accessed on 11/04/2011

APPENDIX A

TPCAD DATA ENTRY FORM

Table A-1 TPCAD Motor Data Entry Form (Single Cage)

Description				
Title				
Date				
#	Name	Description	Value	Unit
1	m	Phase Number		-
2	V	Impressed Voltage		Volt
3	f	Frequency		Hz
4	p	Number of Poles		-
5	C	Number of Conductor		-
6	P_u_pit	Per unit Pitch		-
7	F	Stacking Factor		-
8	K ϕ	Reactance Voltage Drop Factor		-
9	Kr1	Total Flux Factor		-
10	Kp1	Primary Flux Factor		-
11		Throw of Coil (Number of Slot Pitches)		-
12	qm	Number of Parallel Paths in Stator Winding		-
13	A1m	Cross-sectional Area of Conductor		m ²
14	Rhom	Resistivity of Copper		Ω /m
15	Rhor	Resistivity of Aluminium		Ω /m

Table A-1 (cont'd)

#	Name	Description	Value	Unit
16	Tmain	Copper Resistivity Measured At		°C
17	Tbar	Aluminium Resistivity Measuring Temperature		°C
18	Ar1	Cross-Sectional Area of End Ring		m ²
19	Dr1	Mean Diameter of End Ring		m
20	ns	Synchronous Speed		rpm
21	n	Rotor Speed		rpm
22		Friction Loss		W
23		Windage Loss		W
24	Γ	Extension of Coil from Core		m
25	T	Final Temperature		°C
26	P rated	Rated Output Power		W
27	Khi	High Frequency Loss Constant		-
28	Ab	Bar Cross Sectional Area		m ²
29	RhoFe	Density of Iron		Kg/m ³
30	Ar2	Cross Sectional Area of End Rings		m ²
31	Dr2	End Ring Diameters		m
32		Coreloss Resistance Constant		-
33	D	Stator Outside Diameter		m
34	D1	Stator Bore Diameter		m
35	L1	Stator Stack Length		m
36	t1	Stator Tooth width		m
37	d01	Stator Tooth Depth		m
38	S1	Number of Stator Slots		-
39	w10	Stator Slot Opening		m
40	d11	Stator Tip Depth		m
41	d10	Stator Mouth Depth		m
42	d14			m
43	w13	Stator Slot Top Width		m
44	w11	Stator Slot Bottom Width		m
45	SA1	Stator Slot Area		m ²
46	SHL	Total Length of the Shaft		m

Table A-1 (cont'd)

#	Name	Description	Value	Unit
47	D2	Rotor Outside Diameter		m
48	Db	Rotor Shaft Diameter		m
49	L2	Rotor Stack Length		m
50	t2	Rotor Tooth width		m
51	d02	Rotor Tooth Depth		m
52	S2	Number of Rotor Slots		-
53	w20	Rotor Slot Opening		m
54	d21	Rotor Tip Depth		m
55	d20	Rotor Mouth Depth		m
56	w21	Rotor Slot Top Width		m
57	SA2	Rotor Slot Area		m ²
58	w23	Rotor Slot Bottom Width		m
59	α	Rotor Skew Angle		°

Table A-2 TPCAD Motor Data Entry Form (Double Cage)

Description				
Title				
Date				
#	Name	Description	Value	Unit
1	m	Phase Number		-
2	V	Impressed Voltage		Volt
3	f	Frequency		Hz
4	p	Number of Poles		-
5	C	Number of Conductor		-
6	P_u_pit	Per unit Pitch		-
7	F	Stacking Factor		-
8	K ϕ	Reactance Voltage Drop Factor		-
9	Kr1	Total Flux Factor		-
10	Kp1	Primary Flux Factor		-
11		Throw of Coil (Number of Slot Pitches)		-
12	qm	Number of Parallel Paths in Stator Winding		-
13	A1m	Cross-sectional Area of Conductor		m ²
14	Rhom	Resistivity of Copper		Ω /m
15	Rhor	Resistivity of Aluminium		Ω /m
16	Tmain	Copper Resistivity Measured At		°C
17	Tbar	Aluminium Resistivity Measuring Temperature		°C
18	Ar1	Cross-Sectional Area of End Ring		m ²
19	Dr1	Mean Diameter of End Ring		m
20	ns	Synchronous Speed		rpm
21	n	Rotor Speed		rpm
22		Friction Loss		W
23		Windage Loss		W
24	Γ	Extension of Coil from Core		m
25	T	Final Temperature		°C
26	P rated	Rated Output Power		W
27	Khi	High Frequency Loss Constant		-

Table A-2 (cont'd)

#	Name	Description	Value	Unit
28	Ab	Bar Cross Sectional Area		m ²
29	RhoFe	Density of Iron		Kg/m ³
30	Ar2	Cross Sectional Area of End Rings		m ²
31	Dr2	End Ring Diameters		m
32		Coreloss Resistance Constant		-
33	D	Stator Outside Diameter		m
34	D1	Stator Bore Diameter		m
35	L1	Stator Stack Length		m
36	t1	Stator Tooth width		m
37	d01	Stator Tooth Depth		m
38	S1	Number of Stator Slots		-
39	w10	Stator Slot Opening		m
40	d11	Stator Tip Depth		m
41	d10	Stator Mouth Depth		m
42	d14			m
43	w13	Stator Slot Top Width		m
44	w11	Stator Slot Bottom Width		m
45	SA1	Stator Slot Area		m ²
46	SHL	Total Length of the Shaft		m
47	D2	Rotor Outside Diameter		m
48	Db	Rotor Shaft Diameter		m
49	L2	Rotor Stack Length		m
50	α	Rotor Skew Angle		°
51	S2	Number of Rotor Slots		-
52	t2	Top Cage Tooth Width		m
53	d02	Top Cage Tooth Depth		m
54	w20	Top Cage Slot Opening		m
55	d21	Top Cage Tip Depth		m
56	d20	Top Cage Mouth Depth		m
57	w21	Top Cage Slot Top Width		m
58	w23	Top Cage Slot Bottom Width		m

Table A-2 (cont'd)

#	Name	Description	Value	Unit
59	SA2	Top Cage Slot Area		m ²
60	t2	Bottom Cage Tooth Width		m
61	d02	Bottom Cage Tooth Depth		m
62	w20	Bottom Cage Slot Opening		m
63	d21	Bottom Cage Tip Depth		m
64	d20	Bottom Cage Mouth Depth		m
65	w21	Bottom Cage Slot Top Width		m
66	w23	Bottom Cage Slot Bottom Width		m
67	SA2	Bottom Cage Slot Area		m ²

APPENDIX B

SPCAD DATA ENTRY FORM

Table B-1 SPCAD Data Entry Form

Description				
Title				
Date				
#	Name	Description	Value	Unit
1	V	Impressed Voltage		Volt
2	f	Frequency		Hz
3	p	Number of Poles		-
4	C	Number of Conductor		-
5	F	Stacking Factor		-
6	$K\phi$	Reactance Voltage Drop Factor		-
7	Kr1	Total Flux Factor		-
8	Kp1	Primary Flux Factor		-
9	qm	Number of Parallel Paths in Stator Winding		-
10	A1m	Cross-sectional Area of Conductor		m ²
11	Rhom	Resistivity of Copper		Ω/m
12	Rhor	Resistivity of Aluminium		Ω/m
13	Tmain	Copper Resistivity Measured At		°C
14	Tbar	Aluminium Resistivity Measuring Temperature		°C
15	Ar1	Cross-Sectional Area of End Ring		m ²

Table B-1 (cont'd)

#	Name	Description	Value	Unit
16	Dr1	Mean Diameter of End Ring		m
17	Ar2	Cross Sectional Area of End Rings		m ²
18	Dr2	End Ring Diameters		m
19	ns	Synchronous Speed		rpm
20	n	Rotor Speed		rpm
21		Friction and Windage Loss		W
22	Γ	Extension of Coil from Core		m
23	T	Final Temperature		°C
24	P rated	Rated Output Power		W
25	Khi	High Frequency Loss Constant		-
26	Krad	Radiator Factor		-
27		Saturation Factor		-
28	Ab	Bar Cross Sectional Area		m ²
29	RhoFe	Density of Iron		Kg/m ³
30	D	Stator Outside Diameter		m
31	D1	Stator Bore Diameter		m
32	L1	Stator Stack Length		m
33	t1	Stator Tooth width		m
34	d01	Stator Tooth Depth		m
35	S1	Number of Stator Slots		-
36	w10	Stator Slot Opening		m
37	d11	Stator Tip Depth		m
38	d10	Stator Mouth Depth		m
39	d14			m
40	w13	Stator Slot Top Width		m
41	w11	Stator Slot Bottom Width		m
42	SA1	Stator Slot Area		m ²
43	SHL	Total Length of the Shaft		m
44	D2	Rotor Outside Diameter		m
45	Db	Rotor Shaft Diameter		m
46	L2	Rotor Stack Length		m

Table B-1 (cont'd)

#	Name	Description	Value	Unit
47	t2	Rotor Tooth width		m
48	d02	Rotor Tooth Depth		m
49	S2	Number of Rotor Slots		-
50	w20	Rotor Slot Opening		m
51	d21	Rotor Tip Depth		m
52	d20	Rotor Mouth Depth		m
53	w21	Rotor Slot Top Width		m
54	SA2	Rotor Slot Area		m ²
55	w23	Rotor Slot Bottom Width		m
56	α	Rotor Skew Angle		°
57	C1m	Number of Conductors in Slot 1		-
58	C2m	Number of Conductors in Slot 2		-
59	C3m	Number of Conductors in Slot 3		-
60	C4m	Number of Conductors in Slot 4		-
61	C5m	Number of Conductors in Slot 5		-
62	C6m	Number of Conductors in Slot 6		-
63	C7m	Number of Conductors in Slot 7		-
64	C8m	Number of Conductors in Slot 8		-
65	C9m	Number of Conductors in Slot 9		-
66	T1m	Throw of Coil C1m, in Number of Slot Spanned		-
67	T2m	Throw of Coil C2m, in Number of Slot Spanned		-
68	T3m	Throw of Coil C3m, in Number of Slot Spanned		-
69	T4m	Throw of Coil C4m, in Number of Slot Spanned		-
70	T5m	Throw of Coil C5m, in Number of Slot Spanned		-
71	T6m	Throw of Coil C6m, in Number of Slot Spanned		-
72	T7m	Throw of Coil C7m, in Number of Slot Spanned		-
73	T8m	Throw of Coil C8m, in Number of Slot Spanned		-
74	T9m	Throw of Coil C9m, in Number of Slot Spanned		-
75		Number of Conductors in Aux Winding		-
76		Number of Parallel Paths in Aux Winding		-
77		Cross-sectional Area of Aux Winding Conductor		m ²

Table B-1 (cont'd)

#	Name	Description	Value	Unit
78		Resistivity of Aux Winding Conductor		Ω/m
79		Voltage Impressed on Main Phase		V
80		Voltage Impressed on Aux Phase Including C		V
81		Value of External Capacitor		μF
82		Resistance of External Capacitor		Ω
83		Speed at Aux Winding Off		rpm
84		Aux Winding Resistivity Measuring Temperature		$^{\circ}\text{C}$
85		Aux Winding Coil Extension		m
86		Winding Ratio		-
87	C1a	Number of Conductors in Slot 1		-
88	C2a	Number of Conductors in Slot 2		-
89	C3a	Number of Conductors in Slot 3		-
90	C4a	Number of Conductors in Slot 4		-
91	C5a	Number of Conductors in Slot 5		-
92	C6a	Number of Conductors in Slot 6		-
93	T1a	Throw of coil C1a, in Number of Slot Spanned		-
94	T2a	Throw of coil C2a, in Number of Slot Spanned		-
95	T3a	Throw of coil C3a, in Number of Slot Spanned		-
96	T4a	Throw of coil C4a, in Number of Slot Spanned		-
97	T5a	Throw of coil C5a, in Number of Slot Spanned		-
98	T6a	Throw of coil C6a, in Number of Slot Spanned		-
99		Are Aux Windings Wound Asymmetrically?		-
100	C1a2	Number of Conductors in Slot 1		-
101	C2a2	Number of Conductors in Slot 2		-
102	C3a2	Number of Conductors in Slot 3		-
103	C4a2	Number of Conductors in Slot 4		-
104	C5a2	Number of Conductors in Slot 5		-
105	C6a2	Number of Conductors in Slot 6		-
106	T1a2	Throw of Coil C1a2, in Number of Slot Spanned		-
107	T2a2	Throw of Coil C2a2, in Number of Slot Spanned		-
108	T3a2	Throw of Coil C3a2, in Number of Slot Spanned		-

Table B-1 (cont'd)

#	Name	Description	Value	Unit
109	T4a2	Throw of Coil C4a2, in Number of Slot Spanned		-
110	T5a2	Throw of Coil C5a2, in Number of Slot Spanned		-
111	T6a2	Throw of Coil C6a2, in Number of Slot Spanned		-

APPENDIX C

ANALYSIS DATA OF TEST MOTORS - TPCAD

Table C-1 Analysis Data of Single Cage Motors - 1

#	90L4A	NM112M - 6	NM112M - 4	132S4C	Unit
1	3	3	3	3	-
2	220	218	380	380	Volt
3	50	50	50	50	Hz
4	4	6	4	4	-
5	564	480	576	456	-
6	1	1	1	1	-
7	0.96	0.96	0.96	0.96	-
8	0.94	0.94	0.94	0.94	-
9	0.96	0.96	0.96	0.96	-
10	0.96	0.98	0.98	0.96	-
11	9	6	9	9	-
12	2	1	1	1	-
13	4.92602E-07	9.05721E-07	7.6969E-07	9.55672E-07	m ²
14	1.75E-08	1.75E-08	1.75E-08	1.7E-08	Ω/m
15	2.85E-08	2.65E-08	2.65E-08	2.8E-08	Ω/m
16	20	20	20	25	°C
17	20	20	20	25	°C
18	0.000148104	0.0001387	0.000242	0.00026775	m ²

Table C-1 (cont'd)

#	90L4A	NM112M - 6	NM112M - 4	132S4C	Unit
19	0.06465	0.094	0.079	0.0955	m
20	1500	1000	1500	1500	rpm
21	1436	952.5	1439.323	1448.119	rpm
22	4.5	6	5	45	W
23	4.5	10	10	40	W
24	0.37	0.1	0.12	0.19	m
25	45	55	43	25	°C
26	1500	2200	4000	5500	W
27	1.65	2.65	2.65	1.5	-
28	4.3E-05	4.5E-05	5.32E-05	8.123E-05	m ²
29	7750	7750	7750	7750	Kg/m ³
30	0.000148104	0.0001387	0.000242	0.00026775	m ²
31	0.06465	0.094	0.079	0.0955	m
32	1	1.397	1.495	1	-
33	0.135	0.17	0.17	0.19	m
34	0.085	0.115	0.103	0.125	m
35	0.1	0.13	0.13	0.14	m
36	0.0036	0.0054	0.0049	0.00573	m
37	0.01032	0.0162	0.0173	0.0105	m
38	36	36	36	36	-
39	0.0022	0.0025	0.0025	0.003	m
40	0.00031	0.00223	0.00188	0.00069	m
41	0.00035	0.00062	0.00064	0.0005	m
42	0.00966	0.01335	0.01478	0.00931	m
43	0.0057	0.00724	0.00691	0.007	m
44	0.0032	0.00512	0.00451	0.0054	m
45	6.3E-05	9.448E-05	9.44E-05	8.446E-05	m ²
46	0.31	0.4	0.4	0.438	m
47	0.0844	0.11435	0.10215	0.1242	m
48	0.03	0.038	0.038	0.043	m
49	0.1	0.13	0.13	0.14	m

Table C-1 (cont'd)

#	90L4A	NM112M - 6	NM112M - 4	132S4C	Unit
50	0.0045	0.006	0.0062	0.008129	m
51	0.01356	0.01633	0.01718	0.01944	m
52	28	34	28	26	-
53	0.0008	0.001	0.001	0	m
54	0.00219	0.00199	0.002286	0.003	m
55	0.00052	0.00078	0.00068	0.00054	m
56	0.00438	0.0041	0.00468	0.006	m
57	4.4E-05	4.5E-05	5.32E-05	8.123E-05	m ²
58	0.00196	0.00176	0.0015	0.0022	m
59	10	4	4	10	°

Table C-2 Analysis Data of Single Cage Motors - 2

#	132M4B	132S2C	160L4A	180M4B	Unit
1	3	3	3	3	-
2	380	380	380	380	Volt
3	50	50	50	50	Hz
4	4	2	4	4	-
5	384	360	300	288	-
6	1	0.78	0.78	1	-
7	0.96	0.96	0.96	0.96	-
8	0.94	0.94	0.94	0.94	-
9	0.96	9.96	0.96	0.96	-
10	0.96	0.98	0.96	0.96	-
11	9	14	7	7	-
12	1	1	2	1	-
13	1.7E-06	1.135E-06	1.9E-06	4.52389E-06	m ²
14	1.7E-08	1.7E-08	1.7E-08	1.7E-08	Ω/m
15	2.8E-08	2.87E-08	2.8E-06	2.8E-08	Ω/m
16	25	25	20	25	°C
17	25	25	20	25	°C
18	0.00036	0.0003096	0.000252	0.000372	m ²
19	0.112	0.084	0.133	0.143	m
20	1500	3000	1500	1500	rpm
21	1458.475	2921.113	1456.57	1449.341	rpm
22	60	200	60	100	W
23	40	60	44	50	W
24	0.215	0.24	0.18	0.2	m
25	35	30	35	35	°C
26	7500	7500	15000	18500	W
27	2.1	1.9	1	4	-
28	0.00012346	6.618E-05	7.7E-05	8.141E-05	m ²
29	7750	7750	7750	7750	Kg/m ³
30	0.00036	0.0003096	0.000252	0.000372	m ²

Table C-2 (cont'd)

#	132M4B	132S2C	160L4A	180M4B	Unit
31	0.112	0.084	0.133	0.143	m
32	1	1	1.0158	0.97	-
33	0.225	0.19	0.24	0.27	m
34	0.146	0.109	0.158	0.178	m
35	0.15	0.14	0.21	0.21	m
36	0.007	0.00432	0.0071	0.00744	m
37	0.0135	0.0105	0.01925	0.0195	m
38	36	36	36	36	-
39	0.003	0.003	0.003	0.003	m
40	0.0007	0.00069	0.001125	0.001375	m
41	0.0005	0.0005	0.00075	0.00075	m
42	0.0123	0.00931	0.017375	0.017375	m
43	0.008	0.007	0.01	0.0115	m
44	0.0058	0.0054	0.0075	0.0085	m
45	0.000110088	7.99E-05	0.0002	0.00023498	m ²
46	0.479	0.438	0.59	0.629	m
47	0.14505	0.108	0.1564	0.1765	m
48	0.048	0.043	0.055	0.062	m
49	0.15	0.14	0.21	0.21	m
50	0.00974	0.00505	0.0047	0.005	m
51	0.022375	0.01409	0.01533	0.01844	m
52	26	28	46	46	-
53	0	0	0	0	m
54	0.0034	0.0031	0.0028	0.00327	m
55	0.000575	0.00059	0.00033	0.00044	m
56	0.0068	0.0062	0.0056	0.00654	m
57	0.00012346	6.615E-05	7.7E-05	8.141E-05	m ²
58	0.0024	0.0044	0.004	0.0049	m
59	8.5	10.1	10.3	10.3	°

Table C-3 Analysis Data of Double Cage Motors

#	NM250M - 4	NM315Ma - 4	Unit
1	3	3	-
2	380	380	Volt
3	50	50	Hz
4	4	4	-
5	128	70	-
6	1	1	-
7	0.96	0.96	-
8	0.94	0.94	-
9	0.96	0.96	-
10	0.98	0.98	-
11	10	13	-
12	2	4	-
13	5.49779E-06	1.19459E-05	m ²
14	1.75E-08	1.7E-08	Ω/m
15	2.75E-08	2.65E-08	Ω/m
16	18.4	20	°C
17	18.4	20	°C
18	0.000670375	0.001062	m ²
19	0.19075	0.259	m
20	1500	1500	rpm
21	1469.807	1478.431	rpm
22	60	21	W
23	700	1500	W
24	0.29	0.4	m
25	37.6	59	°C
26	55000	160000	W
27	1.6	1.6	-
28	0.0001499	0.0003332	m ²
29	7750	7750	Kg/m ³
30	0.000670375	0.001062	m ²

Table C-3 (cont'd)

#	NM250M - 4	NM315Ma - 4	Unit
31	0.19075	0.259	m
32	1.028	0.673	-
33	0.375	0.5	m
34	0.24	0.325	m
35	0.26	0.36	m
36	0.00938	0.01	m
37	0.0273	0.0406	m
38	48	60	-
39	0.0025	0.00315	m
40	0.00703	0.0016	m
41	0.0006	0.00071	m
42	0.01967	0.03829	m
43	0.01	0.01117	m
44	0.00714	0.00575	m
45	0.000221	0.00037	m ²
46	0.889	1.27	m
47	0.2386	0.3235	m
48	0.085	0.115	m
49	0.26	0.36	m
50	3.46	3.75	°
51	40	48	-
52	0.01014	0.0123	m
53	0.0087	0.01107	m
54	0.0011	0.002	m
55	0	0	m
56	0.0018	0.00333	m
57	0.007	0.008	m
58	0	0	m
59	3.73E-05	5E-05	m ²
60	0.01014	0.01	m
61	0.02705	0.04493	m

Table C-3 (cont'd)

#	NM250M - 4	NM315Ma - 4	Unit
62	0.0011	0.002	m
63	0.00299	0.0015	m
64	0.00504	0.00543	m
65	0.00608	0.00876	m
66	0.0031	0.00426	m
67	0.0001126	0.00028322	m ²

APPENDIX D

ANALYSIS DATA OF TEST MOTORS - SPCAD

Table D-1 Analysis Data of Single Phase Motors

#	77C014	87C012	87A0345B	97C100	97A1005B	Unit
1	220	220	220	220	200	Volt
2	50	50	50	50	50	Hz
3	4	4	2	4	2	-
4	1568	1008	624	784	568	-
5	0.96	0.96	0.96	0.96	0.96	-
6	0.94	0.94	0.94	0.94	0.94	-
7	0.94	0.94	0.94	0.94	0.94	-
8	0.96	0.96	0.98	0.96	0.98	-
9	1	1	1	1	1	-
10	2.4E-07	4.41E-07	6.63E-07	1E-06	1.135E-06	m ²
11	1.72E-08	1.72E-08	1.72E-08	1.7E-08	1.72E-08	Ω/m
12	2.78E-08	2.78E-08	2.78E-08	2.8E-08	2.78E-08	Ω/m
13	25	25	20	20	25	°C
14	20	20	20	20	25	°C
15	0.00012	0.000118	0.0001125	0.00011825	0.000231	m ²
16	0.054	0.054	0.0455	0.07475	0.0565	m
17	0.00012	0.000118	0.0001125	0.00011825	0.000231	m ²
18	0.054	0.054	0.0455	0.07475	0.0565	m

Table D-1 (cont'd)

#	77C014	87C012	87A0345B	97C100	97A1005B	Unit
19	1500	1500	3000	1500	3000	rpm
20	1447.361	1443.717	2888.322	1441.287	2922.713	rpm
21	4	15	15	15	45	W
22	0.09	0.093	0.107	0.087	0.1559	m
23	25	25	65	45	68	°C
24	180	370	550	750	750	W
25	4.4	3.66	3	1.5	1.4	-
26	0	0	1.8	1.63	1	-
27	1	0	1	1	1.4	-
28	1.7E-05	1.651E-05	1.78E-05	2.13E-05	3.135E-05	m ²
29	7750	7750	7750	7750	7750	Kg/m ³
30	0.12458	0.12445	0.12458	0.1457	0.146	m
31	0.073	0.073	0.061011	0.0889	0.076213	m
32	0.048	0.076	0.072	0.08	0.075	m
33	0.00333	0.00333	0.003508	0.00381	0.00381	m
34	0.0133	0.0133	0.01172	0.01415	0.01414	m
35	36	36	24	36	24	-
36	0.00216	0.00216	0.00208	0.00254	0.00254	m
37	0.00025	0.00025	0.001524	0.0008	0.00139	m
38	0.00075	0.00075	0.000369	0.00055	0.0008	m
39	0.0123	0.0123	0.009827	0.0128	0.01195	m
40	0.00536	0.00536	0.00752	0.0064	0.0098	m
41	0.003217	0.003217	0.00498	0.00421	0.00681	m
42	6.5E-05	6.5E-05	8.78E-05	0.0001	0.000143	m ²
43	0.25	0.25	0.25	0.25	0.339	m
44	0.0724	0.0724	0.060411	0.0884	0.075613	m
45	0.01905	0.01905	0.01905	0.02	0.02	m
46	0.048	0.076	0.072	0.08	0.075	m
47	0.00225	0.00225	0.00243	0.00254	0.00218	m
48	0.00985	0.00985	0.00553	0.00752	0.008567	m
49	48	48	30	44	34	-

Table D-1 (cont'd)

#	77C014	87C012	87A0345B	97C100	97A1005B	Unit
50	0	0	0	0	0	m
51	0.00115	0.00115	0.00171	0.00175	0.00183	m
52	0.00035	0.00035	0.00039	0.0004	0.000467	m
53	0.0023	0.0023	0.00344	0.00351	0.00439	m
54	1.65E-05	1.651E-05	1.78E-05	2.13E-05	3.135E-05	m ²
55	0.00128	0.00128	0.00274	0.00288	0.00323	m
56	10	10	15	10	15	°
57	20	20	44	12	28	-
58	44	44	44	22	34	-
59	64	64	42	32	38	-
60	68	68	26	32	42	-
61	0	0	0	0	0	-
62	0	0	0	0	0	-
63	0	0	0	0	0	-
64	0	0	0	0	0	-
65	0	0	0	0	0	-
66	2	2	11	2	5	-
67	4	4	9	4	7	-
68	6	6	7	6	9	-
69	8	8	5	8	11	-
70	0	0	0	0	0	-
71	0	0	0	0	0	-
72	0	0	0	0	0	-
73	0	0	0	0	0	-
74	0	0	0	0	0	-
75	1744	1344	904	896	728	-
76	1	1	1	1	1	-
77	9.6E-08	9.6E-08	1.256E-07	2.82E-07	2.376E-07	m ²
78	1.72E-08	1.72E-08	1.72E-08	1.72E-08	1.72E-08	Ω/m
79	220	220	220	220	200	V
80	220	220	220	220	200	V

Table D-1 (cont'd)

#	77C014	87C012	87A0345B	97C100	97A1005B	Unit
81	49.4	71.2	72.7	149.8	151	μF
82	3.35	3.42	2.75	1.75	1.77	Ω
83	1080	1100	2150	1120	2110	rpm
84	25	25	25	20	25	°C
85	0.08	0.03	0.06	0.068	0.1315	m
86	0	0	0.69	0	0	-
87	0	0	84	38	52	-
88	0	0	78	48	62	-
89	0	0	64	56	68	-
90	64	64	0	0	0	-
91	100	80	0	0	0	-
92	108	112	0	0	0	-
93	0	0	11	5	7	-
94	0	0	9	7	9	-
95	0	0	7	9	11	-
96	5	5	0	0	0	-
97	7	7	0	0	0	-
98	9	9	0	0	0	-
99	Yes	Yes	No	Yes	No	-
100	64	32	0	38	0	-
101	100	80	0	48	0	-
102	0	0	0	0	0	-
103	0	0	0	0	0	-
104	0	0	0	0	0	-
105	0	0	0	0	0	-
106	5	5	0	5	0	-
107	7	7	0	7	0	-
108	0	0	0	0	0	-
109	0	0	0	0	0	-
110	0	0	0	0	0	-
111	0	0	0	0	0	-

APPENDIX E

TPCAD FLOWCHARTS

In this part, calculations used in TPCAD to obtain machine parameters and performances are explained by flowcharts. Main body of the program is given in Figure E-1.

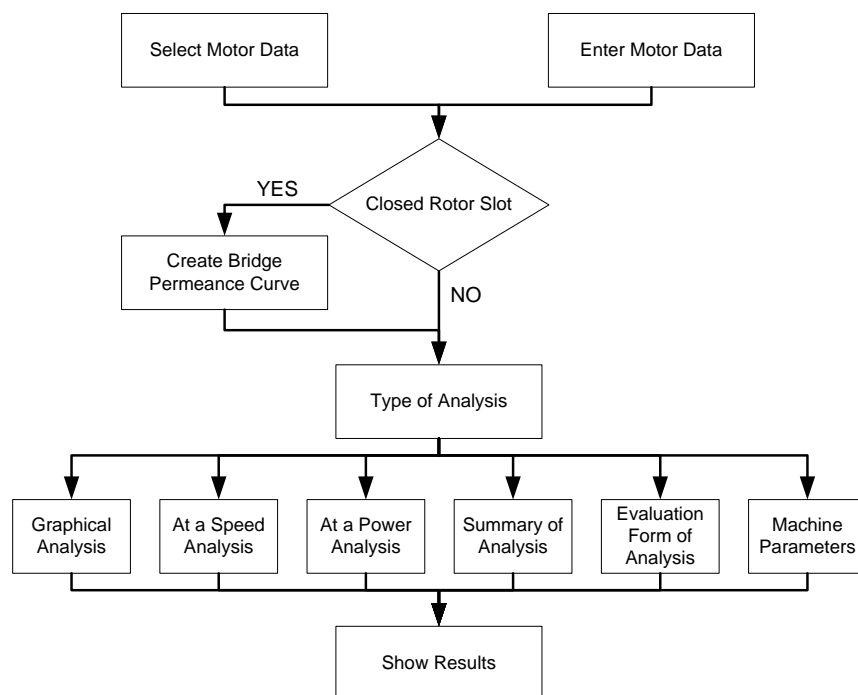


Figure E-1 Main Body of TPCAD

Performance calculations are done according to the steps given in Figure E-2.

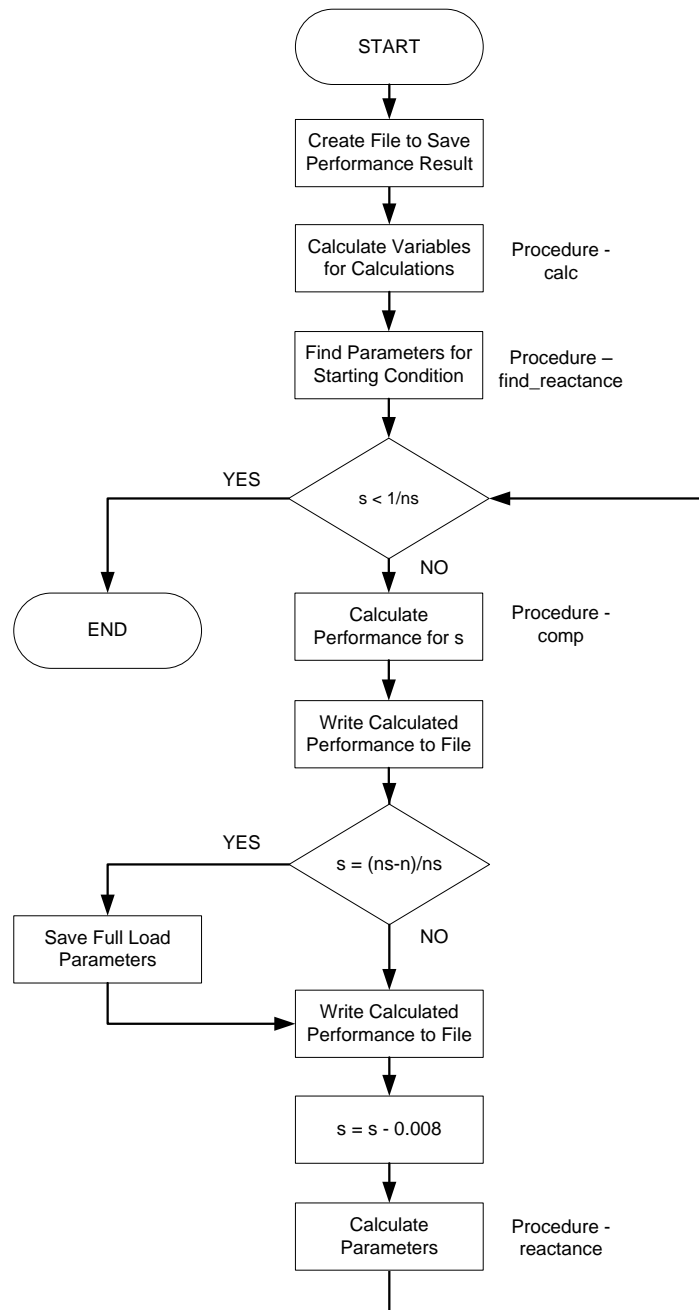


Figure E-2 Flowchart of the Performance Calculation

“calc” Procedure: This procedure performs the initial calculations for the motor parameters.

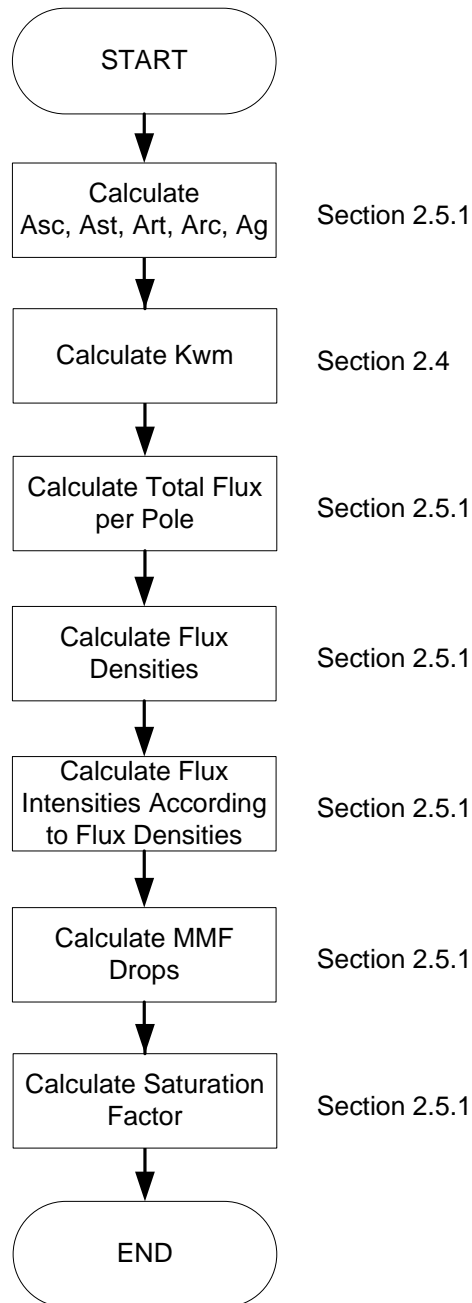


Figure E-3 Flowchart of Calc Procedure

“find_reactance” Procedure: This procedure performs the calculation of reactances at the starting condition.

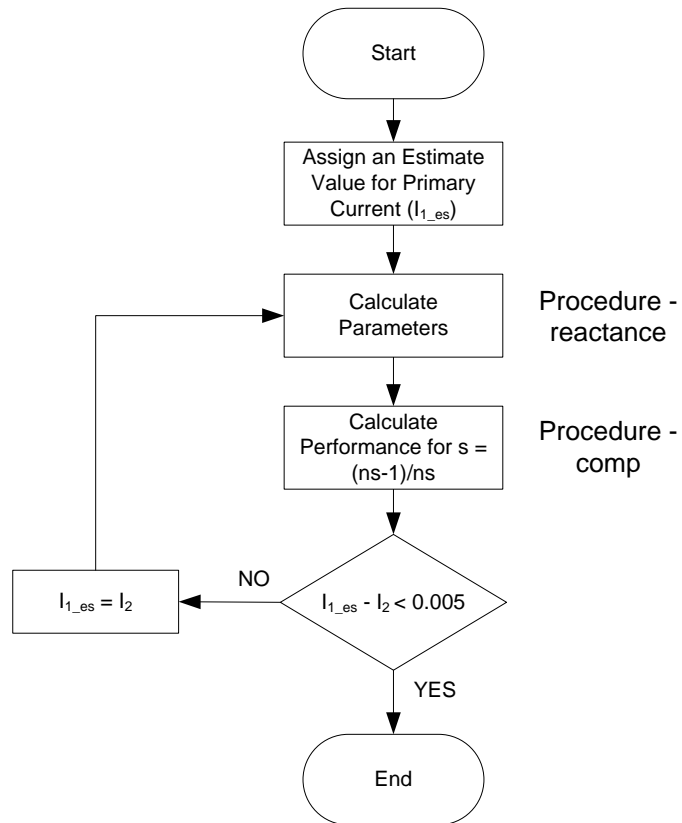


Figure E-4 Flowchart of find_reactance Procedure

“comp” Procedure: This procedure calculates the motor performance according to the desired slip value.

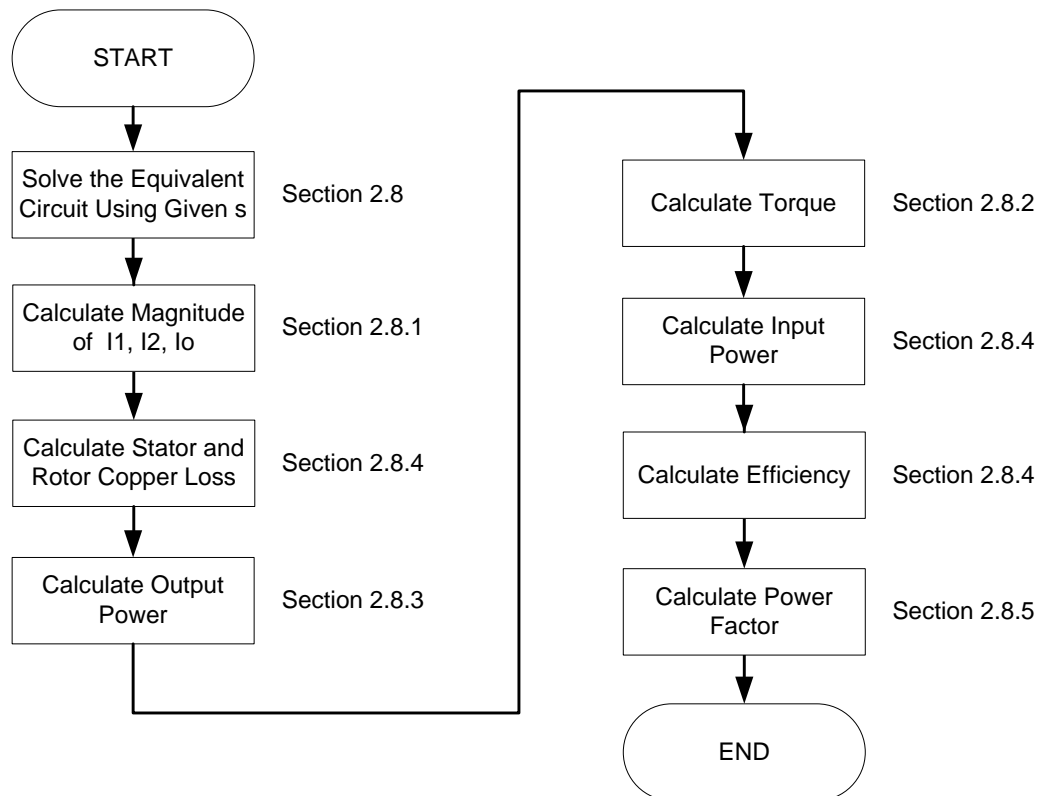


Figure E-5 Flowchart of comp Procedure

“reactance” Procedure: This procedure calculates the reactances according to line current.

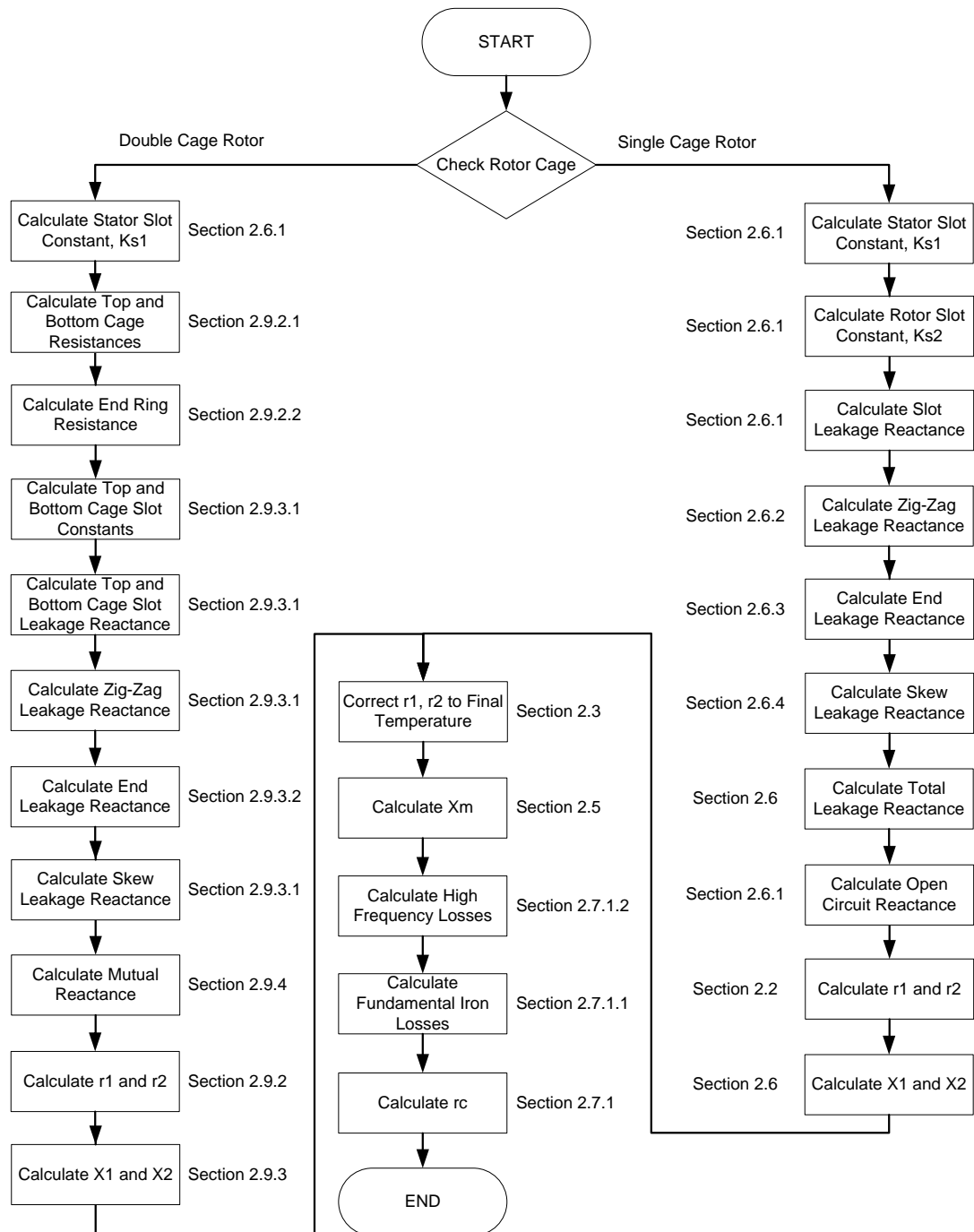


Figure E-6 Flowchart of reactance Procedure

APPENDIX F

SPCAD FLOWCHARTS

In this part, calculations used in SPCAD to obtain machine parameters and performances are explained by flowcharts. Main body of the program is given in Figure F-1.

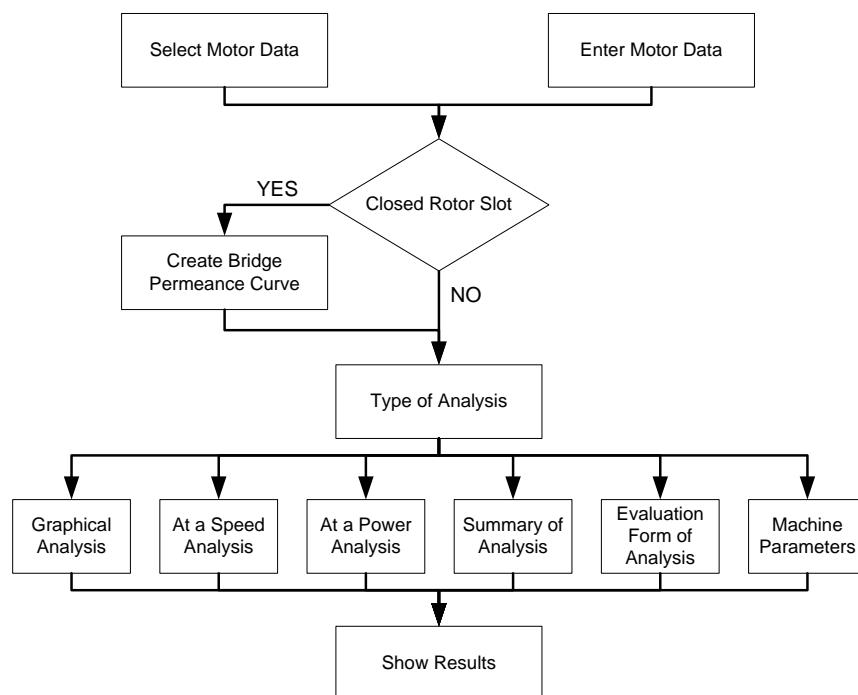


Figure F-1 Main Body of SPCAD

Performance calculations are done according to the steps given in Figure F-2.

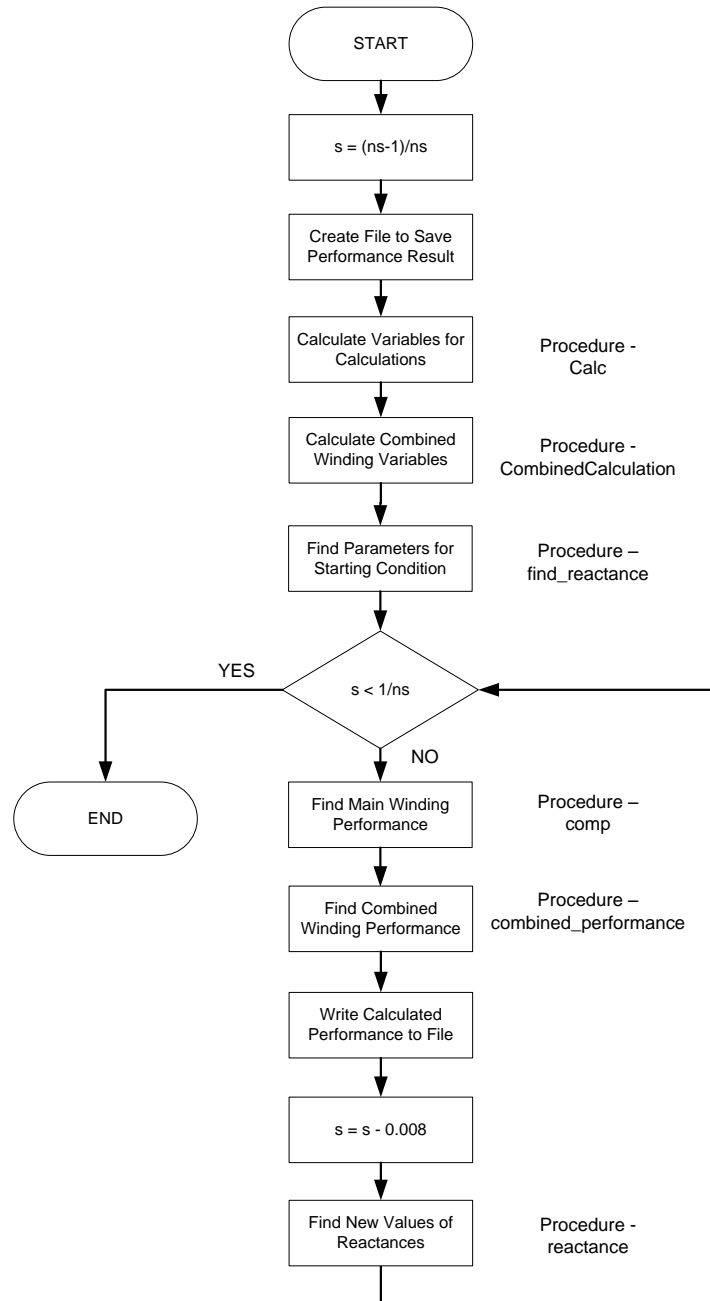


Figure F-2 Flowchart of the Performance Calculation

“calc” Procedure: This procedure performs the initial calculations for the main winding motor parameters.

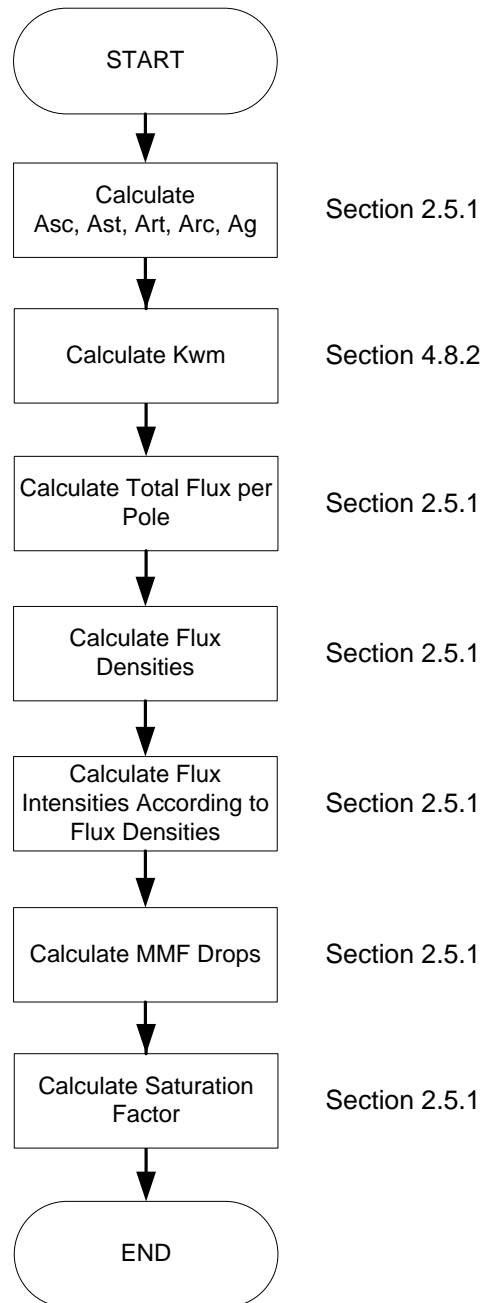


Figure F-3 Flowchart of Calc Procedure

“CombinedCalculation” Procedure: This procedure performs the initial calculations for the auxiliary winding motor parameters.

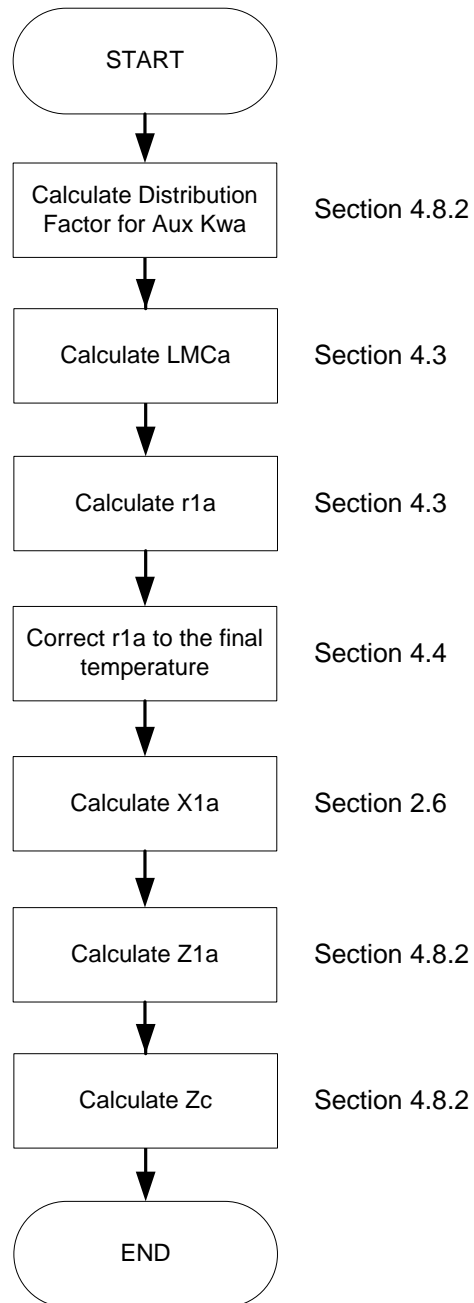


Figure F-4 Flowchart of CombinedCalculation Procedure

“find_reactance” Procedure: This procedure performs the calculation of reactances at the starting condition.

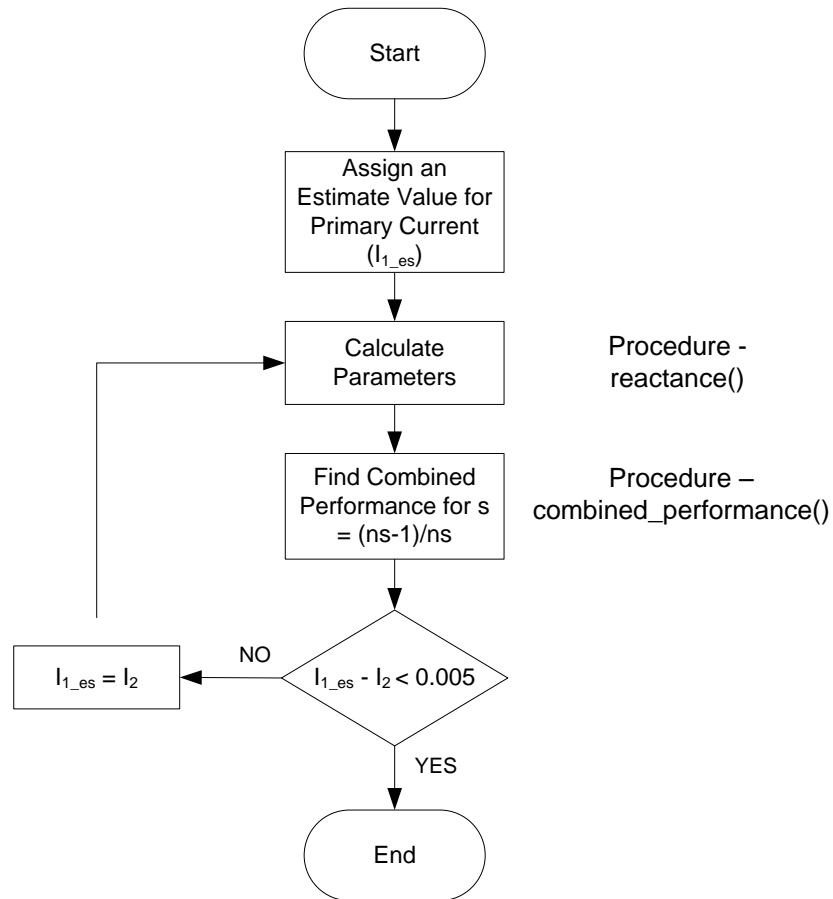


Figure F-5 Flowchart of find_reactance Procedure

“comp” Procedure: This procedure calculates the main winding performance of the motor according to the desired slip value.

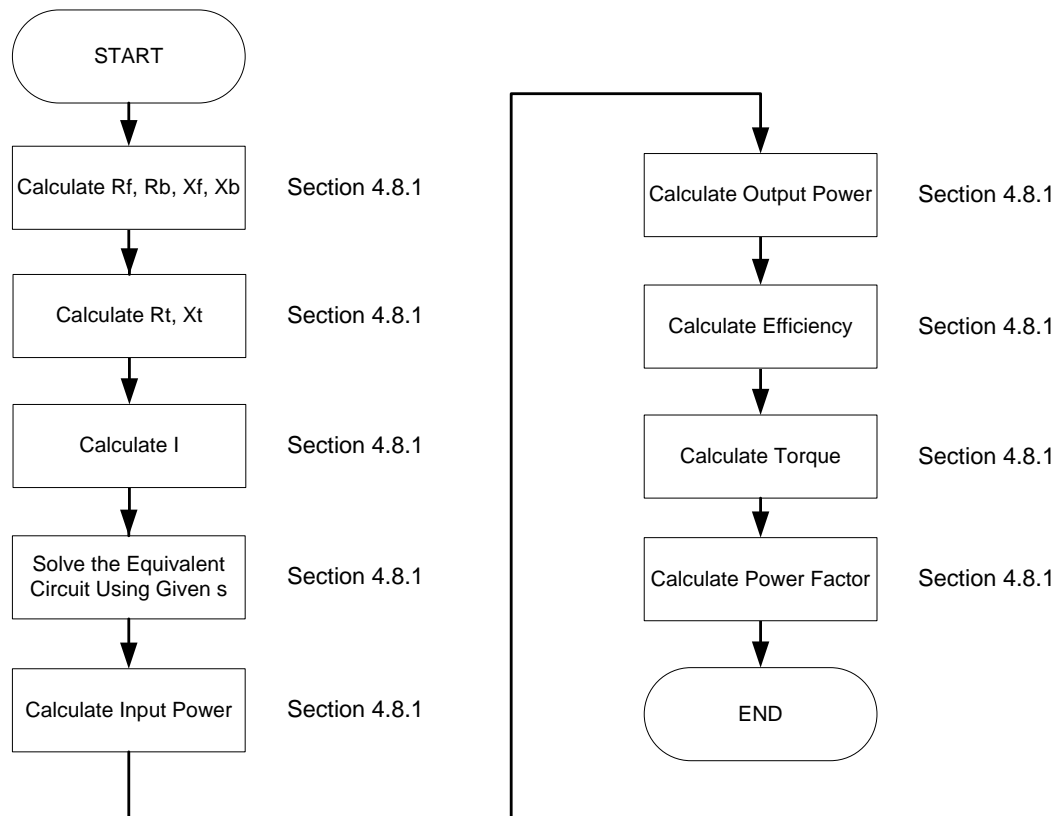


Figure F-6 Flowchart of comp Procedure

“combined_performance” Procedure: This procedure calculates the combined winding performance of the motor according to the desired slip value.

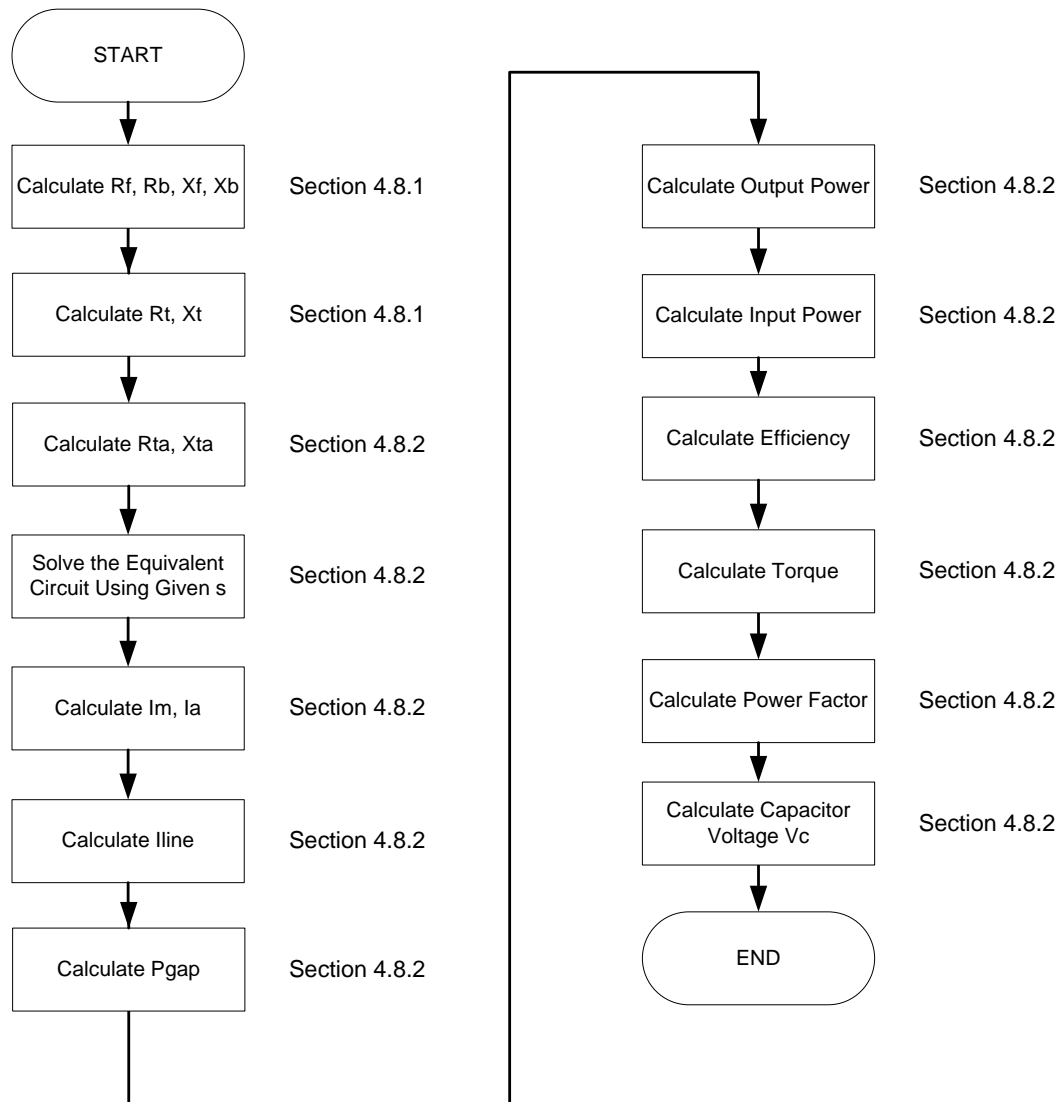


Figure F-7 Flowchart of combined_performance Procedure

“reactance” Procedure: This procedure calculates the reactances according to line current.

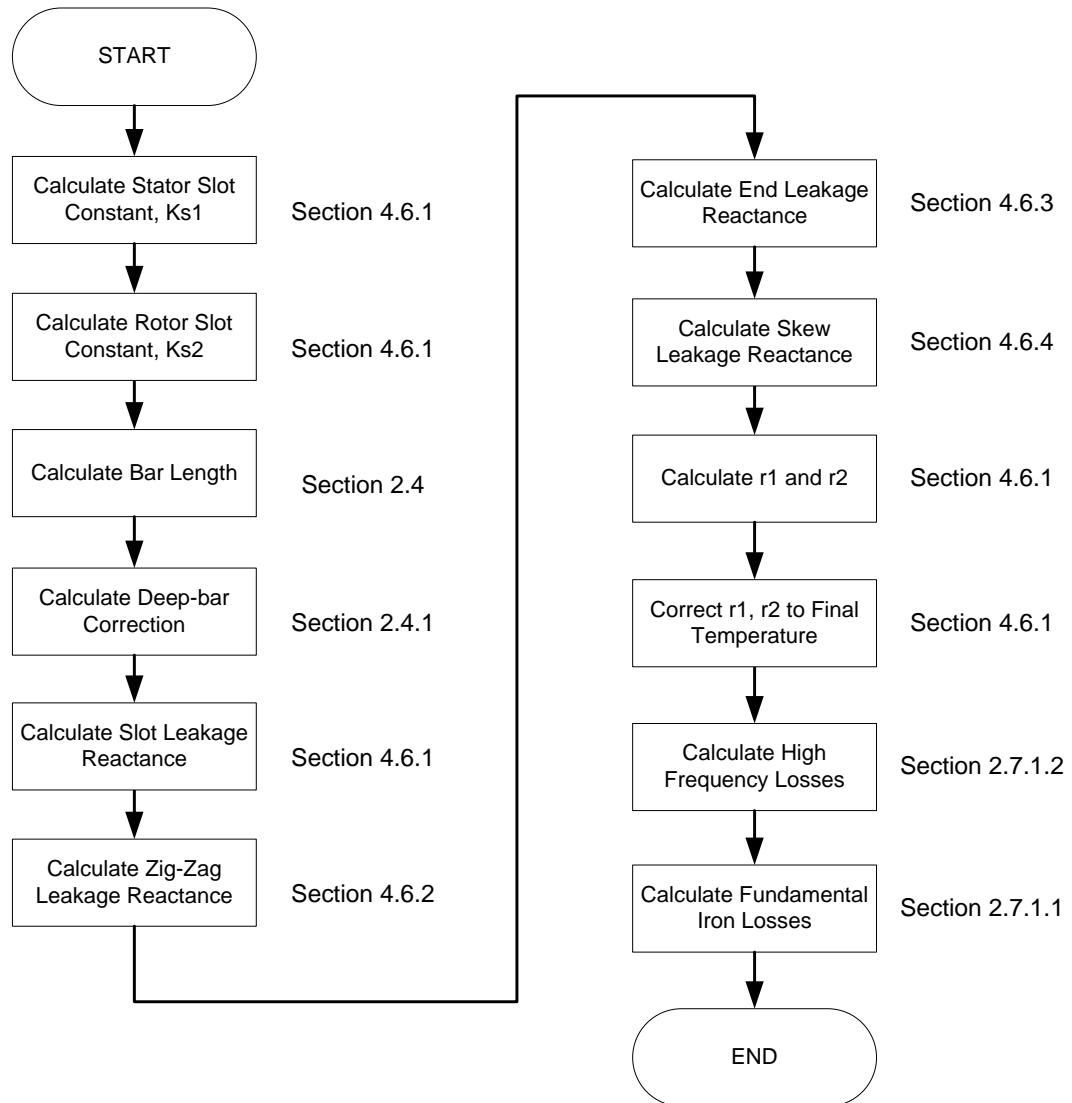


Figure F-8 Flowchart of reactance Procedure

APPENDIX G

B-H CURVE DATA

In this part, the B-H curve data used in TPCAD and SPCAD for calculations are given in Table G-1 and Table G-2 respectively.

Table G-1 TPCAD B-H Curve Data

B (T)	H (AT)
0.10	0.96
0.11	11
0.20	30
0.45	40
0.63	54
0.76	66
0.92	100
0.98	150
1.05	162
1.15	254
1.27	316
1.40	512
1.50	1106
1.55	1650
1.65	4500
1.75	8000

Table G-1 (cont'd)

B (T)	H (AT)
1.85	15000
1.95	25000
2.00	30000
2.05	35000
2.10	40000
2.15	45000
2.20	50000

Table G-2 SPCAD B-H Curve Data

B (T)	H (AT)
0.00	66.8
0.67	141.42
1.05	282.84
1.25	424.26
1.32	565.68
1.40	707.1
1.51	1414.2
1.56	2121.3
1.59	2828.4
1.61	3535.53
1.63	4242.64
1.66	4949.74
1.67	6363.96
1.69	7071.06
1.70	7778.17
1.71	8485.28
1.73	9192
1.75	10606.6
1.76	11313.7
1.78	12021

Table G-2 (cont'd)

B (T)	H (AT)
1.80	13435
1.81	14839